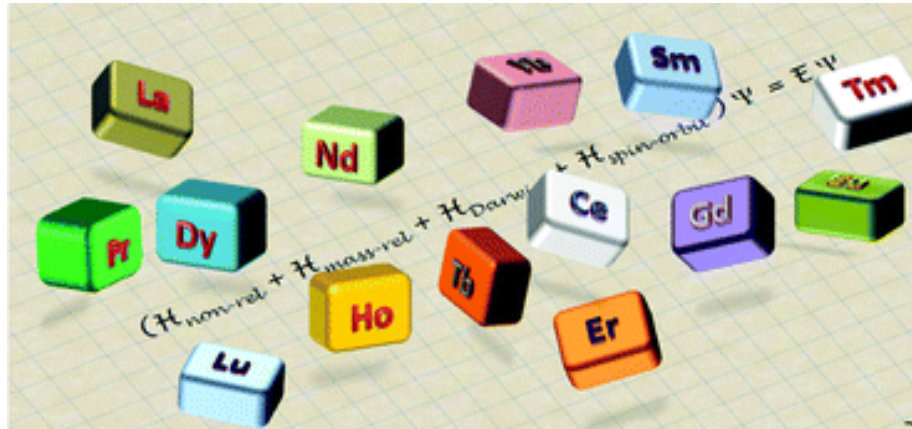


Introduction to the Magnetism of Lanthanides Ions



Kevin Bernot

Institut des Sciences Chimiques de Rennes (ISCR)

Basics of Rare-Earth & Lanthanide Elements

Rare-Earth & Lanthanides elements

1 1.00794 H hydrogène	2 6.941 Li lithium	3 9.012182 Be beryllium	4 22.98976 11 Na sodium	5 24.3050 12 Mg magnésium	6 50.9415 23 Sc scandium	7 51.9962 24 Ti titane	8 54.93804 25 V vanadium	9 55.845 26 Cr chrome	10 58.93319 27 Mn manganèse	11 58.6934 28 Fe fer	12 63.546 29 Co cobalt	13 65.38 30 Ni nickel	14 69.723 31 Cu cuivre	15 72.64 32 Zn zinc	16 74.92160 33 Al aluminium	17 78.96 34 Si silicium	18 80.9008 35 B bore	19 83.798 36 C carbone	20 87.904 35 N azote	21 90.1797 10 O oxygène	22 93.948 18 F fluor	23 95.945 17 Ne néon
39.0983 19 K potassium	40.078 20 Ca calcium	44.95591 21 Sc scandium	47.867 22 Ti titane	50.9415 23 V vanadium	51.9962 24 Cr chrome	54.93804 25 Mn manganèse	55.845 26 Fe fer	58.93319 27 Co cobalt	58.6934 28 Ni nickel	63.546 29 Cu cuivre	65.38 30 Zn zinc	69.723 31 Ga gallium	72.64 32 Ge germanium	74.92160 33 As arsenic	78.96 34 Se sélénum	79.904 35 Br brome	83.798 36 Kr krypton					
85.4678 37 Rb rubidium	87.62 38 Sr strontium	88.90585 39 Y yttrium	91.224 40 Zr zirconium	92.90638 41 Nb niobium	95.96 42 Mo molybdène	98 43 Tc technétium	101.07 44 Ru ruthénium	102.9055 45 Rh rhodinium	106.42 46 Pd palladium	107.8682 47 Ag argent	112.441 48 Cd cadmium	114.818 49 In indium	118.710 50 Sn étain	121.760 51 Sb antimoine	127.60 52 Te tellure	126.9044 53 I iode	131.293 54 Xe xénon					
132.9054 55 Cs césium	137.327 56 Ba barium	138.9054 57-71 lanthanides	178.49 72 Hf hafnium	180.9478 73 Ta tantale	183.84 74 W tungstène	186.207 75 Re rhénium	190.23 76 Os osmium	192.217 77 Ir iridium	195.084 78 Pt platine	196.9665 79 Au or	200.59 80 Hg mercure	204.3833 81 Tl thallium	207.2 82 Pb plomb	208.9804 83 Bi bismuth	210 84 Po polonium	210 85 At astate	220 86 Rn radon					
223 87 Fr francium	226 88 Ra radium	226 89-103 actinides	261 104 Rf rutherfordium	262 105 Db dubrium	266 106 Sg seaborgium	264 107 Bh bohrium	277 108 Hs hassium	268 109 Mt meitnérium	271 110 Ds darmstadium	272 111 Rg roentgenium	285 112 Cn copernicium	284 113 Nh nihonium	289 114 Fl flérovium	288 115 Mc moscovium	292 116 Lv livermorium	292 117 Ts tennessine	294 118 Og oganesson					
			138.9054 57 La lanthane	140.116 58 Ce	140.9076 59 Pr	144.242 60 Nd	145 61 Pm	150.36 62 Sm	151.954 63 Eu	157.25 64 Gd	158.9253 65 Tb	162.500 66 Dy	164.9303 67 Ho	167.259 68 Er	168.9342 69 Tm	173.054 70 Yb	174.9566 71 Lu					
			227 89 Ac actinium	232.0380 90 Th thorium	231.0358 91 Pa protactinium	238.0289 92 U uranium	237 93 Np neptunium	244 94 Pu plutonium	243 95 Am américium	247 96 Cm curium	247 97 Bk berkélium	251 98 Cf californium	252 99 Es einsteinium	257 100 Fm fermium	258 101 Md mendélévium	259 102 No nobélium	262 103 Lr lawrencium					

Rare-Earths (RE)

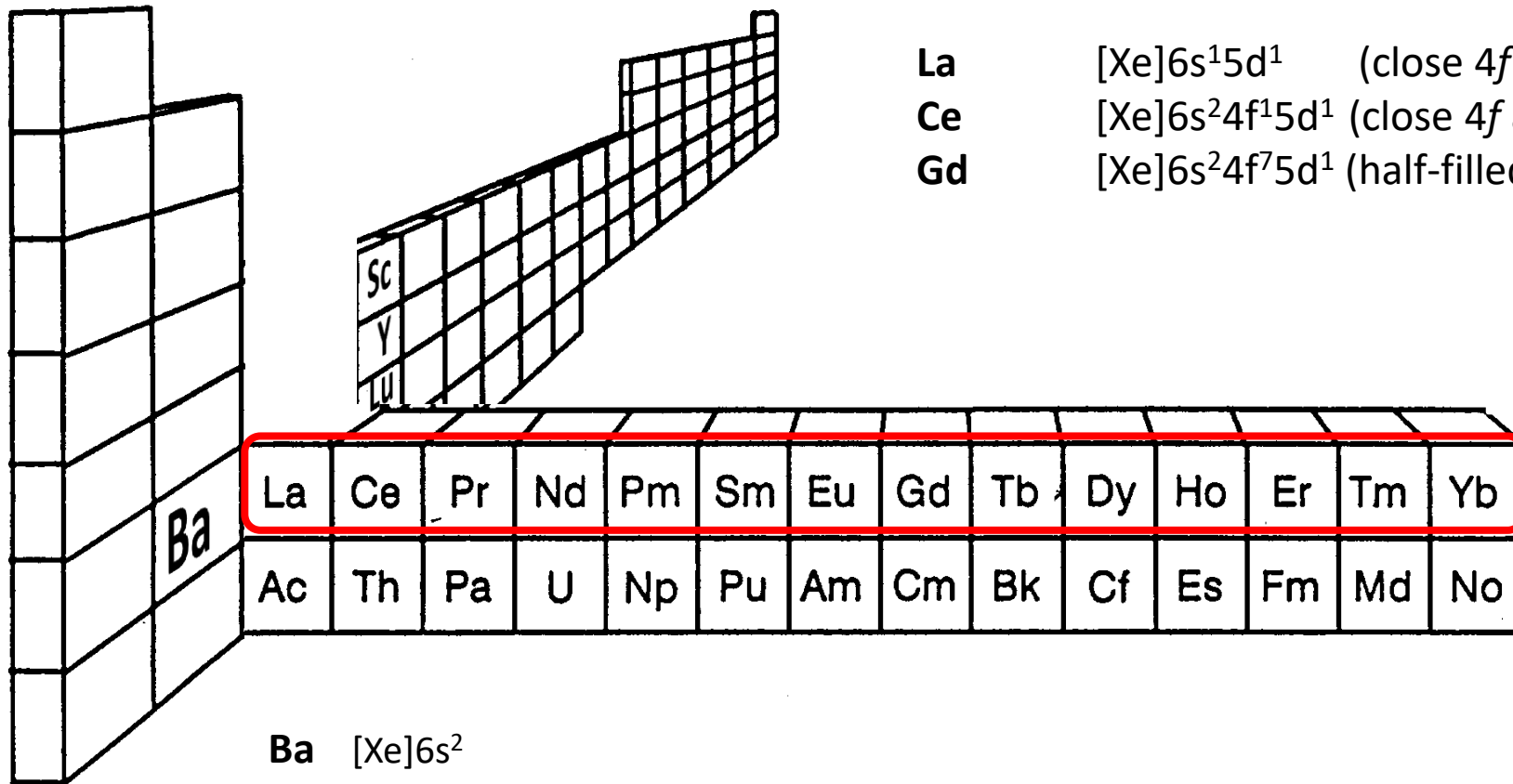
Lanthanides (Ln)

Lanthanoids

Ceric lanthanoids (Ce-Eu) → « big lanthanides »

Yttric lanthanoids (Gd-Lu) → « small lanthanides »

Think about periodic table in 3D...!

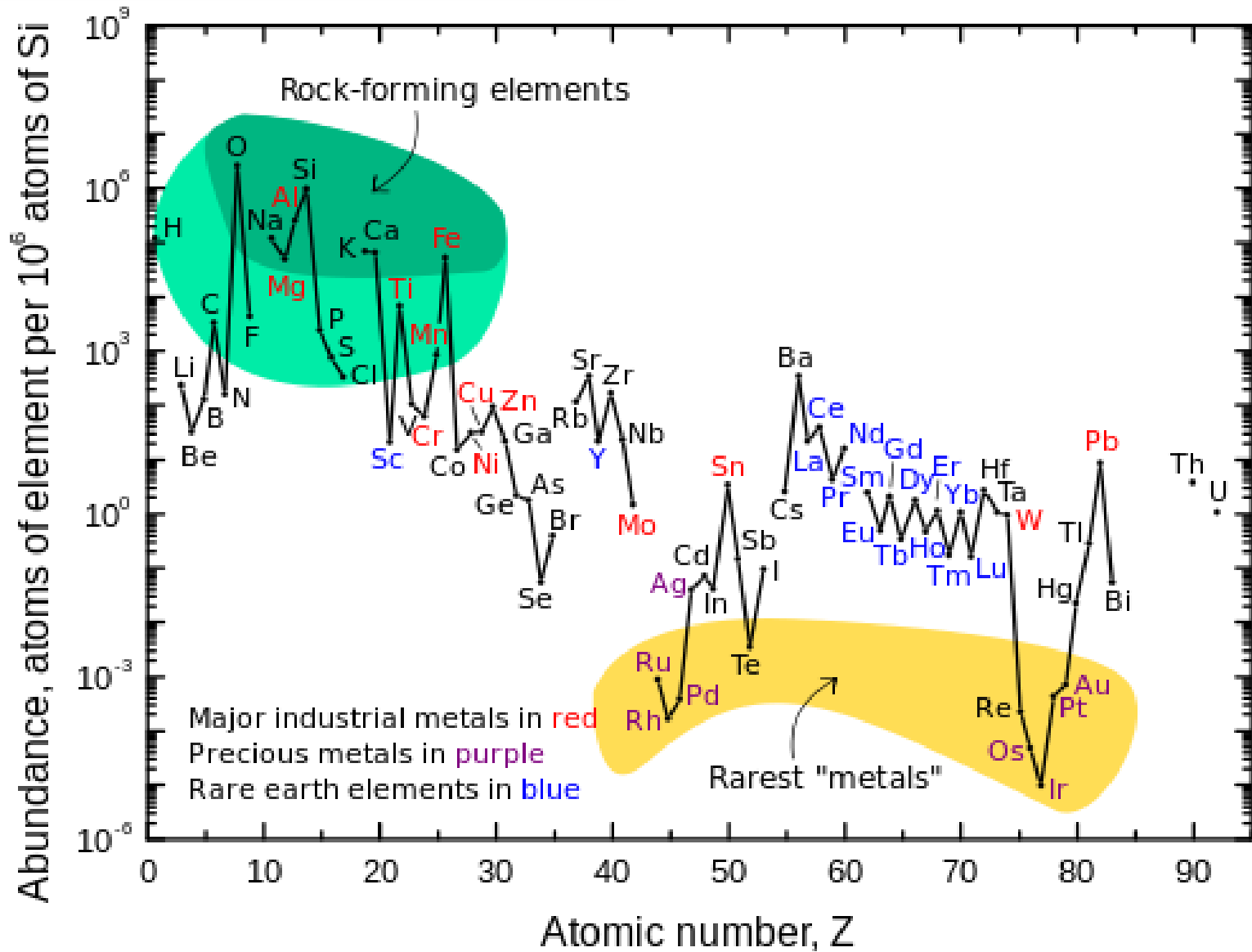


Sc	[Ar]4s ² 3d ¹
Y	[Kr]5s ² 4d ¹
Pr-Yb	[Xe]6s ² 4f ⁿ $3 \leq n \leq 14$
Lu	[Xe]6s ² 4f ¹⁴ 5d ¹

Exception to Klechkowski's rule:

La	[Xe]6s ¹ 5d ¹	(close 4f and 5d)
Ce	[Xe]6s ² 4f ¹ 5d ¹	(close 4f and 5d)
Gd	[Xe]6s ² 4f ⁷ 5d ¹	(half-filled)

Rare-Earth elements are not...rare



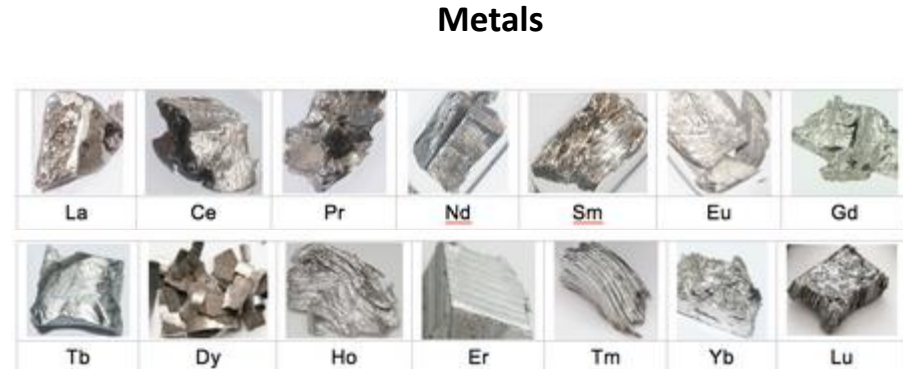
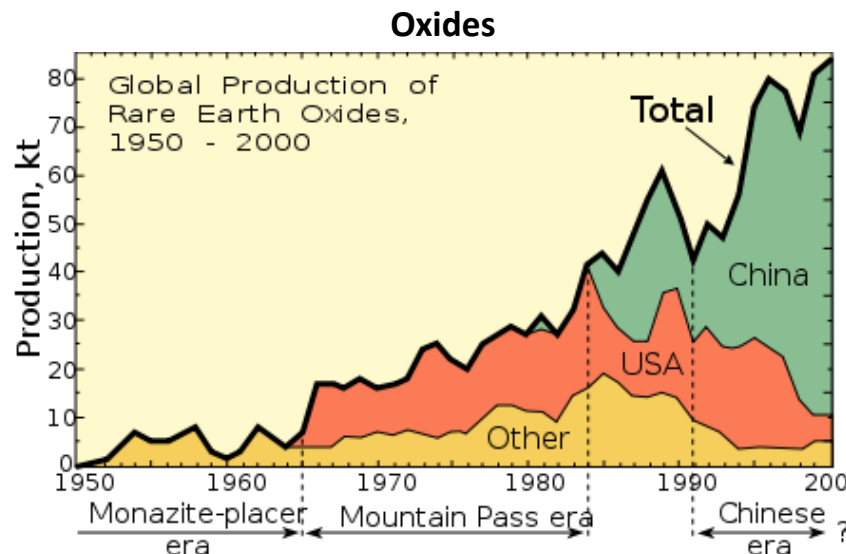
Rare-Earth elements are rare...in every mine

Oxydes de TR, Sc, Th et U	Formule	Teneur de l'écorce terrestre (en ppm)	Concentrés miniers (teneurs* en %)			Concentrés chimiques (teneurs* en %)			Prix des oxydes, en \$/kg, 99 % de pureté, en juillet 2016
			Monazite	Bastnaésite	Loparite	Bayan Obo (Chine)	Mountain Pass (Etats -Unis)	Central Lanthanide Deposit, Mount Weld (Australie)	
Total oxyde de TR		150	~ 60	60-70	~ 32	100	100	100	
Lanthane	La ₂ O ₃	18	24	32	28	23,0	34,0	23,88	5,1 ¹
Cérium	CeO ₂	46	46	49	57	50,0	48,8	47,55	5,2 ¹
Praséodyme	Pr ₆ O ₁₁	5,5	5	4	4	6,2	4,2	5,16	81,3 ¹
Néodyme	Nd ₂ O ₃	24	17	13,5	9	18,5	11,7	18,13	51 ¹
Samarium	Sm ₂ O ₃	6,5	2,5	0,5	0,9	0,8	0,79	2,44	15 ¹
Europium	Eu ₂ O ₃	0,5	0,05	0,1	0,1	0,2	0,13	0,53	285 ¹
Gadolinium	Gd ₂ O ₃	6,4	1,5	0,3	0,2	0,7	0,21	1,09	45 ¹
Terbium	Tb ₄ O ₇	0,9	0,04	0,01	0,07	0,1		0,09	559 ¹
Dysprosium	Dy ₂ O ₃	5	0,7	0,03	0,09	0,1		0,25	259 ¹
Holmium	Ho ₂ O ₃	1,2	0,05	0,01	0,03	-		0,03	82 ²
Erbium	Er ₂ O ₃	4	0,2	0,01	0,07	-		0,06	37 ¹
Thulium	Tm ₂ O ₃	0,4	0,01	0,02	0,07	-		0,01	275 ²
Ytterbium	Yb ₂ O ₃	2,7	0,1	0,01	0,3	-		0,03	65 ²
Lutécium	Lu ₂ O ₃	0,8	0,04	0,01	0,05	-		0	1 550 ²
Yttrium	Y ₂ O ₃	28	2,4	0,1	0,15	-	0,12	0,76	34 ¹
Thorium	ThO ₂	10	6,7	0,35	0,65	0,032			
Uranium	U ₃ O ₈	4	0,3	< 0,05					
Scandium	Sc ₂ O ₃	16							2 150 ²

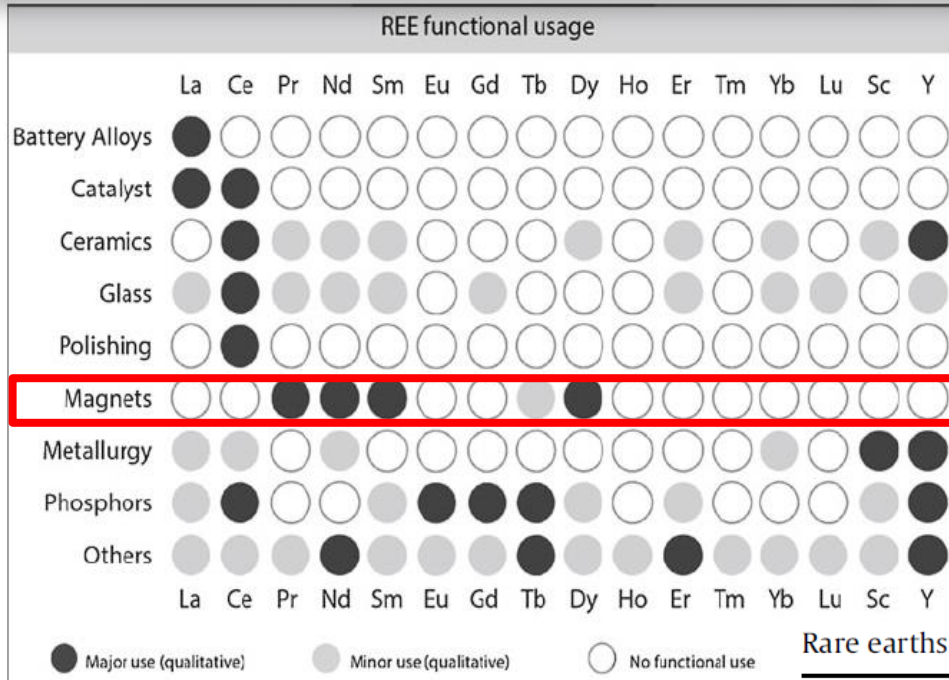
Sources : ¹Mineral Info, ²Panorama 2014 BRGM

Rare-Earth elements are rare...in every mine

Element	Upper crust	Middle crust	Lower crust	Total crust	Composition of the Earth's crust	Bulk composition of the Earth
	ppm					
Sc	14	19	31	21.9	20 ppm	10.1 ± 2 ppm
Y	21	20	16	19	31.5 ppm	2.4 ± 0.2 ppm
Cu	28	26	26	27	68 ppm	64.7 ± 5 ppm
La	31	24	8	20	35 ppm	415 ± 10 ppb
Ce	63	53	20	43	68 ppm	1088 ± 20 ppb
Pr	7.1	5.8	2.4	4.9	9.5 ppm	165 ± 5 ppb
Nd	27	25	11	20	40 ppm	814 ± 10 ppb
Sm	4.7	4.6	2.8	3.9	7.5 ppm	259 ± 3 ppb
Dy	3.9	3.8	3.1	3.6	6.2 ppm	424 ± 10 ppb
Tb	0.7	0.7	0.48	0.6	1.2 ppm	66.6 ± 5 ppb
Lu	0.31	0.4	0.25	0.3	0.81 ppm	42.5 ± 2 ppb
Pt	0.5	0.85	2.7	1.5	0.004 ppm	1562 ± 40 ppb
Au	1.5	0.66	1.6	1.3	0.0041 ppm	102 ± 20 ppb



Rare-earth elements are key ingredients....



Rare earths usage by application, in % (Curtis, 2010).^a

Application	La	Ce	Pr	Nd	Sm	Eu	Gd	Tb	Dy	Y	Other
Magnets				23.4	69.4		2	0.2	5		
Battery alloys	50	33.4	3.3	10	3.3						
Metallurgy	26	52	5.5	16.5							
Auto catalysts	5	90	2	3							
FCC	90	10									
Polishing powders	31.5	65		3.5							
Glass additives	24	66	1	3						2	4
Phosphors	8.5	11				4.9	1.8	4.6		69.2	
Ceramics	17	12	6	12							53
Others	19	39	4	15	2		1				19

^a The percentages are estimated average consumption distribution by application; the actual distribution varies from manufacturer to manufacturer.

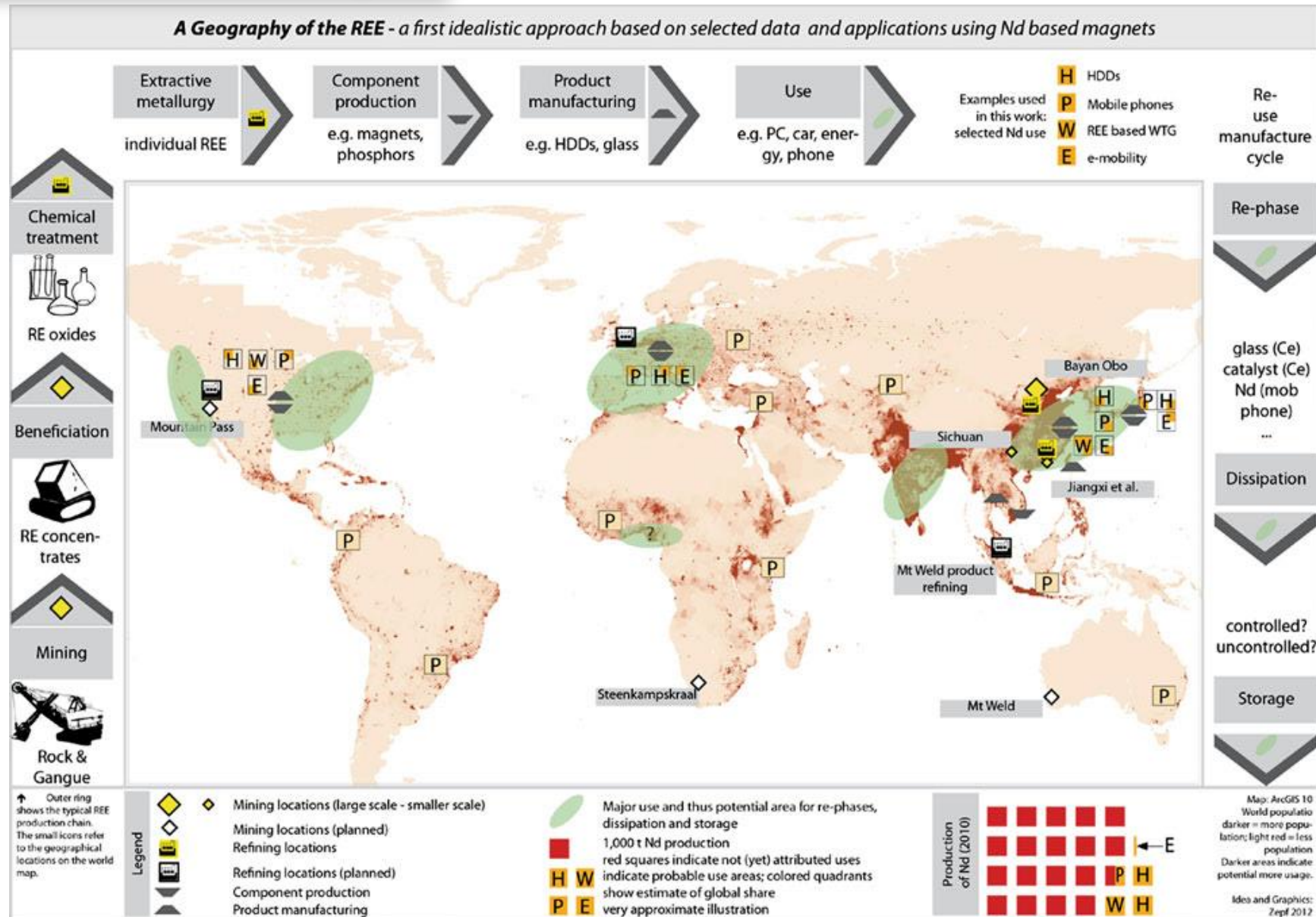
Rare-earth elements are key ingredients....

Typical dysprosium content in NdFeB magnets for different applications (Constantinides, 2011).

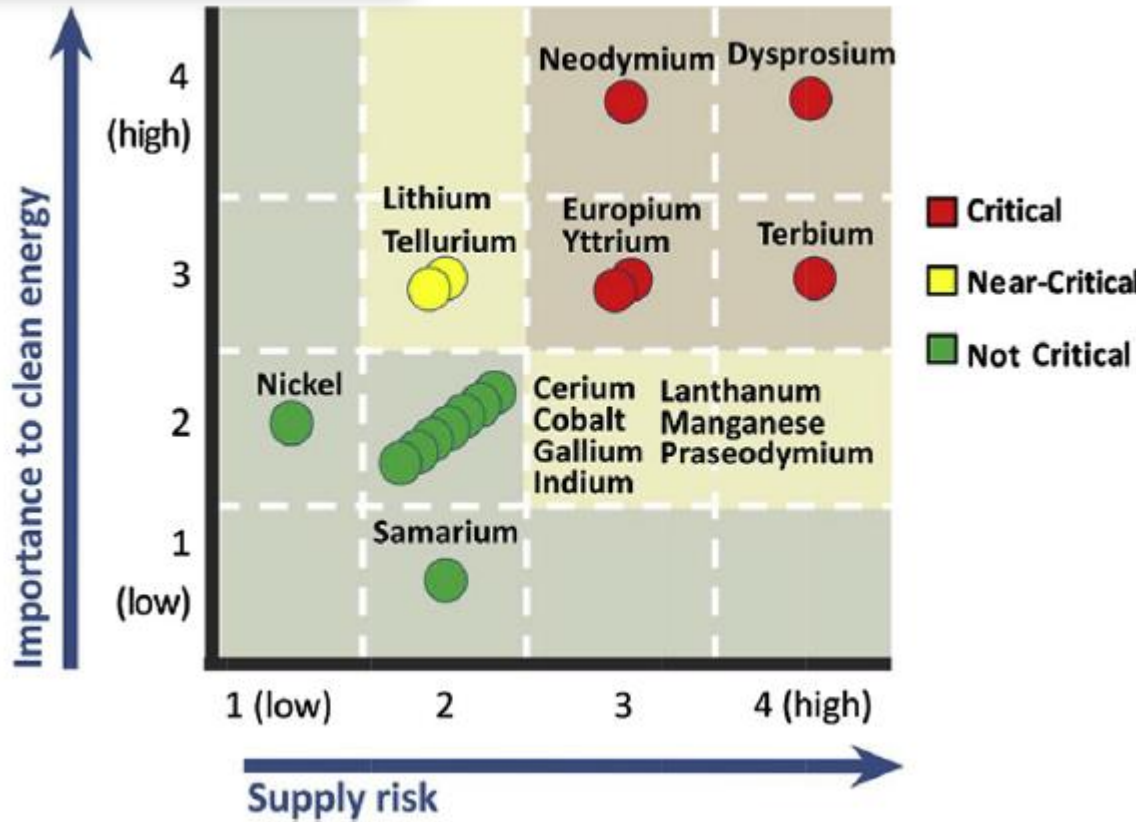
Application	Typical Dy content (%) ^a
Hybrid and electric cars	8.7
Generators	6.4
Wave guides: TWT, undulators, wigglers	6.4
Electric bikes	4.1
Electric storage systems	4.1
Magnetic brakes	4.1
Magnetically levitated transportation	4.1
Motors, industrial, cars, etc.	4.1
Pipe inspection systems	4.1
Relays and switches	4.1
Reprographics	4.1
Torque coupled drives	4.1
Wind turbines	4.1
Gauges	2.8
Hysteresis clutch	2.8
Magnetic separators	2.8
Magnetic refrigerators	1.4
MRI scanners	1.4
Sensors	1.4
HDDs, CDs, DVDs	0.0
Transducers and loudspeakers	0.0
Toys and gadgets	0.0

^a % of Dy compared to the other rare earths.

Rare-Earth elements cycle



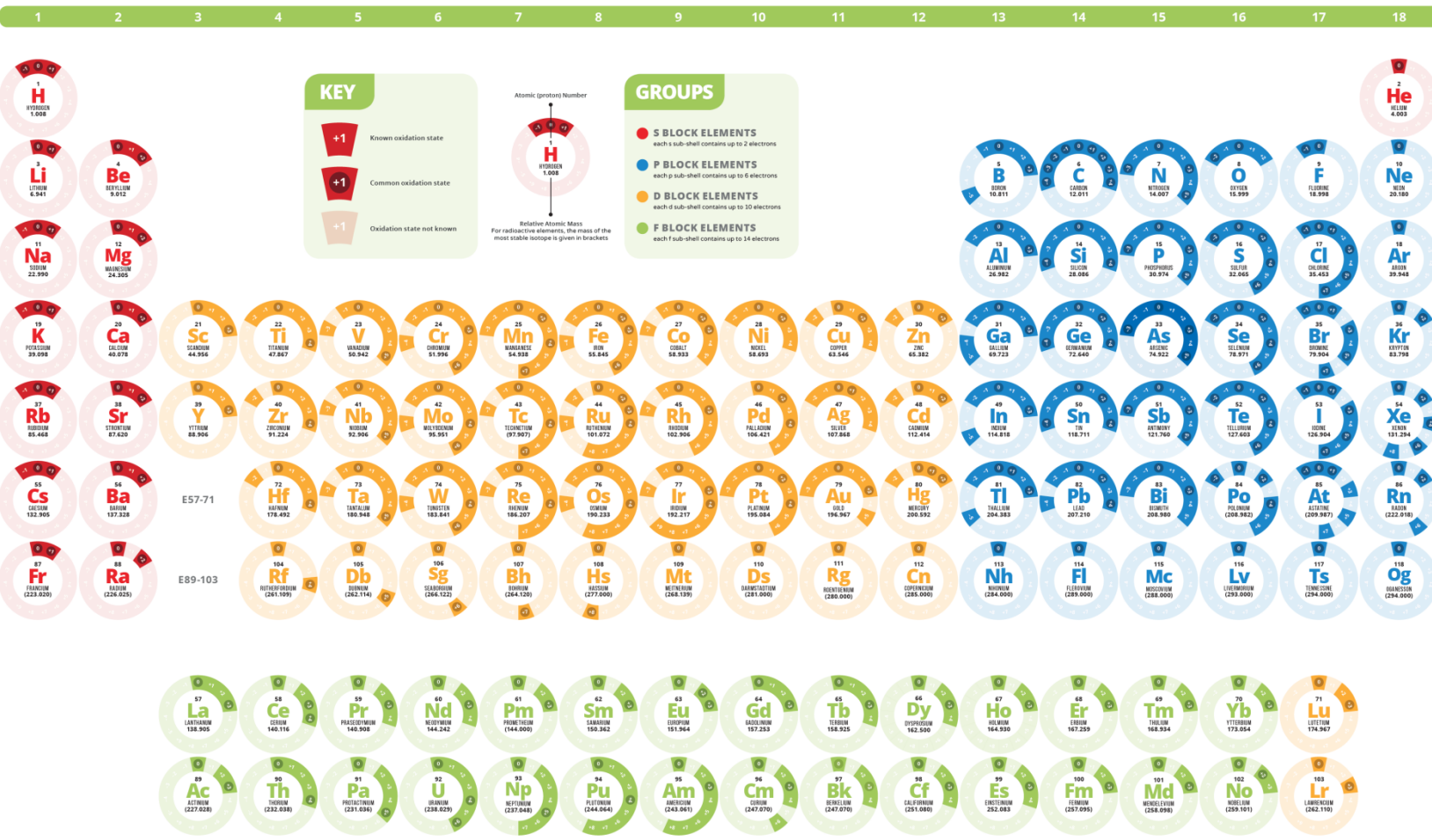
Rare-Earth elements (re)cycle



Recycling potentials for REE from magnets, nickel-metal-hydride batteries and phosphors.

REE application	Estimated REE stocks in 2020 (tons)	Estimated average lifetime (years)	Estimated REE old scrap in 2020 (tons)	Pessimistic scenario: recycled REE in 2020 (tons)	Optimistic scenario: recycled REE in 2020 (tons)
Magnets	300,000	15	20,000	3300	6600
Lamp Phosphors	25,000	6	4167	1333	2333
Nickel-metal-hydride batteries	50,000	10	5000	1000	1750
Total	375,000		29,167	5633	10,683

THE PERIODIC TABLE OF OXIDATION STATES



The chemists periodic table !



For trivalent lanthanides ions : $[Xe] 4f^n$

$n = 0 \quad 1 \quad 2 \quad 3 \quad 4 \quad 5 \quad 6 \quad 7 \quad 8 \quad 9 \quad 10 \quad 11 \quad 12 \quad 13 \quad 14$

Ln	χ_P	I_3	I_{1-3}	$E_{r,3-0}^0$	$E_{r,3-2}^0$
La	1.10	1850	3455	-2.379	-3.1
Ce	1.12	1949	3523	-2.336	-2.92(8)
Pr	1.13	2086	3627	-2.353	-2.84(6)
Nd	1.14	2130	3694	-2.323	-2.62(5)
Pm	1.13	2150	3738	-2.30	-2.44(5)
Sm	1.17	2260	3871	-2.304	-1.50(1)
Eu	1.2	2404	4035	-1.991	-0.34(1)
Gd	1.20	1990	3750	-2.279	-2.85(7)
Tb	1.1	2114	3790	-2.28	-2.83(7)
Dy	1.22	2200	3898	-2.295	-2.56(5)
Ho	1.23	2204	3924	-2.33	-2.79(6)
Er	1.24	2194	3934	-2.331	-2.87(8)
Tm	1.25	2285	4045	-2.319	-2.22(5)
Yb	1.1	2415	4194	-2.19	-1.18(1)
Lu	1.27	2033	3896	-2.28	n.a.
Y	1.22	1980	3777	-2.372	n.a.

Most stable oxidation state is +III

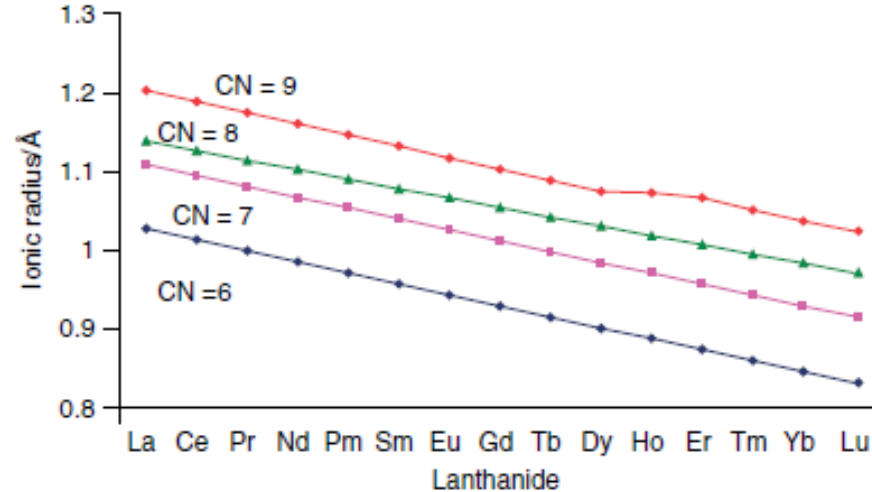
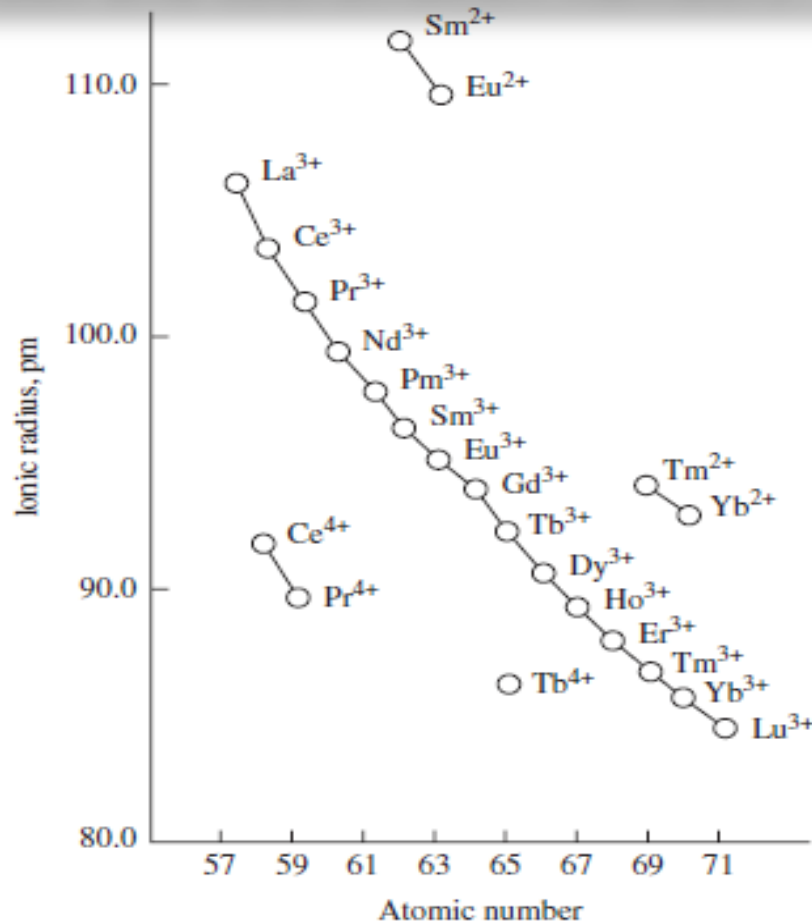
Rare-Earth main properties

Table 1. Selected properties of lanthanides, yttrium, and their trivalent ions.

Ln	χ_P	I_3	I_{1-3}	$E_{r,3-0}^0$	$E_{r,3-2}^0$	ΔH_h^0	$\log * \beta_{11}$	pH	$r_i(6)$	$r_i(9)$	$r_i(12)$
La	1.10	1850	3455	-2.379	-3.1	-3326	-9.01	7.47	103	122	136
Ce	1.12	1949	3523	-2.336	-2.92(8)	-3380	-10.6	7.10	101	120	134
Pr	1.13	2086	3627	-2.353	-2.84(6)	-3421	-8.55	6.96	99	118	132
Nd	1.14	2130	3694	-2.323	-2.62(5)	-3454	-8.43	6.78	98	116	130
Pm	1.13	2150	3738	-2.30	-2.44(5)	-3482	n.a.	n.a.	97	114	128
Sm	1.17	2260	3871	-2.304	-1.50(1)	-3512	-8.34	6.65	96	113	127
Eu	1.2	2404	4035	-1.991	-0.34(1)	-3538	-8.31	6.61	95	112	125
Gd	1.20	1990	3750	-2.279	-2.85(7)	-3567	-8.35	6.58	94	111	124
Tb	1.1	2114	3790	-2.28	-2.83(7)	-3600	-8.16	6.47	92	110	123
Dy	1.22	2200	3898	-2.295	-2.56(5)	-3634	-8.10	6.24	91	108	122
Ho	1.23	2204	3924	-2.33	-2.79(6)	-3663	-8.04	6.20	90	107	121
Er	1.24	2194	3934	-2.331	-2.87(8)	-3692	-7.99	6.14	89	106	119
Tm	1.25	2285	4045	-2.319	-2.22(5)	-3717	-7.95	5.98	88	105	118
Yb	1.1	2415	4194	-2.19	-1.18(1)	-3740	-7.92	5.87	87	104	117
Lu	1.27	2033	3896	-2.28	n.a.	-3759	-7.90	5.74	86	103	116
Y	1.22	1980	3777	-2.372	n.a.	-3640	-8.36	n.a.	90	108	n.a.

Notes: Key: χ_P = Pauling's electronegativity; I_3 = third ionization energy (rounded to 1 kJ mol^{-1}) [8]; I_{1-3} = sum of the first three ionization energies (rounded to 1 kJ mol^{-1}) [8]; $E_{r,3-0}^0$ = standard redox potential $\text{Ln}^{+3}/\text{Ln}^0$ in V at pH 0 [12]; $E_{r,3-2}^0$ = redox potential $\text{Ln}^{+3}/\text{Ln}^{+2}$ in V [13], value for La is calculated; ΔH_h^0 = standard hydration enthalpies in kJ mol^{-1} calculated by semi-empirical methods (Born–Haber cycles) [14]; $*\beta_{11} = [(\text{LnOH})^{2+}][\text{H}^+]/[\text{Ln}^{3+}]$, ionic strength = 0.3 M [15]; pH = pH at which hydroxide precipitation starts in $\text{Ln}(\text{NO}_3)_3$ solutions 0.1 M in water [16]; $r_i(n)$ = ionic radii for coordination numbers $n = 6, 9$, and 12 in pm [17].

Ionic radii and coordination numbers

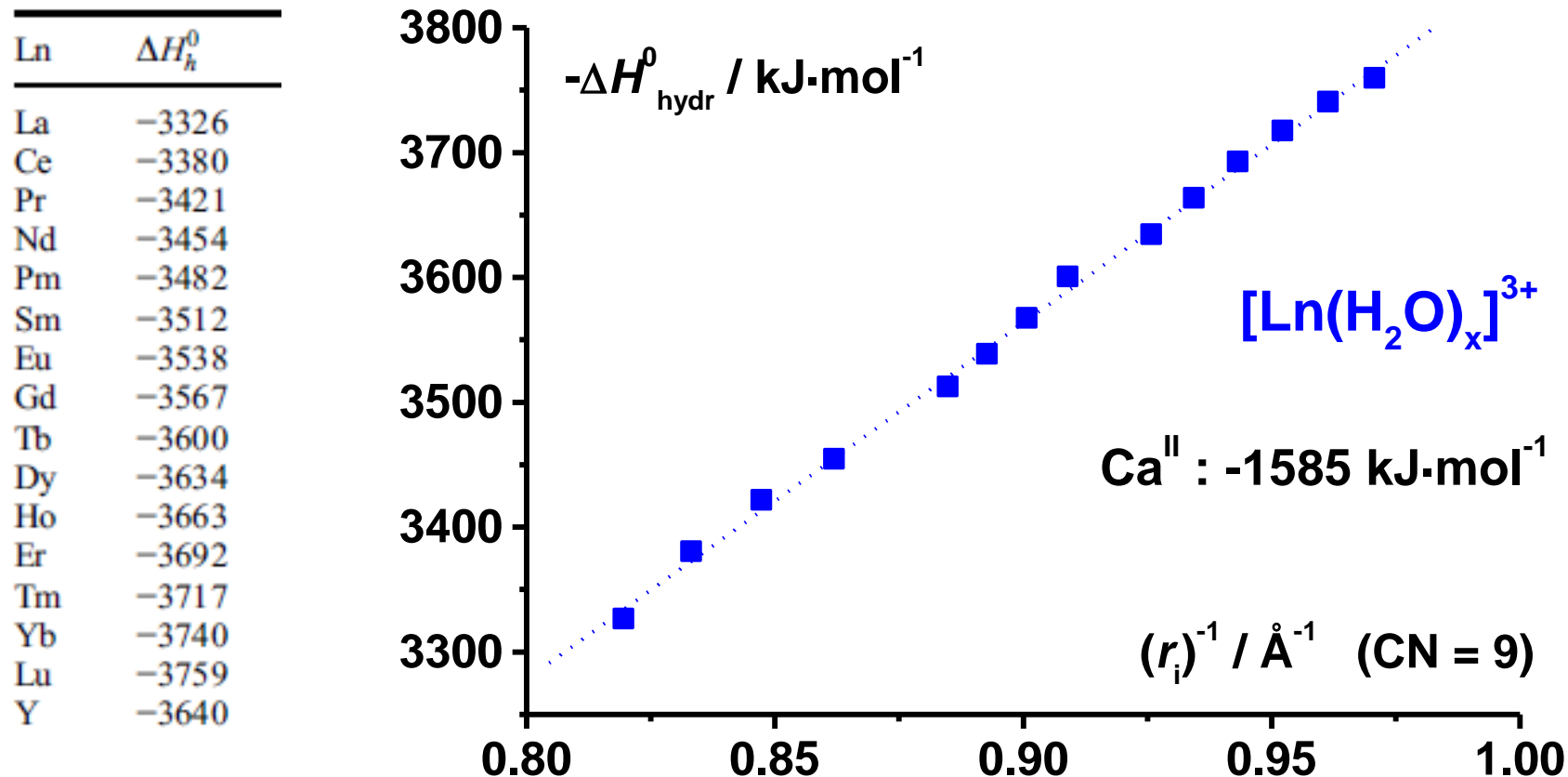


When C.N. is increased → increase of r_i

The relationship between ionic radius and atomic number of lanthanide ions

- Trend on the series,
- Decrease of r_i by 0.2 Å from La to Lu → **Ianthanide contraction**
- "gadolinium break"

Hydratation enthalpies



- Very large hydration enthalpies (most of Ln salts are hygroscopic)
- Trend along the series
- Ligands have to substitute water molecules
- Ln^{III} ions have hard Lewis character → hard bases for ligands such as carboxylates, etc...

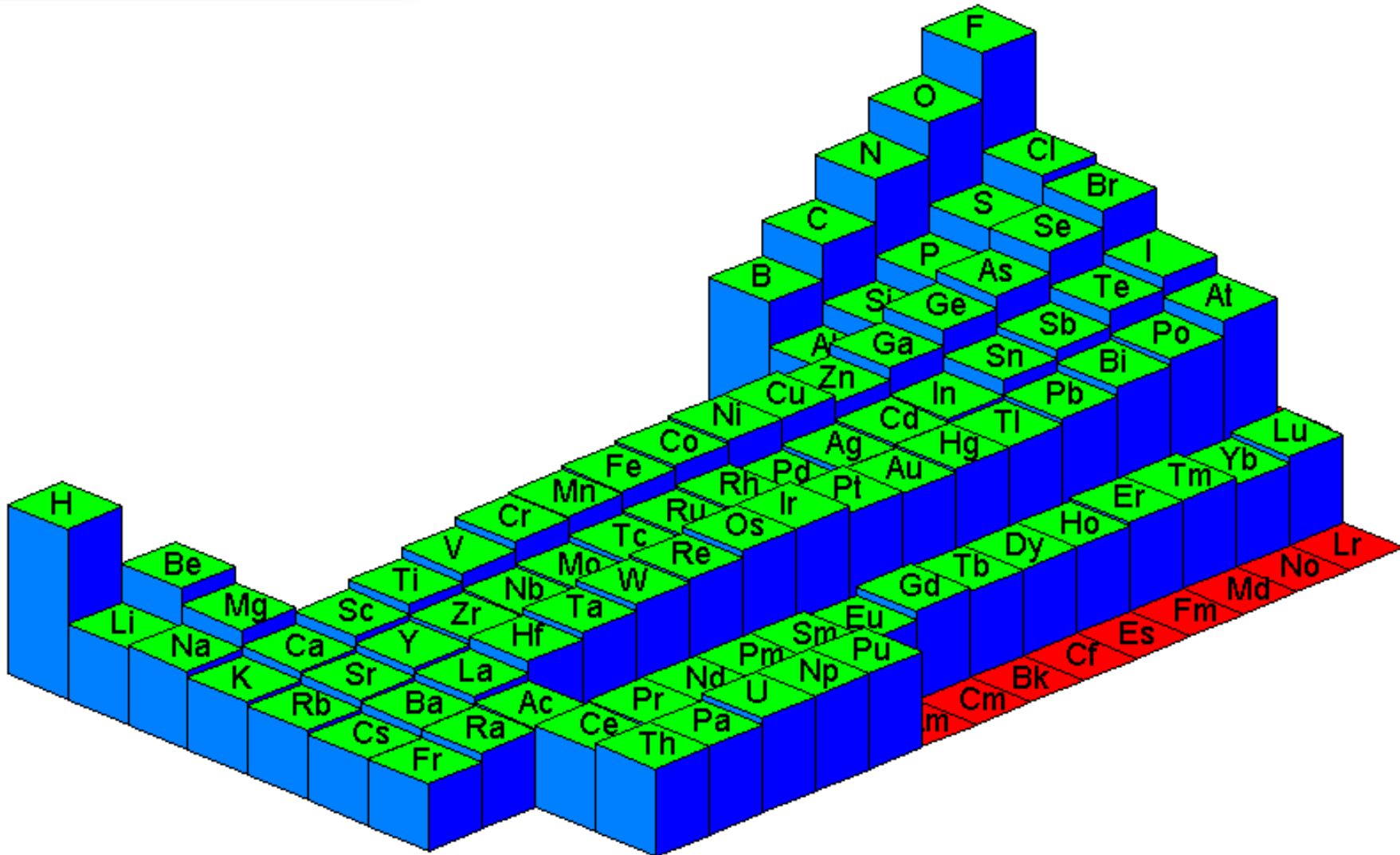
Electronegativity

Table 1. Selected properties of lanthanides, yttrium, and their trivalent ions.

Ln	χ_P	I_3	I_{1-3}	$E_{r,3-0}^0$	$E_{r,3-2}^0$	ΔH_h^0	$\log \beta_{11}^*$	pH	$r_i(6)$	$r_i(9)$	$r_i(12)$
La	1.10	1850	3455	-2.379	-3.1	-3326	-9.01	7.47	103	122	136
Ce	1.12	1949	3523	-2.336	-2.92(8)	-3380	-10.6	7.10	101	120	134
Pr	1.13	2086	3627	-2.353	-2.84(6)	-3421	-8.55	6.96	99	118	132
Nd	1.14	2130	3694	-2.323	-2.62(5)	-3454	-8.43	6.78	98	116	130
Pm	1.13	2150	3738	-2.30	-2.44(5)	-3482	n.a.	n.a.	97	114	128
Sm	1.17	2260	3871	-2.304	-1.50(1)	-3512	-8.34	6.65	96	113	127
Eu	1.2	2404	4035	-1.991	-0.34(1)	-3538	-8.31	6.61	95	112	125
Gd	1.20	1990	3750	-2.279	-2.85(7)	-3567	-8.35	6.58	94	111	124
Tb	1.1	2114	3790	-2.28	-2.83(7)	-3600	-8.16	6.47	92	110	123
Dy	1.22	2200	3898	-2.295	-2.56(5)	-3634	-8.10	6.24	91	108	122
Ho	1.23	2204	3924	-2.33	-2.79(6)	-3663	-8.04	6.20	90	107	121
Er	1.24	2194	3934	-2.331	-2.87(8)	-3692	-7.99	6.14	89	106	119
Tm	1.25	2285	4045	-2.319	-2.22(5)	-3717	-7.95	5.98	88	105	118
Yb	1.1	2415	4194	-2.19	-1.18(1)	-3740	-7.92	5.87	87	104	117
Lu	1.27	2033	3896	-2.28	n.a.	-3759	-7.90	5.74	86	103	116
Y	1.22	1980	3777	-2.372	n.a.	-3640	-8.36	n.a.	90	108	n.a.

Notes: Key: χ_P = Pauling's electronegativity; I_3 = third ionization energy (rounded to 1 kJ mol⁻¹) [8]; I_{1-3} = sum of the first three ionization energies (rounded to 1 kJ mol⁻¹) [8]; $E_{r,3-0}^0$ = standard redox potential $\text{Ln}^{+3}/\text{Ln}^0$ in V at pH 0 [12]; $E_{r,3-2}^0$ = redox potential $\text{Ln}^{+3}/\text{Ln}^{+2}$ in V [13], value for La is calculated; ΔH_h^0 = standard hydration enthalpies in kJ mol⁻¹ calculated by semi-empirical methods (Born–Haber cycles) [14]; ${}^*\beta_{11} = [(\text{LnOH})^{2+}][\text{H}^+]/[\text{Ln}^{3+}]$, ionic strength = 0.3 M [15]; pH = pH at which hydroxide precipitation starts in $\text{Ln}(\text{NO}_3)_3$ solutions 0.1 M in water [16]; $r_i(n)$ = ionic radii for coordination numbers $n = 6, 9$, and 12 in pm [17].

Electronegativity



Similar electronegativities → difficult separation of each RE in RE ore.

Stability toward hydroxides (Ln(OH)_2^- , Ln(OH)_3^-) and oxo-hydroxides is different

Table 1. Selected properties of lanthanides, yttrium, and their trivalent ions.

Ln	χ_p	I_3	I_{1-3}	$E_{r,3-0}^0$	$E_{r,3-2}^0$	ΔH_h^0	$\log \beta_{11}^*$	pH	$r_i(6)$	$r_i(9)$	$r_i(12)$
La	1.10	1850	3455	-2.379	-3.1	-3326	-9.01	7.47	103	122	136
Ce	1.12	1949	3523	-2.336	-2.92(8)	-3380	-10.6	7.10	101	120	134
Pr	1.13	2086	3627	-2.353	-2.84(6)	-3421	-8.55	6.96	99	118	132
Nd	1.14	2130	3694	-2.323	-2.62(5)	-3454	-8.43	6.78	98	116	130
Pm	1.13	2150	3738	-2.30	-2.44(5)	-3482	n.a.	n.a.	97	114	128
Sm	1.17	2260	3871	-2.304	-1.50(1)	-3512	-8.34	6.65	96	113	127
Eu	1.2	2404	4035	-1.991	-0.34(1)	-3538	-8.31	6.61	95	112	125
Gd	1.20	1990	3750	-2.279	-2.85(7)	-3567	-8.35	6.58	94	111	124
Tb	1.1	2114	3790	-2.28	-2.83(7)	-3600	-8.16	6.47	92	110	123
Dy	1.22	2200	3898	-2.295	-2.56(5)	-3634	-8.10	6.24	91	108	122
Ho	1.23	2204	3924	-2.33	-2.79(6)	-3663	-8.04	6.20	90	107	121
Er	1.24	2194	3934	-2.331	-2.87(8)	-3692	-7.99	6.14	89	106	119
Tm	1.25	2285	4045	-2.319	-2.22(5)	-3717	-7.95	5.98	88	105	118
Yb	1.1	2415	4194	-2.19	-1.18(1)	-3740	-7.92	5.87	87	104	117
Lu	1.27	2033	3896	-2.28	n.a.	-3759	-7.90	5.74	86	103	116
Y	1.22	1980	3777	-2.372	n.a.	-3640	-8.36	n.a.	90	108	n.a.

Notes: Key: χ_p = Pauling's electronegativity; I_3 = third ionization energy (rounded to 1 kJ mol^{-1}) [8]; I_{1-3} = sum of the first three ionization energies (rounded to 1 kJ mol^{-1}) [8]; $E_{r,3-0}^0$ = standard redox potential $\text{Ln}^{+3}/\text{Ln}^0$ in V at pH 0 [12]; $E_{r,3-2}^0$ = redox potential $\text{Ln}^{+3}/\text{Ln}^{+2}$ in V [13], value for La is calculated; ΔH_h^0 = standard hydration enthalpies in kJ mol^{-1} calculated by semi-empirical methods (Born–Haber cycles) [14]; $*\beta_{11} = [(\text{LnOH})^{2+}][\text{H}^+]/[\text{Ln}^{3+}]$, ionic strength = 0.3 M [15]; pH = pH at which hydroxide precipitation starts in $\text{Ln}(\text{NO}_3)_3$ solutions 0.1 M in water [16]; $r_i(n)$ = ionic radii for coordination numbers $n = 6, 9$, and 12 in pm [17].

Coordination numbers

Main CN are 8 and 9

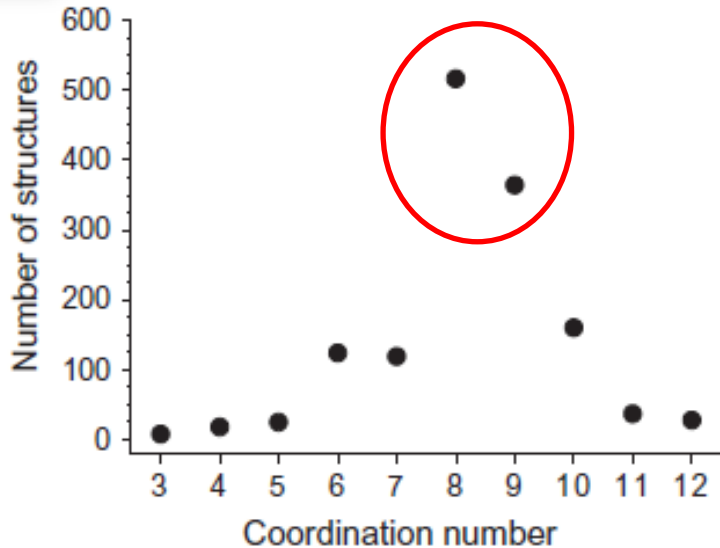
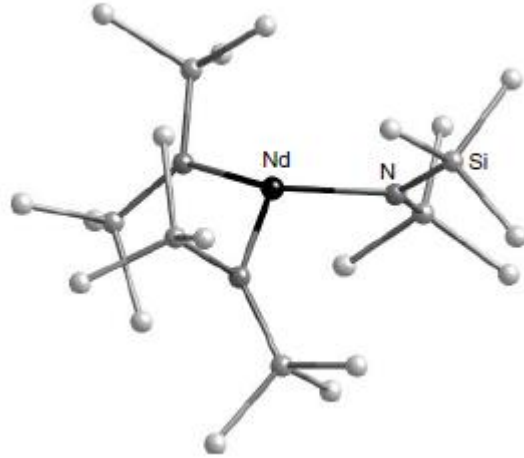
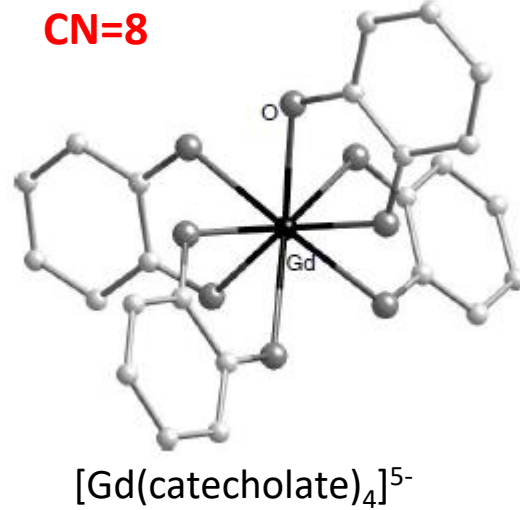


Figure 1. Distribution of coordination numbers among rare earth complexes from 1389 crystal structures published between 1935 and 1995 [91]

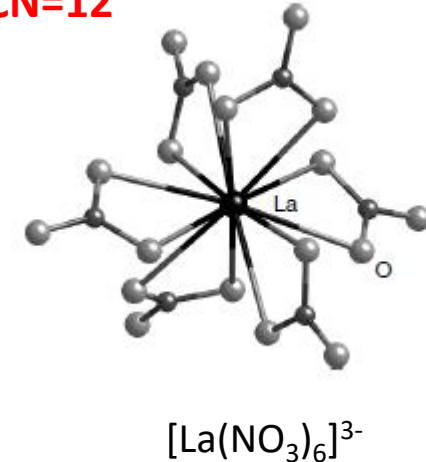
CN=3



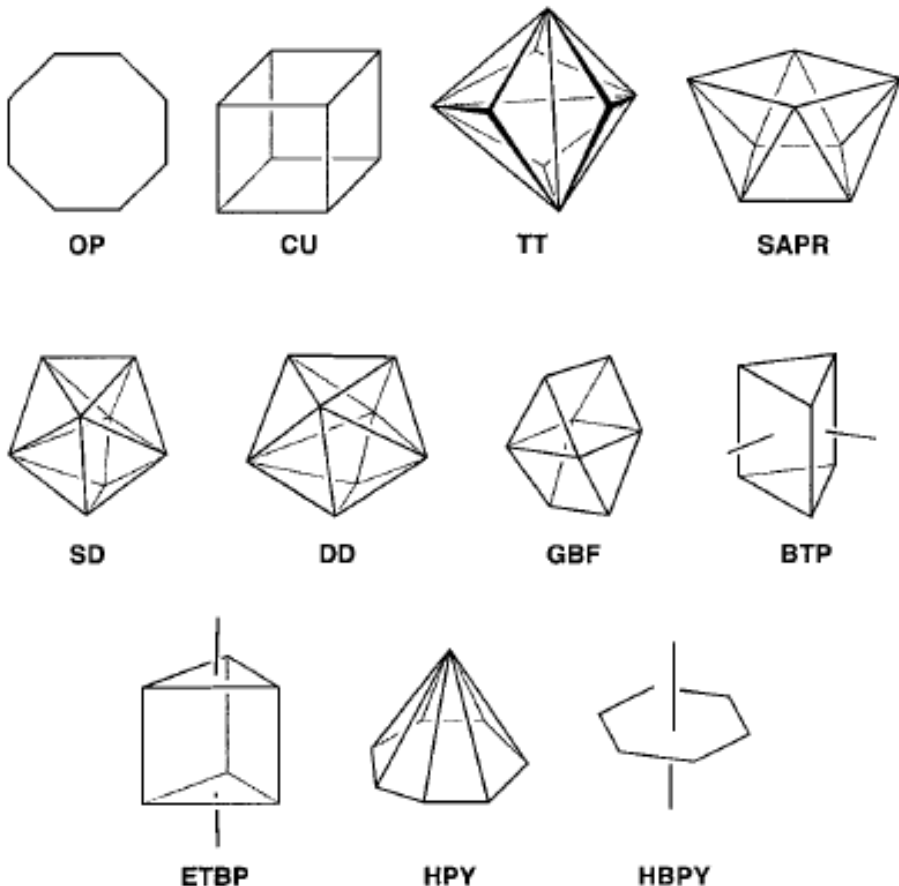
CN=8



CN=12



Coordination polyhedra for CN=8

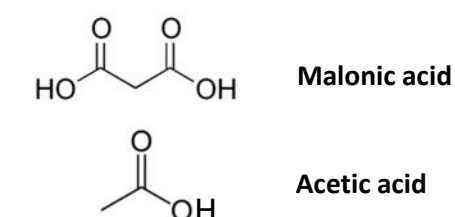
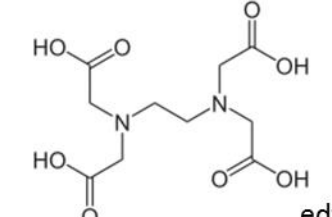
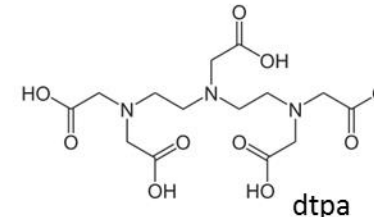
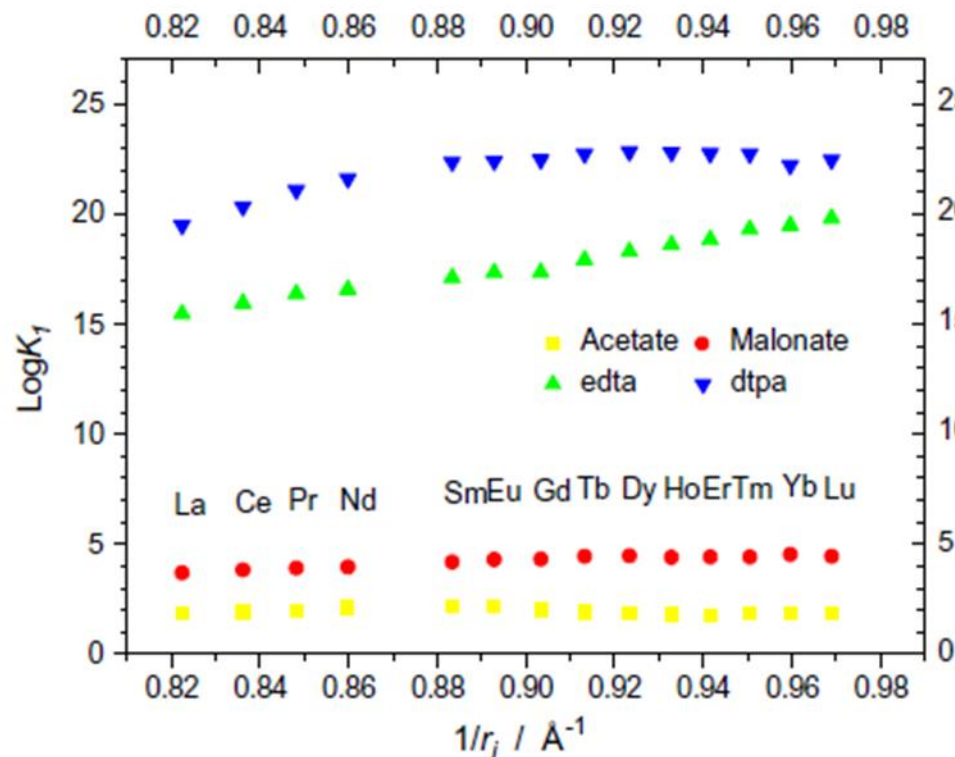
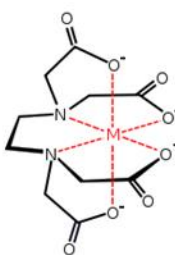


Ideal shape	Abbreviation	Symmetry
octagon	OP	D_{8h}
cube	CU	O_h
triakis-tetrahedron	TT	T_d
square antiprism	SAPR	D_{4d}
snub disphenoid	J-SD	T_d
triangular dodecahedron	DD	D_{2d}
gyrobifastigium	J-GBF	D_{2d}
biaugmented trigonal prism	J-BTP	C_{2v}
	s-BTP	C_{2v}
elongated trigonal bipyramid	J-ETBP	D_{3h}
	s-ETBP	D_{3h}
heptagonal pyramid	HPY	D_{7h}
hexagonal bipyramid	HBPY	D_{6h}

See also SHAPE program from Univ Barcelona

S. Alvarez, P. Alemany, M. Llunel

Stability



Stability constants for the formation of 1:1 complexes in water at 298 K vs. reciprocal ionic radii for coordination number 9.

- Polydentate ligands vs monodentate ligands:
dtpa complexes are 20 orders of magnitude more stable than acetates
→ Entropic stabilization

15-crown-5 $d = 1.7\text{--}2.2 \text{ \AA}$
18-crown-6 $d = 2.6\text{--}3.2 \text{ \AA}$

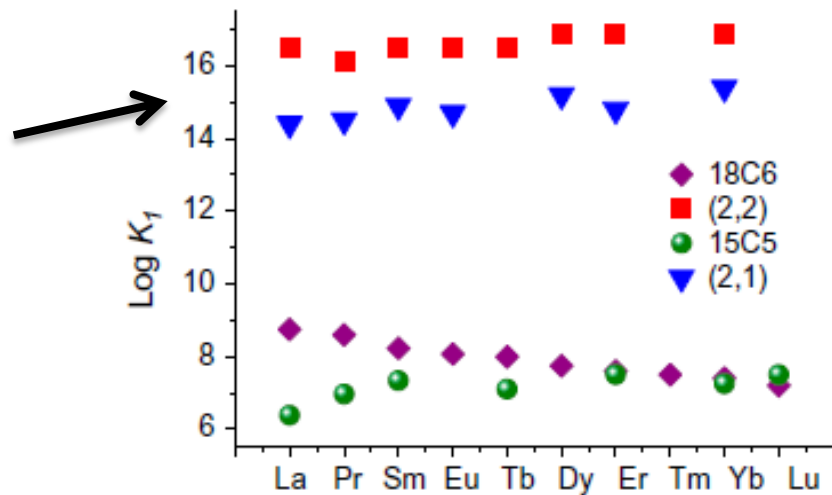
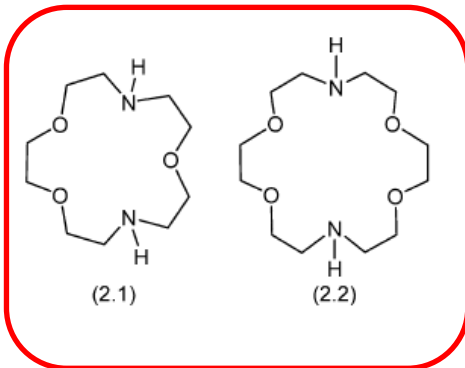
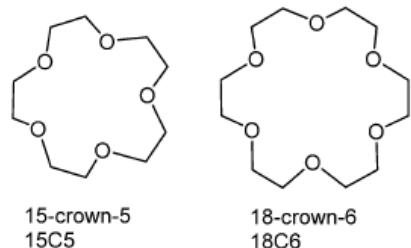
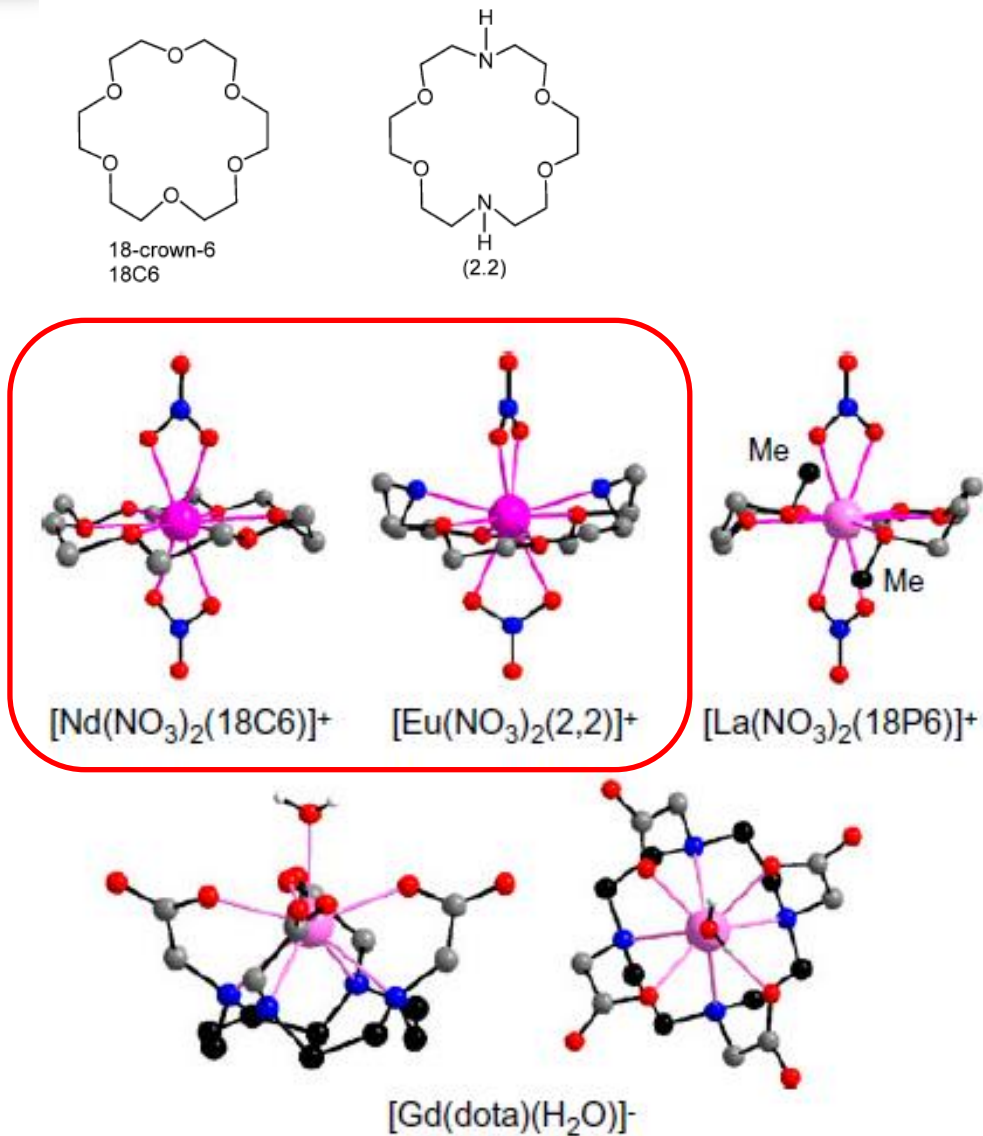
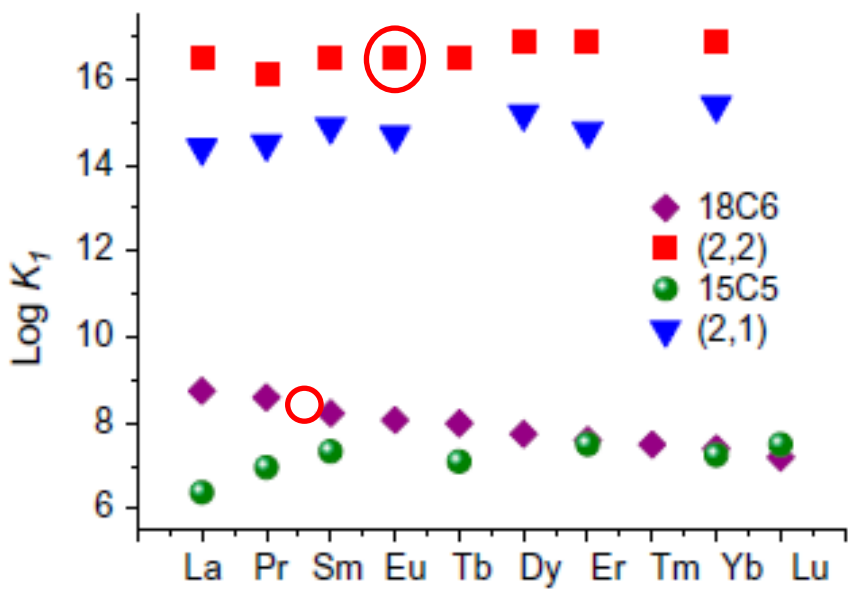


Figure 4. Stability constants of 1:1 coronates in propylene carbonate at 298 K and $\mu = 0.1 \text{ M Et}_4\text{NClO}_4$; drawn from data reported in Ref. [41].

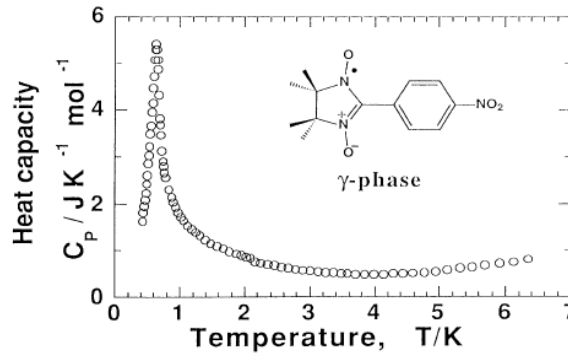
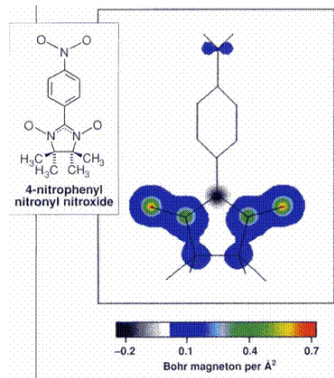
- Variation in cavity dimension (1.7 to 3.2 Å) do not change stability that much (no « lock-and-key » discrimination as with alkaline or 3d ions)
- Variation in the coordinating atoms affords tremendous changes in stability:
→ Enthalpic stabilization

Macrocyclic Lanthanide Chemistry



From Magnetochemistry to Molecular Magnetism : The role of lanthanide ions

The heritage



$\text{NIT-PhNO}_2 \rightarrow \text{First organic magnet } T_c = 0.6 \text{ K}$
Takahashi, M. et al. *Phys. Rev. Lett.* 1991, 67, 746-748

On the Theory of Spin-Lattice Relaxation in Paramagnetic Salts

By R. ORBACH

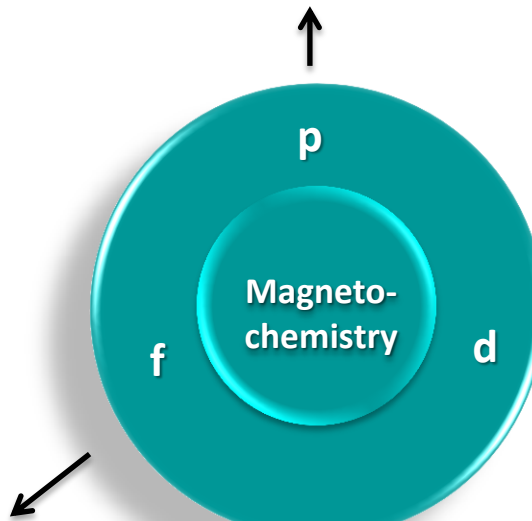
Clarendon Laboratory, Oxford

MS. received 4th November 1960

Trivalent rare-earth ions

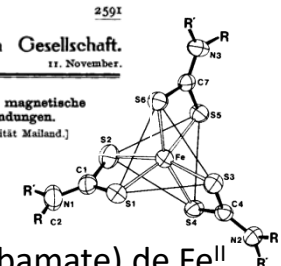
→ Magnetic relaxation theory

Orbach, R. *Proc. R. Soc. London, Ser. A* 1961, 264, 458-484.



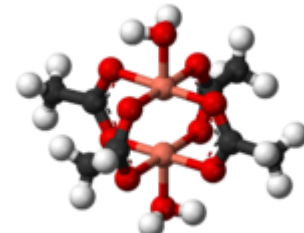
1931. B
Berichte der Deutschen Chemischen Gesellschaft.
1931, Nr. 10. — Abteilung B (Abhandlungen) — 11. November.

421. L. Cambi und L. Szegő: Über die magnetische Suszeptibilität der komplexen Verbindungen.
[Aus d. Istituto di Chimica Industriale d. Universität Mailand.]
(Eingegangen am 18. Juli 1931.)



$\text{Fe}^{II}\text{Tris}(\text{dithiocarbamate})\text{ de } \text{Fe}^{III}$
→ Spin Cross Over

Cambi, L. et al., *Ber. Dtsch. Chem. Ges.* 1931, 64, 2591
Stahl K. et al., *Acta Chem. Scand.* 1983, A37, 729.

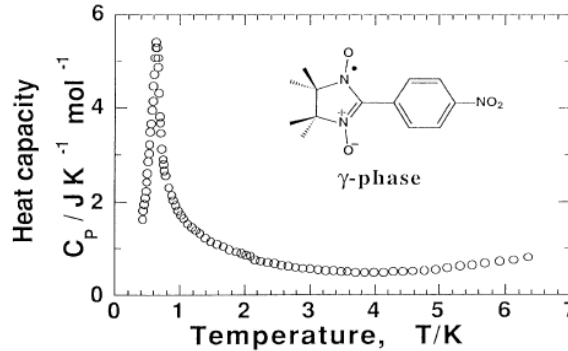
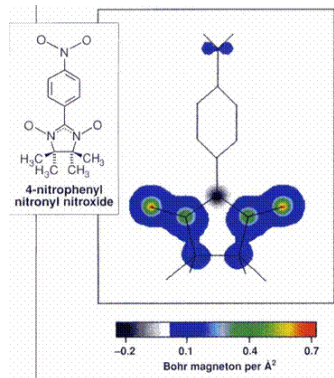


Copper acetate → Magnetic exchange

Guha, B.C. *Proc. Roy. Soc. (London)* 1951, 206, 353.

Bleaney, B. et al., *Proc. Roy. Soc. (London)* 1952, 214, 451 **26**

The heritage



$\text{NIT-PhNO}_2 \rightarrow \text{First organic magnet } T_c = 0.6 \text{ K}$
Takahashi, M. et al. *Phys. Rev. Lett.* 1991, 67, 746-748

On the Theory of Spin-Lattice Relaxation in Paramagnetic Salts

By R. ORBACH

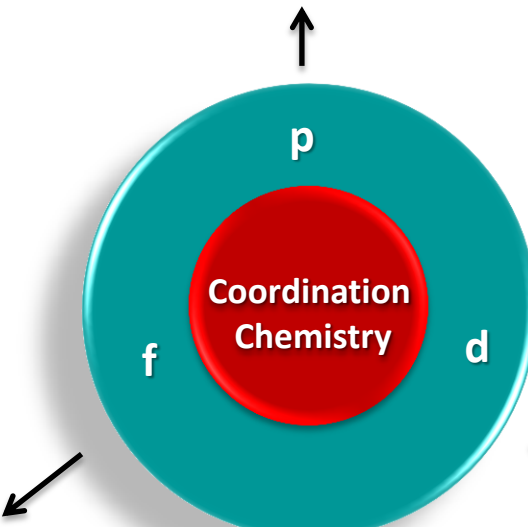
Clarendon Laboratory, Oxford

MS. received 4th November 1960

Trivalent rare-earth ions

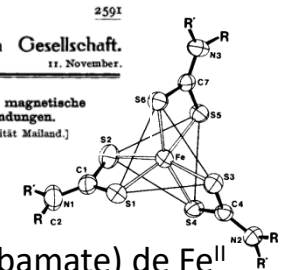
→ Magnetic relaxation theory

Orbach, R. *Proc. R. Soc. London, Ser. A* 1961, 264, 458-484.

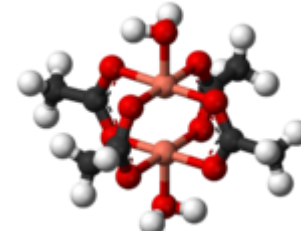


1931. B
Berichte der Deutschen Chemischen Gesellschaft.
1931, Nr. 10. — Abteilung B (Abhandlungen) — 11. November.

421. L. Cambi und L. Szegő: Über die magnetische Suszeptibilität der komplexen Verbindungen.
[Aus d. Istituto di Chimica Industriale d. Universität Mailand.]
(Eingegangen am 18. Juli 1931.)



Fe^{II} Tris(dithiocarbamate) de Fe^{II} → Spin Cross Over
Cambi, L. et al., *Ber. Dtsch. Chem. Ges.* 1931, 64, 2591
Stahl K. et al., *Acta Chem. Scand.* 1983, A37, 729.

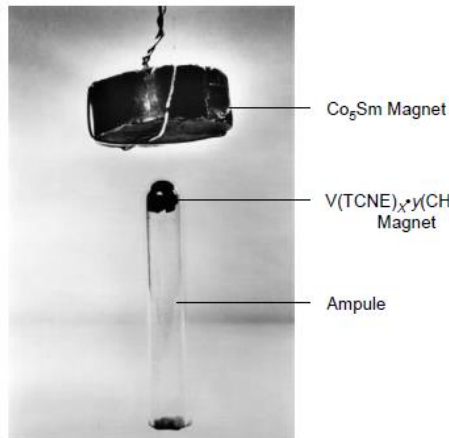
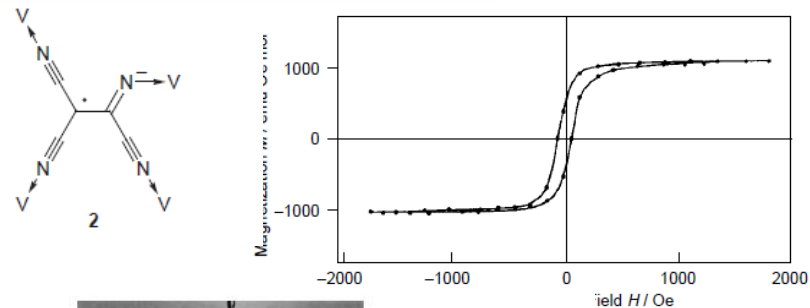


Copper acetate → Magnetic exchange

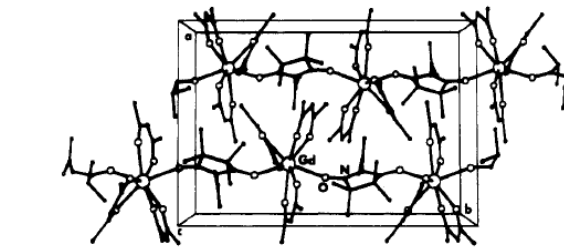
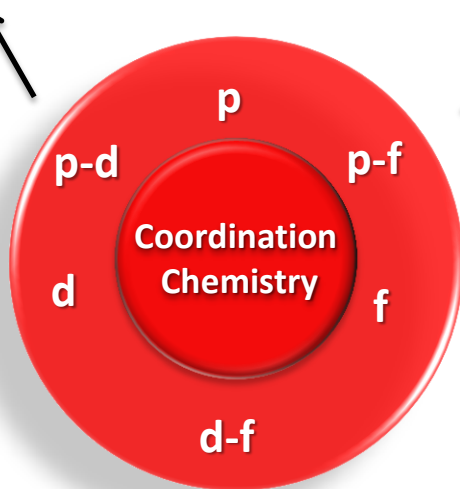
Guha, B.C. *Proc. Roy. Soc. (London)* 1951, 206, 353.

Bleaney, B. et al., *Proc. Roy. Soc. (London)* 1952, 214, 451 27

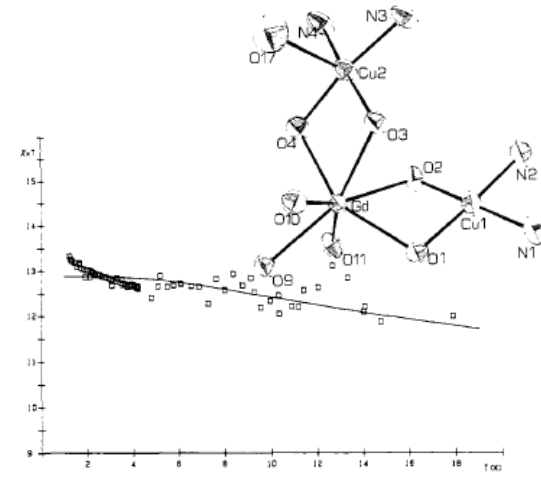
The heritage



$\text{V}(\text{TCNE})_2 \rightarrow$ High T_c permanent magnets
S. Miller, J. et al., *Chem. Commun.* 1998, 1319-1325

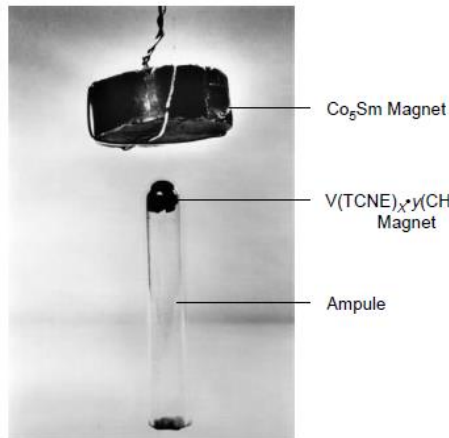
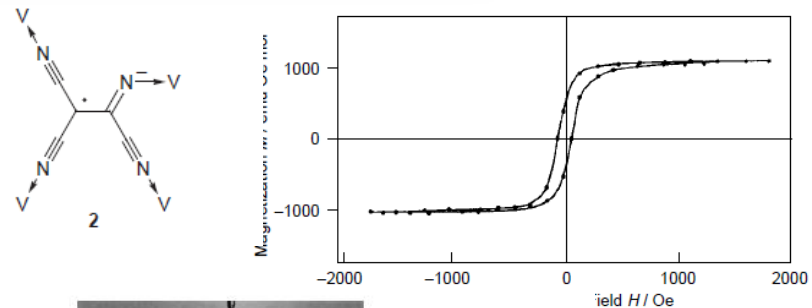


$\text{GdNITiPr} \rightarrow$ Next-nearest neighbor interactions
Benelli, C. et al. *Inorg. Chem.* 1990, 29, 4223

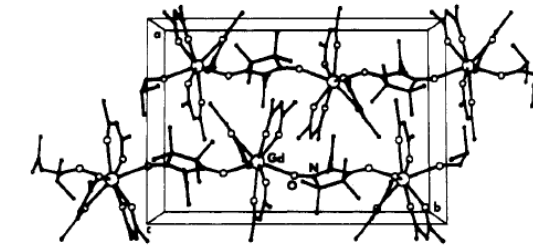
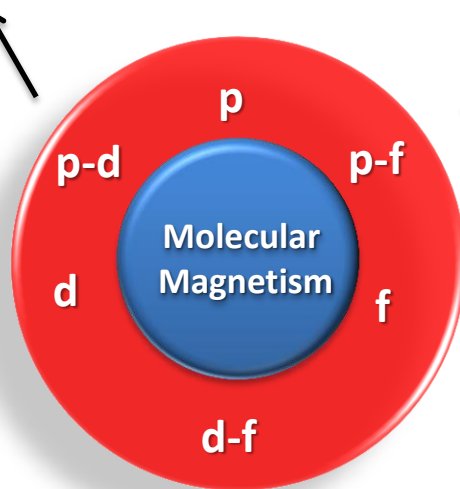


$(\text{CuSalen})_2\text{Gd}(\text{H}_2\text{O})_3]^{3+} \rightarrow$ 3d-4f ferromagnetic coupling
Bencini, A. et al., *J. Am. Chem. Soc.* 1985, 107, 8128

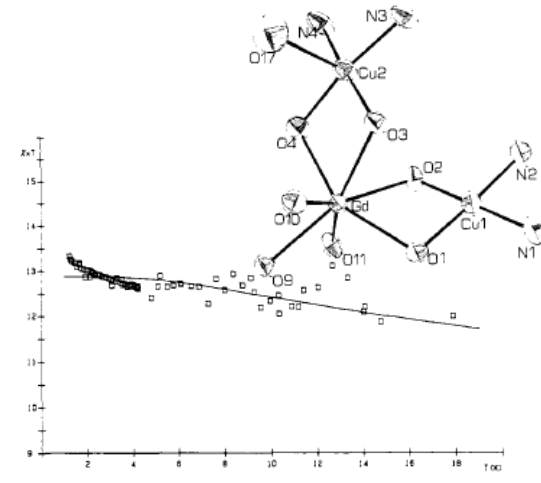
The heritage



$\text{V}(\text{TCNE})_2 \rightarrow$ High T_c permanent magnets
S. Miller, J. et al., *Chem. Commun.* 1998, 1319-1325

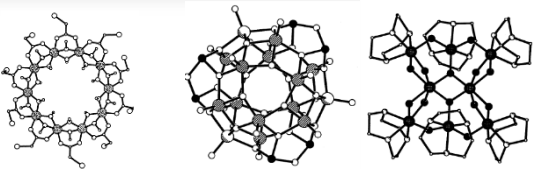


$\text{GdNITiPr} \rightarrow$ Next-nearest neighbor interactions
Benelli, C. et al. *Inorg. Chem.* 1990, 29, 4223



$(\text{CuSalen})_2\text{Gd}(\text{H}_2\text{O})_3]^{3+} \rightarrow$ 3d-4f ferromagnetic coupling
Bencini, A. et al., *J. Am. Chem. Soc.* 1985, 107, 8128

Molecular Magnetism

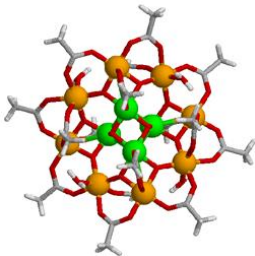


■ ARTICLE

Large Clusters of Metal Ions: The Transition from Molecular to Bulk Magnets

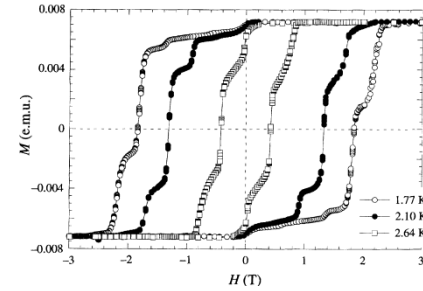
→ **Toward Single-Molecule Magnet (SMM)**

Gatteschi, D. et al., *Science* 1994, 265, 1054



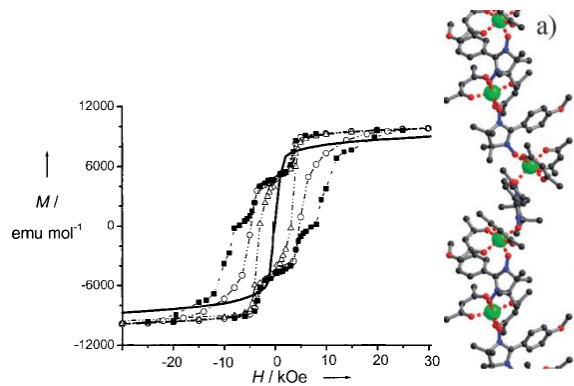
→ **Quantum effects on SMM**

Thomas, L. et al., *Nature* 1996, 383, 145



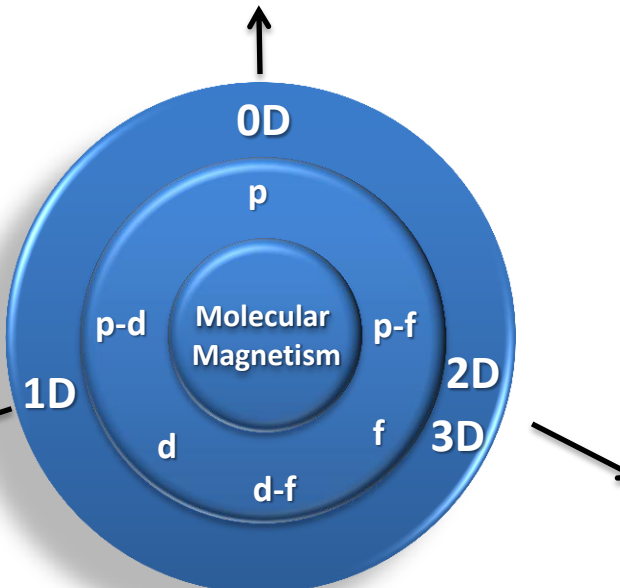
$\text{Mn}_{12} \rightarrow$ **Molecular magnetic bistability**

Sessoli, R. et al., *Nature* 1993, 365, 141



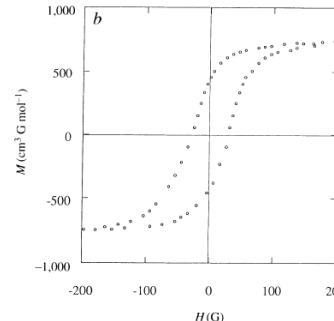
$\text{CoPhOMe} \rightarrow$ **Single-Chain Magnets (SCM)**

Caneschi et al, *Angew. Chem.*, 2001, 40, 1760



LETTERS TO NATURE

A room-temperature organometallic magnet based on Prussian blue

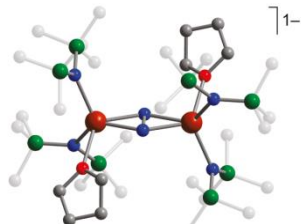
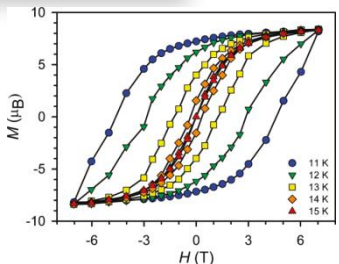


Prussian Blue

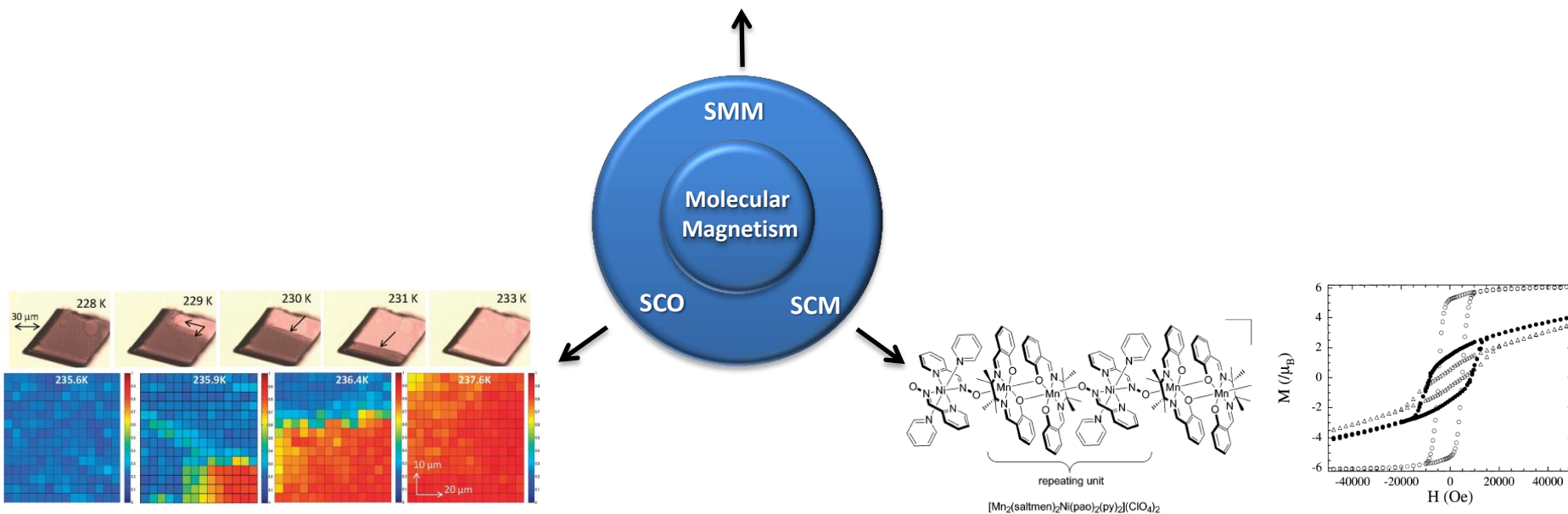
→ **high T_c permanent magnets**

Ferlay, S. et al., *Nature* 1995, 378, 701-703.

Molecular Magnetism



Rinehart, J. D. et al., *J. Am. Chem. Soc.* 2011, 133, 14236



Bedoui, S., *Chem. Phys. Lett.* 2010, 499, 94.

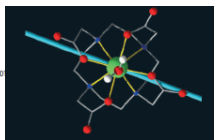
Clérac, R.; et al., *J. Am. Chem. Soc.* 2002, 124, 12837

Molecular Magnetism

Angewandte
Chemie
Communications

Single-Molecule Magnets

Magnetic Anisotropy in a Dysprosium/DOTA Single-Molecule Magnet: Beyond Simple Magneto-Structural Correlations^{10,11}



DOI: 10.1002/anie.2010

Magnetic activity of MRI agents

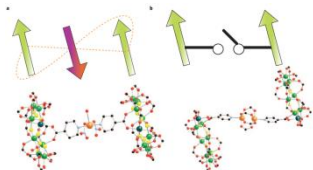
Cucinotta et al., *Angew. Chem. Int. Ed.* 2012, 51, 1606

nature
nanotechnology

ARTICLES

CORRECTED ONLINE: 17 FEBRUARY 2009
PUBLISHED ONLINE: 1 FEBRUARY 2009 DOI: 10.1038/NANO.2008.404

Engineering the coupling between molecular spin qubits by coordination chemistry

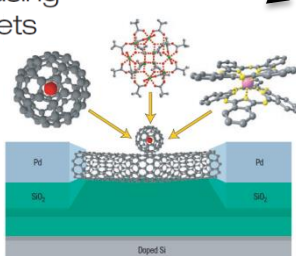


Quantum computing

Timco, G. A. et al., *Nat Nano* 2009, 4, 173

PROGRESS ARTICLE

Molecular spintronics using single-molecule magnets



Spintronics

Bogani, L., et al., *Nat. Mater.* 2008, 7, 179-186.

LETTERS

PUBLISHED ONLINE: 1 FEBRUARY 2009 DOI: 10.1038/NMAT2374

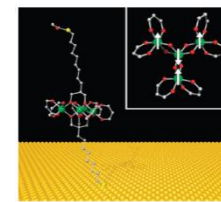
nature
materials

Magnetic memory of a single-molecule quantum magnet wired to a gold surface

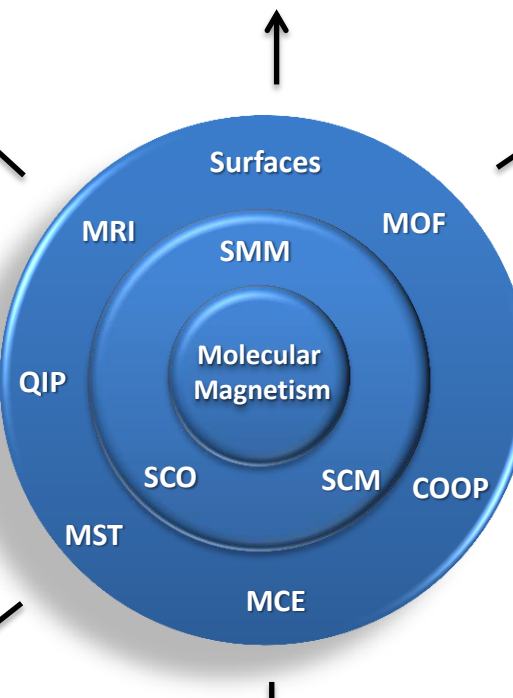
SMM on surfaces

Mannini, M., et al., *Nat. Mater.* 2009, 8, 194

Mannini, M., et al., *Nature* 2010, 468, 417



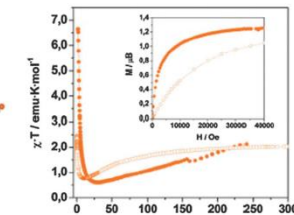
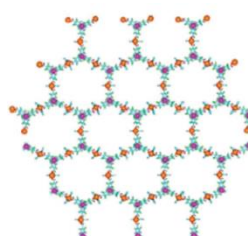
Institut des
Chimiques
de Rennes



LETTERS

PUBLISHED ONLINE: 1 FEBRUARY 2009 DOI: 10.1038/NMAT2374

A nanoporous molecular magnet with reversible solvent-induced mechanical and magnetic properties

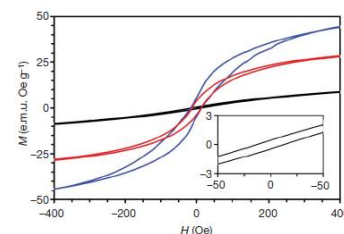


Nanoporous magnets / host-guest systems

Maspoch, D., et al., *Nat. Mater.* 2003, 2, 190

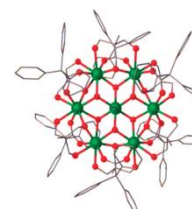
LETTERS

High-temperature metal-organic magnets



Tc > 400 K (Ni2TCNE, TCNQ, BenzoQ)

Jain, R. et al., *Nature* 2007, 445, 291



ARTICLE

Received 18 Jun 2014 | Accepted 19 Sep 2014 | Published 22 Oct 2014

DOI: 10.1038/NCOMMS1221

OPEN

Quantum signatures of a molecular nanomagnet in direct magnetocaloric measurements

Sub-Kelvin nano-coolers

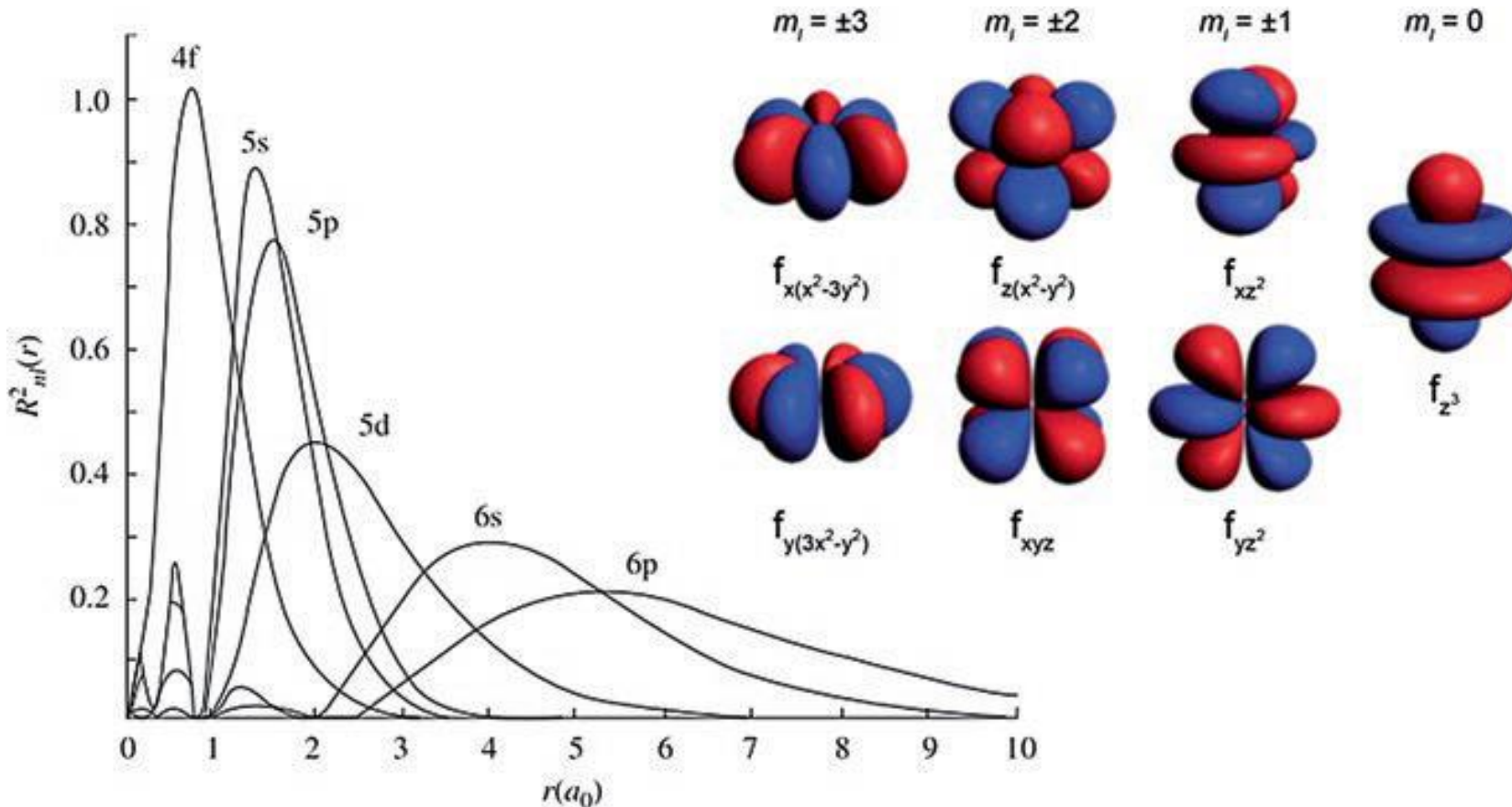
Sharples, J. W. et al., *Nat Commun* 2014, 5

Benelli, C.; Gatteschi, D.

Introduction to Molecular Magnetism: From Transition Metals to Lanthanides, 2015

Basics of Magnetism of Trivalent Lanthanide ions

4f free ion electronic structure



- Radial dependence of 4f orbitals: **shielding** by 5s, 5p
- Angular dependence of 4f orbitals: changes with m_L states → strong **Spin-Orbit coupling**
- **Russel-Saunders coupling scheme:** interelectronic repulsion > SO coupling

4f free ion electronic structure

- Spins of all electrons are coupled:
- Angular momenta are coupled:
- $L = 0, 1, 2, 3, \dots$ provides S, P, D, F,...
- The total momentum J is:

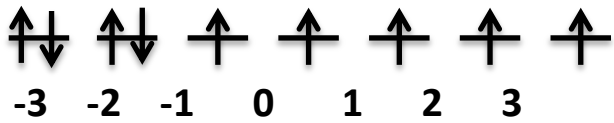
$$(|L - S| \leq J \leq |L + S|)$$

- A multiplet noted $^{2S+1} L_J$ is obtained whose energy is:

$$E(^{2S+1}L_J) = (\lambda/2)[J(J+1) - L(L+1) - S(S+1)]$$

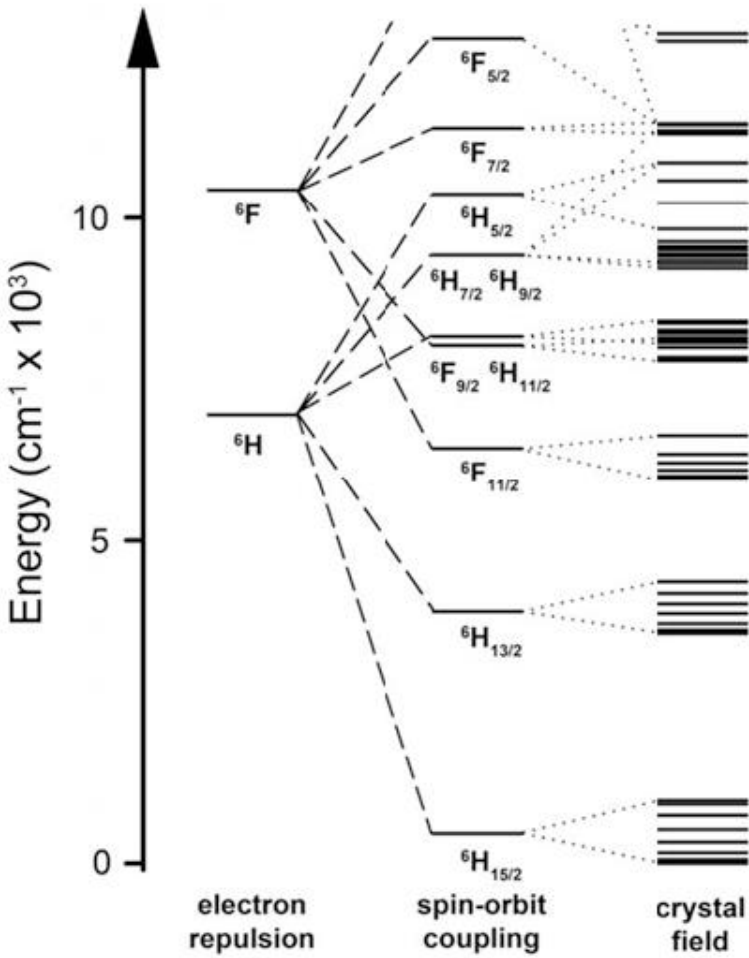
where λ is the spin-orbit coupling constant of the ion

- Ex: Dy^{III}, 4f⁹



$S=5/2;$
 $L=5; \rightarrow H$
 $J=S+L=15/2$

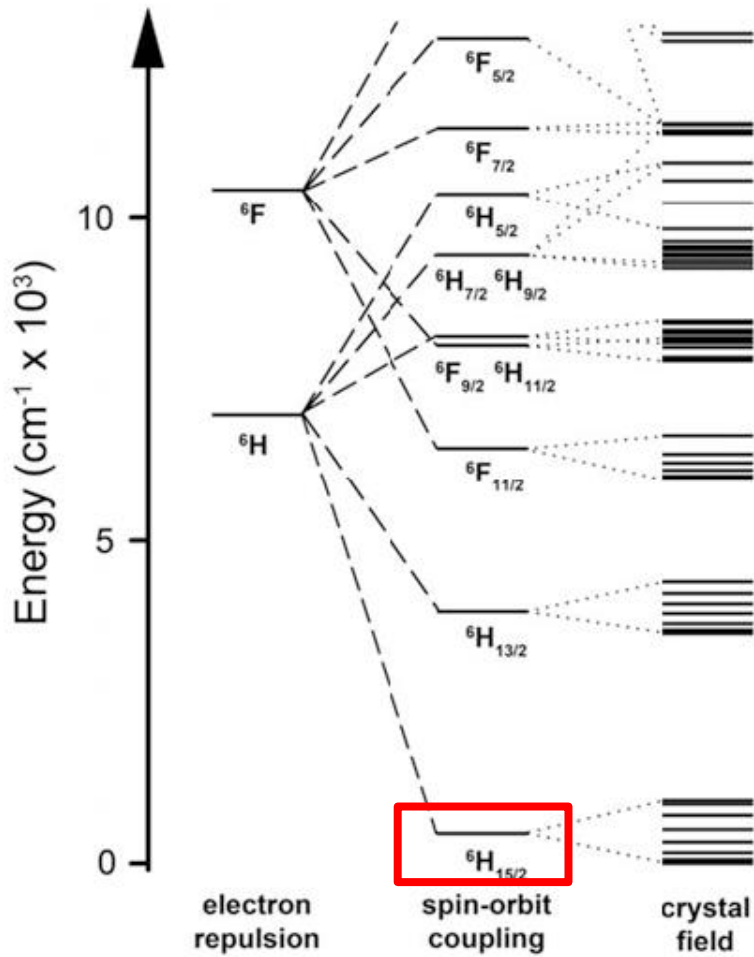
$$^{2S+1}L_J = ^6H_{15/2}$$



4f free ion electronic structure

- SO coupling split the terms with same L and S and different J → the lowest lying J multiplet is the “ground state”
- Except for Eu^{III} and Sm^{III}, S.O. is large so magnetic properties of the ion → magnetic properties of the ground state

Ln ³⁺	4f ⁿ	Ground state	g_J	χT (emu mol ⁻¹ K)	First excited state	Energy separation (cm ⁻¹)
Ce	f^1	$^2F_{5/2}$	6/7	0.8	$^2F_{7/2}$	2200
Pr	f^2	3H_4	4/5	1.6	3H_5	2100
Nd	f^3	$^4I_{9/2}$	8/11	1.64	$^4I_{11/2}$	1900
Pm	f^4	5I_4	3/5	0.9	5I_5	1600
Sm	f^5	$^6H_{5/2}$	2/7	0.09	$^6H_{7/2}$	1000
Eu	f^6	7F_0	0		7F_1	300
Gd	f^7	$^8S_{7/2}$	2	7.88	$^6P_{7/2}$	30,000
Tb	f^8	7F_6	3/2	11.82	7F_5	2000
Dy	f^9	$^6H_{15/2}$	4/3	14.17	$^6H_{13/2}$	–
Ho	f^{10}	5I_8	5/4	14.07	5I_7	–
Er	f^{11}	$^4I_{15/2}$	6/5	11.48	$^4I_{13/2}$	6500
Tm	f^{12}	3H_6	7/6	7.15	3H_5	–
Yb	f^{13}	$^2F_{7/2}$	8/7	2.57	$^2F_{5/2}$	10,000



4f free ion magnetism

- By applying a magnetic field, the degeneracy of the $2J+1$ levels in each $^{2S+1}L_J$ is removed
→ it provides a series of M_J levels : $-J \leq M_J \leq +J$

- The corresponding magnetic moments are:

$$\mu_J = \mu_B g_J J$$

- With the Landé factor that is :

$$g_J = \frac{3}{2} + \frac{S(S+1) - L(L+1)}{2J(J+1)}$$

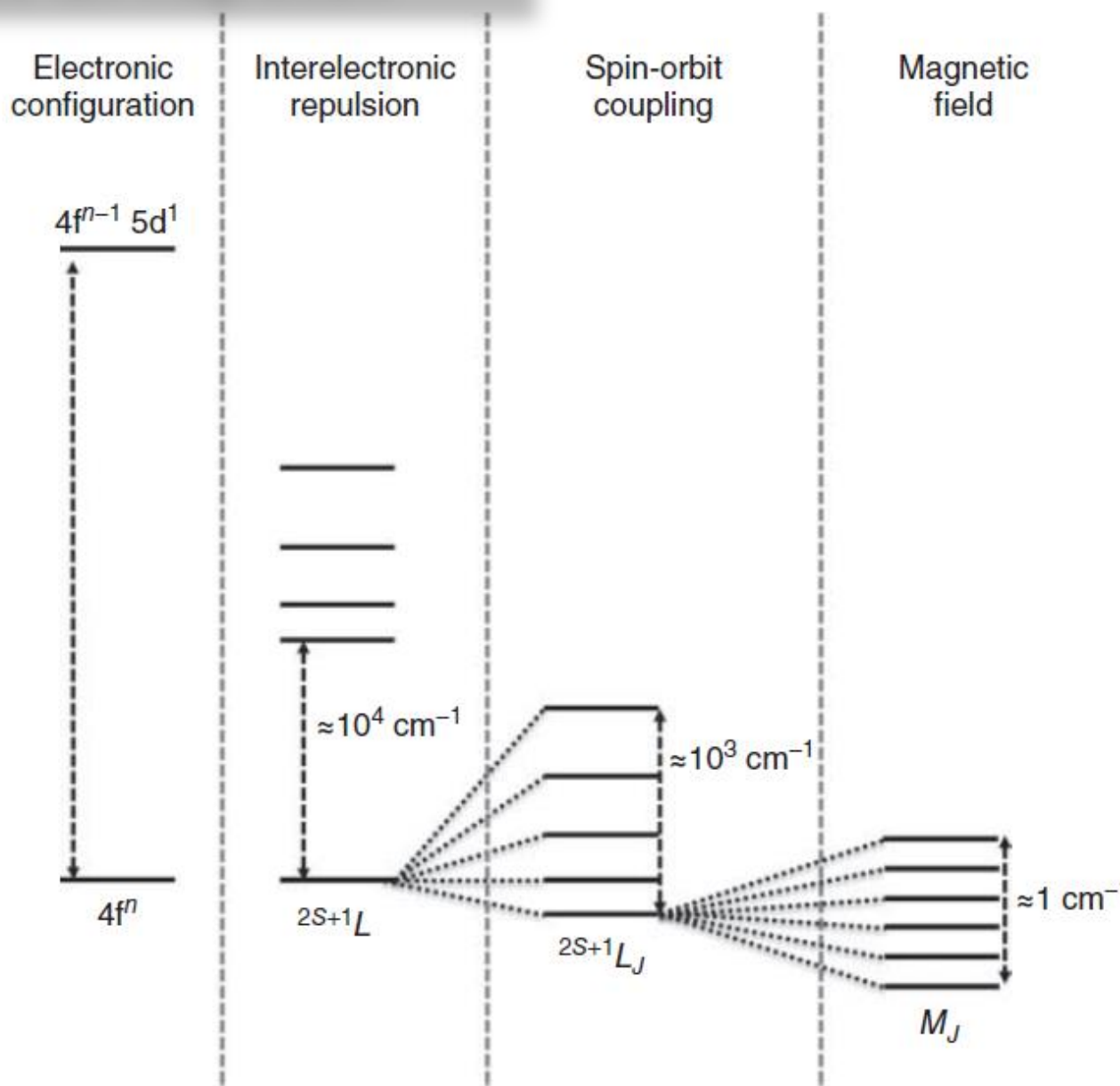
- And the magnetic susceptibility that follows the Curie law: (except Eu³⁺ and Sm³⁺)

$$\chi^M = \frac{N_A g_J^2 \mu_B^2}{3kT} J(J+1)$$

with $N_A \mu_B^2 / 3k_B T = 1/8$

- Ex: for Dy³⁺ ($S=5/2$, $L=5$, $J=15/2$), the $^6H_{15/2}$ multiplet is split in $2J+1$ M_J states = 16
 $g_J = 4/3$ and $\chi_M T_{(300K)} = 14.17 \text{ emu.mol}^{-1}$

4f free ion magnetism

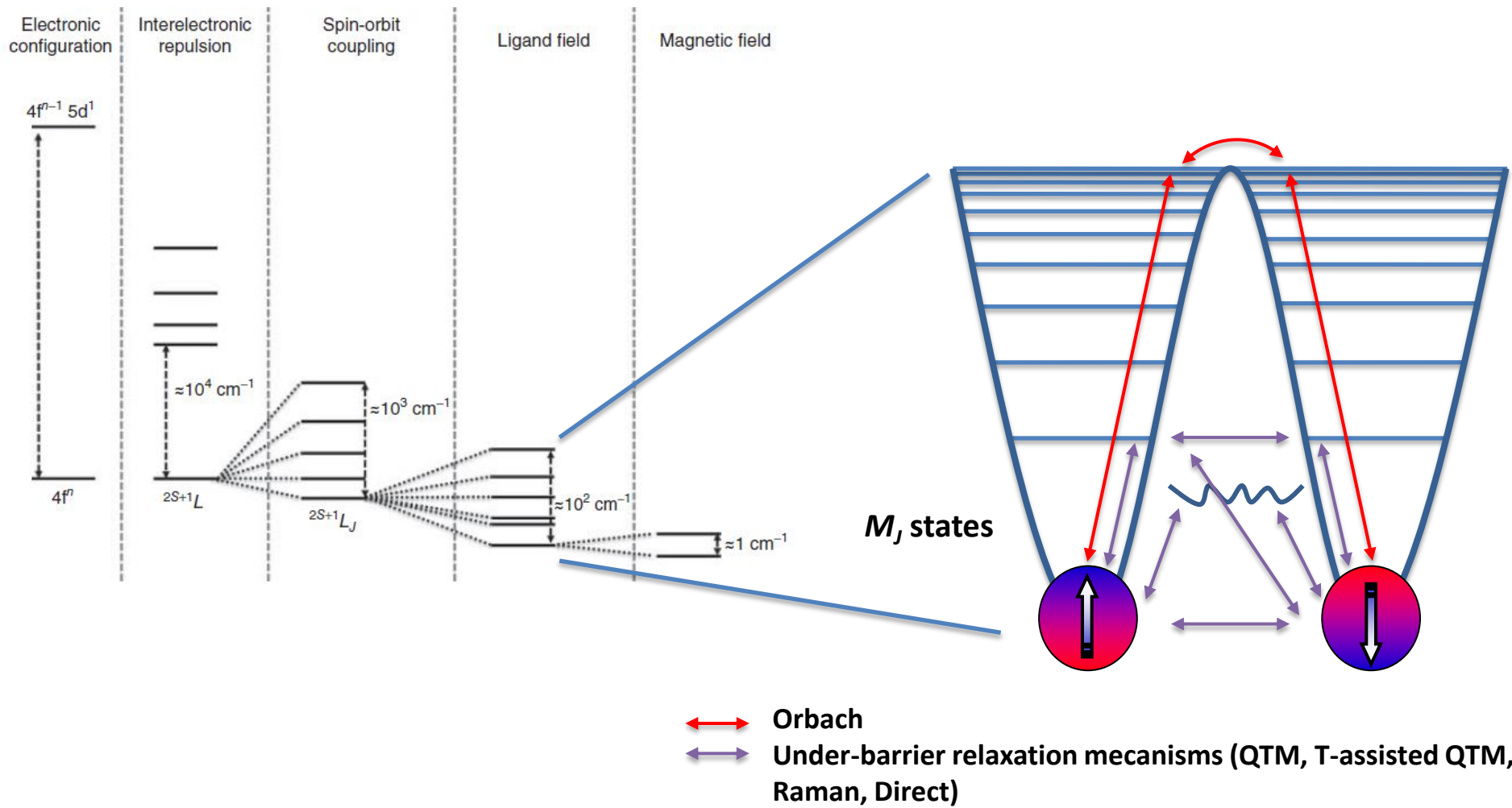


4f anisotropy in a crystal field

- Spin is isotropic but orbital component reflects the symmetry of the system and can be anisotropic
- Magnetic anisotropy → depends of Spin Orbit coupling (SO or LS coupling) and Crystal field (CF)
- For 3d ions: orbital moments are quenched because $LS \ll CF$
- For 4f ions : orbital moments are unquenched because $LS \gg CF$
 → the total angular momentum J is a good quantum number

Group	Shell	Electronic repulsion	LS coupling	CF splitting
Fe	$3d$	10^5	10	10^3
Pd, Pt	$4d, 5d$	10^4	10^2	10^4
RE	$4f$	10^5	10^3	10^2

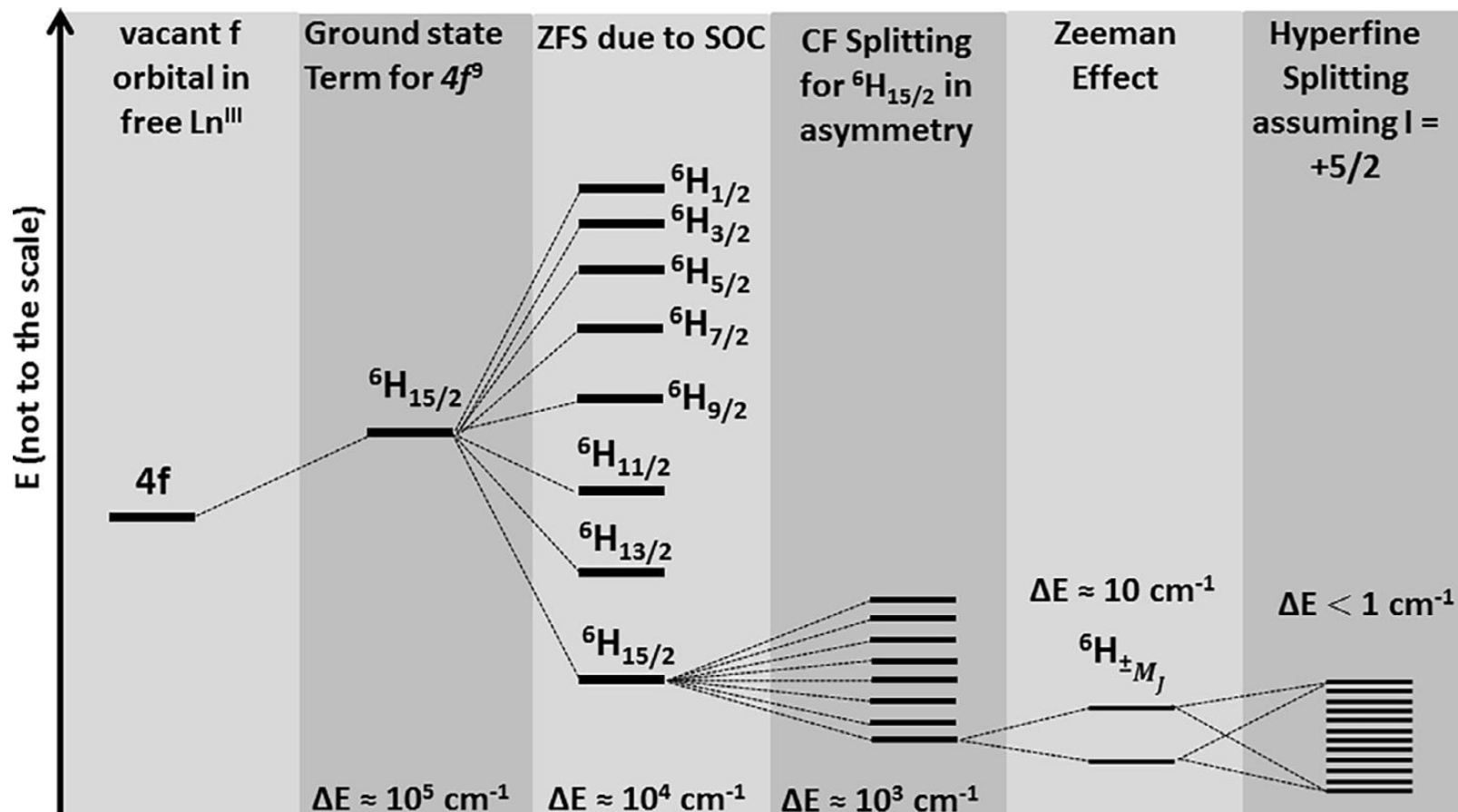
4f anisotropy in a crystal field



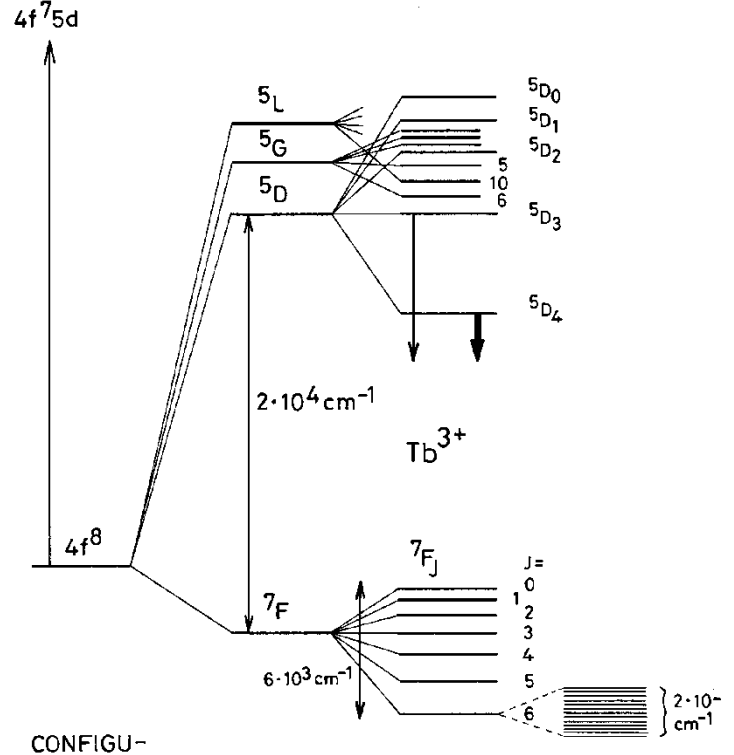
\longleftrightarrow Orbach
 \longleftrightarrow Under-barrier relaxation mechanisms (QTM, T-assisted QTM,
 Raman, Direct)

4f anisotropy in a crystal field

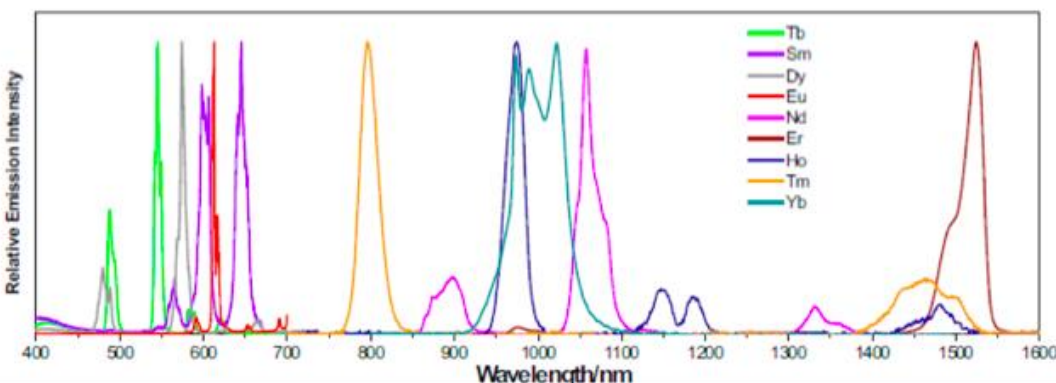
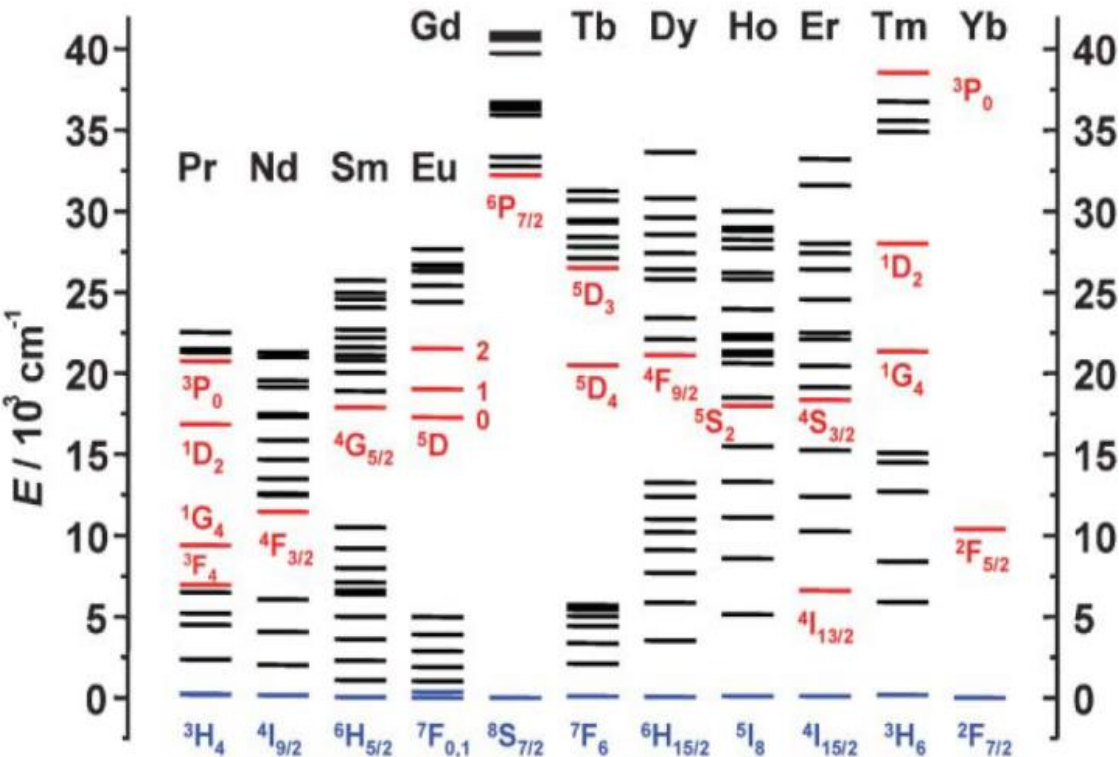
- For $^{161}\text{Dy}^{\text{III}}$:



Basics of Lanthanides luminescence

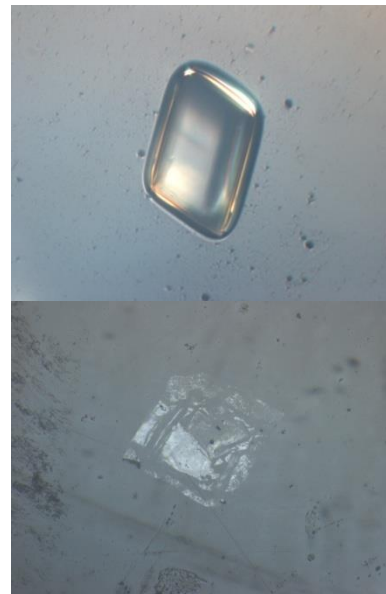
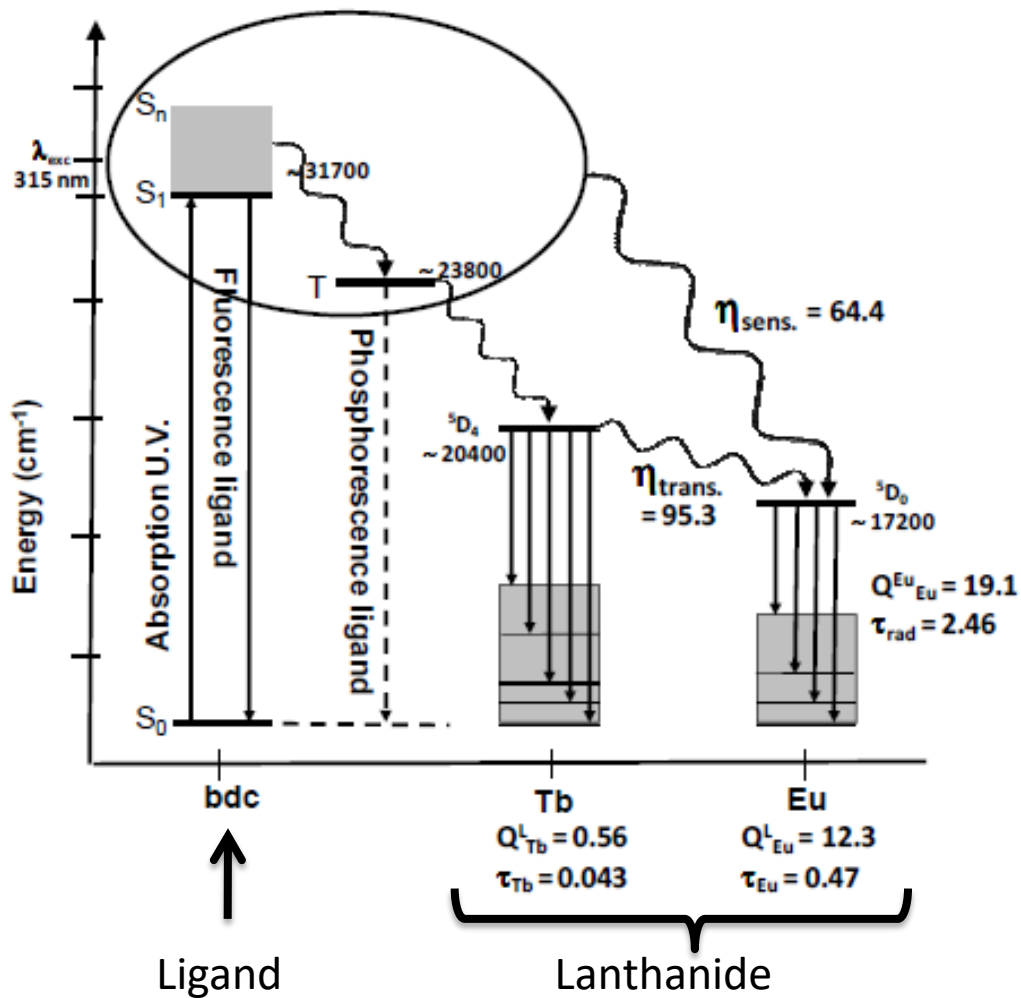


From J.-C. Bünzli



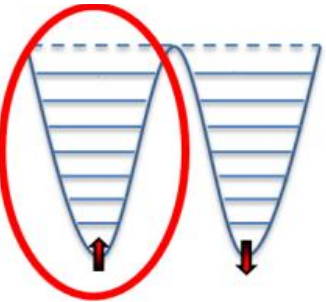
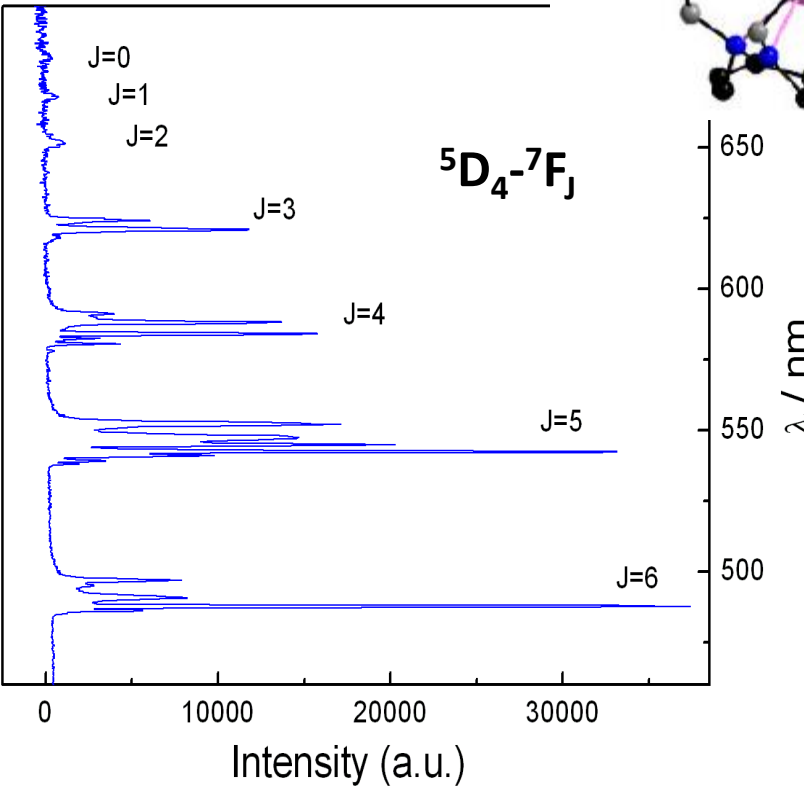
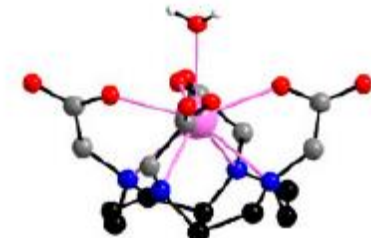
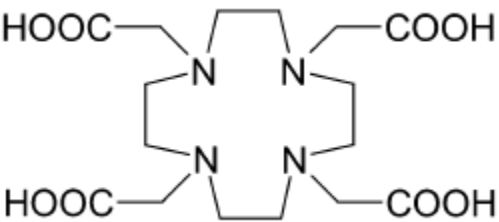
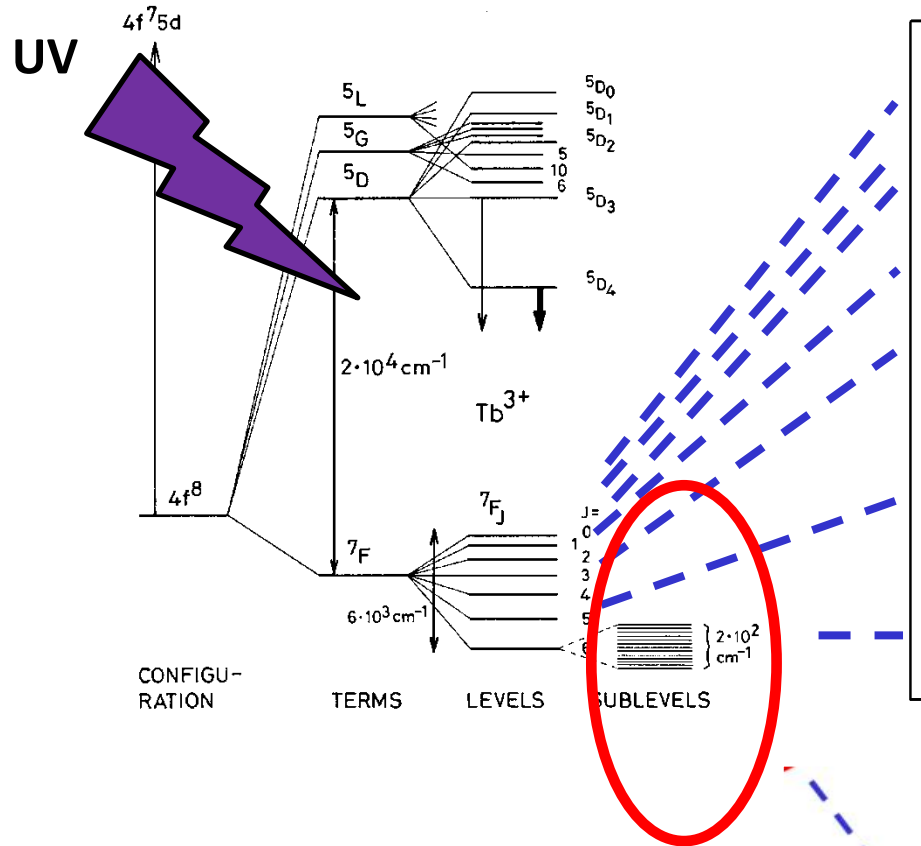
Basics of Lanthanides luminescence

- $f-f$ transitions are Laporte forbidden so **emissions are weak**
- Ln^{III} emissive level can be fed using an organic ligand as energy absorber (UV). If the triplet(s) state(s) of the ligand is (are) at an appropriate energy → transfer toward the Ln^{III} → **antenna effect**
- Antenna effect enhance Ln^{III} emissions by several orders of magnitude



Lanthanides Spectroscopy

TbDOTA



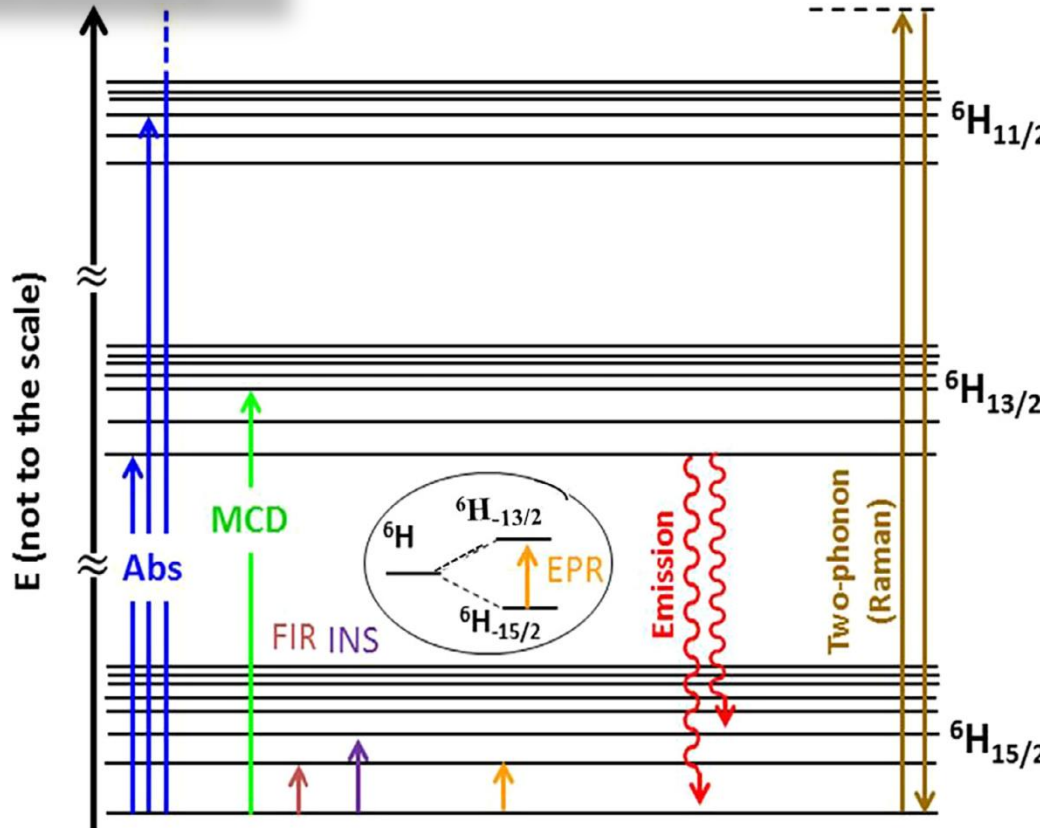
Emission spectroscopy → access to Tb^{III} 's M_J

G. Cucinnotta et al, *Angew. Chem. Int. Ed.* 2012, 51, 1606-1610

M.-E Boulon et al, *Angew. Chem. Int. Ed.* 2013, 52, 350-354

J. Long et al, *Coord. Chem. Rev.* 2018, 363, 57

Lanthanides Spectroscopy



Landscape of Dy(III) ion portraying the energy levels associated in:

- Optical absorption (**Abs**)
- Magnetic circular dichroism (**MCD**)
- Far infra-red (**FIR**)
- Inelastic neutron scattering (**INS**)
- Electron paramagnetic resonance (**EPR**)
- **Emission**
- and **Raman** spectroscopy

Single ion anisotropy

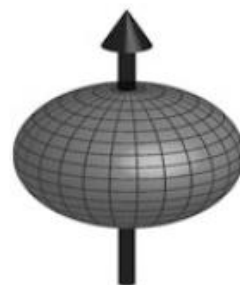
- Single ion anisotropy of lanthanide ions is linked to the charge distribution on the lowest J states whose shape is based on the quadrupole moment:

$$Q_2 = \alpha_J \left\langle r^2 \right\rangle_{4f} (2J^2 - J)$$

r: 4f shell radius
 α_J : second order Stevens coefficient

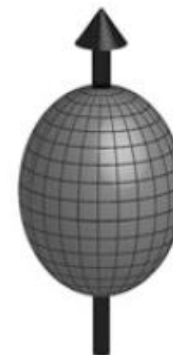
Ln^{3+}	Ground state	α_J	β_J	γ_J	Q_2
Ce	$^2\text{F}_{5/2}$	$\frac{-2}{5 \cdot 7}$	$\frac{2}{3^2 \cdot 5 \cdot 7}$	0	-0.686
Pr	$^3\text{H}_4$	$\frac{-2^2 \cdot 13}{3^2 \cdot 5^2 \cdot 11}$	$\frac{-2^2}{3^2 \cdot 5 \cdot 11^2}$	$\frac{2^4 \cdot 17}{3^4 \cdot 5 \cdot 7 \cdot 11^2 \cdot 13}$	-0.639
Nd	$^4\text{I}_{9/2}$	$\frac{-7}{3^2 \cdot 11^2}$	$\frac{-2^3 \cdot 17}{3^3 \cdot 11^3 \cdot 13}$	$\frac{-5 \cdot 17 \cdot 19}{3^3 \cdot 7 \cdot 11^3 \cdot 13^2}$	-0.232
Pm	$^5\text{I}_4$	$\frac{2 \cdot 7}{3 \cdot 5 \cdot 11^2}$	$\frac{2^3 \cdot 7 \cdot 17}{3^3 \cdot 5 \cdot 11^3 \cdot 13}$	$\frac{2^3 \cdot 17 \cdot 19}{3^3 \cdot 7 \cdot 11^2 \cdot 13^2}$	0.202
Sm	$^6\text{H}_{5/2}$	$\frac{13}{3^2 \cdot 5 \cdot 7}$	$\frac{2 \cdot 13}{3^3 \cdot 5 \cdot 7 \cdot 11}$	0	0.364
Eu	$^7\text{F}_0$	0	0	0	-
Gd	$^8\text{S}_{7/2}$	0	0	0	0
Tb	$^7\text{F}_6$	$\frac{-1}{3^2 \cdot 11}$	$\frac{2}{3^3 \cdot 5 \cdot 11^2}$	$\frac{-1}{3^4 \cdot 7 \cdot 11^2 \cdot 13}$	-0.505
Dy	$^6\text{H}_{15/2}$	$\frac{-2}{3^2 \cdot 5 \cdot 7}$	$\frac{-2^3}{3^3 \cdot 5 \cdot 7 \cdot 11 \cdot 13}$	$\frac{2^2}{3^3 \cdot 7 \cdot 11^2 \cdot 13^2}$	-0.484
Ho	$^5\text{I}_8$	$\frac{-1}{2 \cdot 3^2 \cdot 5^2}$	$\frac{-1}{2 \cdot 3 \cdot 5 \cdot 7 \cdot 11 \cdot 13}$	$\frac{-5}{3^3 \cdot 7 \cdot 11^2 \cdot 13^3}$	-0.185
Er	$^4\text{I}_{15/2}$	$\frac{2^2}{3^2 \cdot 5^2 \cdot 7}$	$\frac{5}{3^2 \cdot 5 \cdot 7 \cdot 11 \cdot 13}$	$\frac{2^3}{3^3 \cdot 7 \cdot 11^2 \cdot 13^3}$	0.178
Tm	$^3\text{H}_6$	$\frac{1}{3^2 \cdot 11}$	$\frac{2^3}{3^4 \cdot 5 \cdot 11^2}$	$\frac{-5}{3^4 \cdot 7 \cdot 11^2 \cdot 13}$	0.427
Yb	$^2\text{F}_{7/2}$	$\frac{2}{3^2 \cdot 7}$	$\frac{-2}{3 \cdot 5 \cdot 7 \cdot 11}$	$\frac{2^2}{3^3 \cdot 7 \cdot 11 \cdot 13}$	0.409

Oblate



Ce³⁺, Pr³⁺, Nd³⁺, Tb³⁺, Dy³⁺, Ho³⁺

Prolate



Sm³⁺, Er³⁺, Tm³⁺, Yb³⁺

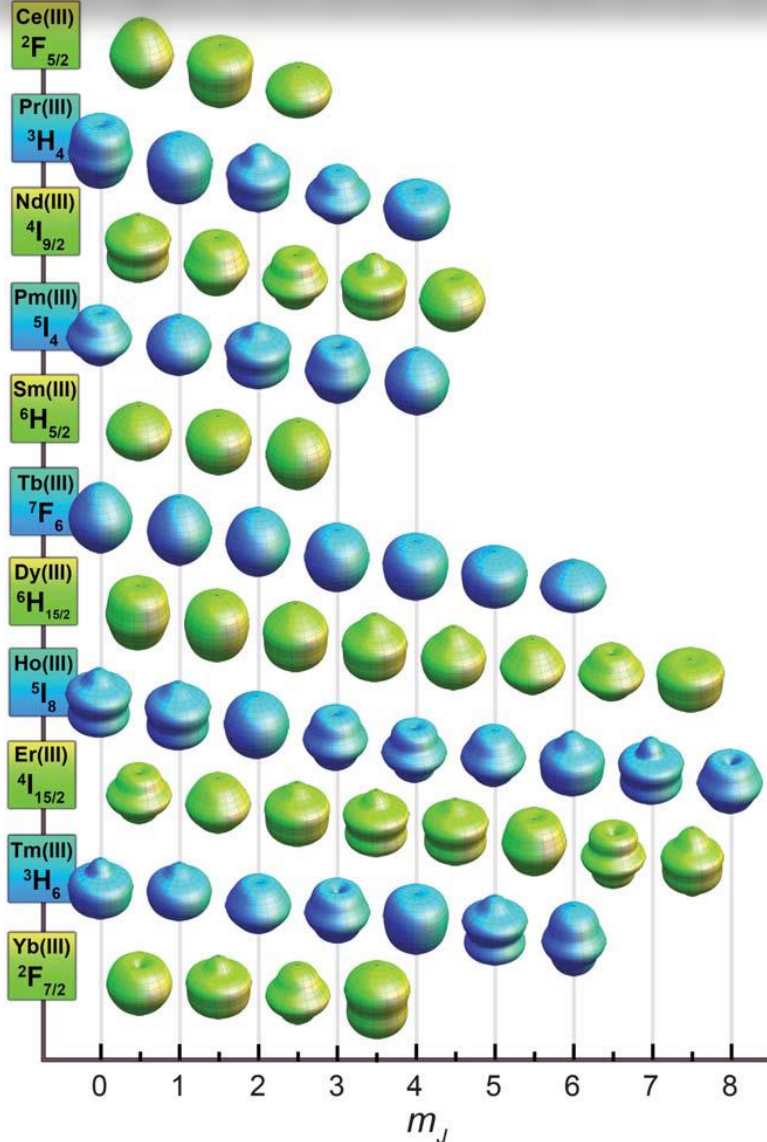
Isotropic



Gd³⁺

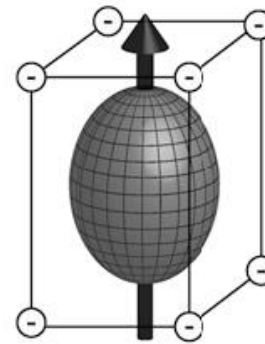
$Q_2 > 0$, prolate electron distribution
 $Q_2 < 0$, oblate electron distribution

Single ion anisotropy and CF

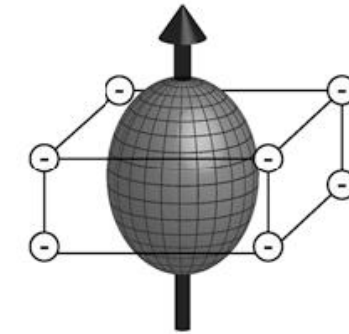


- Example of a prolate ion (Yb^{III}):

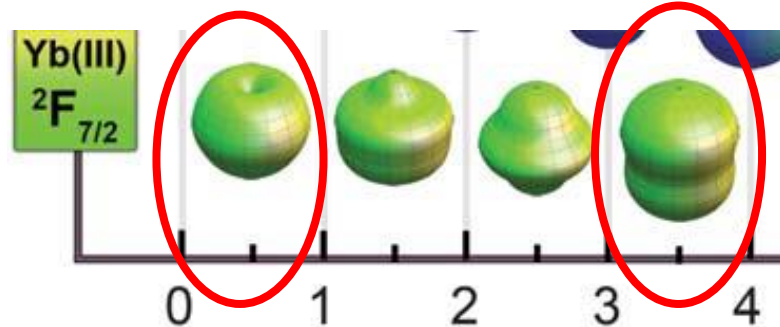
A given CF orient the electronic charge cloud in a energetically favorable direction



Planar Anisotropy
Stabilization of the highest M_J ,



Axial Anisotropy
Stab. of the lowest M_J ,



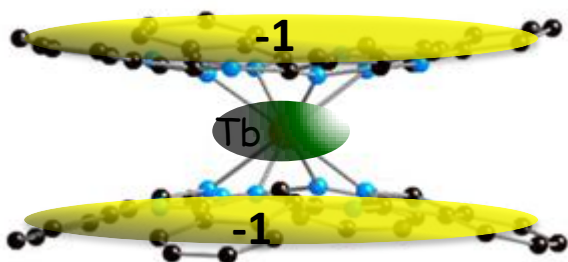
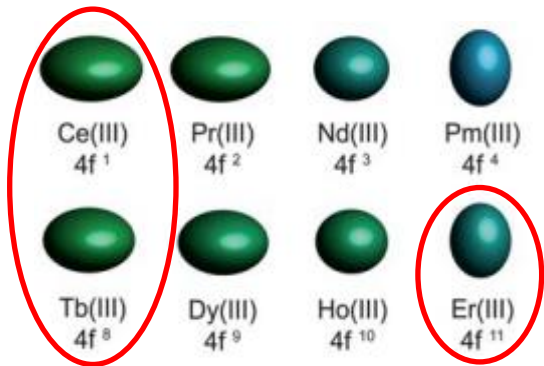
Carlin, R. J. *Magnetochemistry*; Springer: Berlin, 1986

J. D. Rinehart., et al. *Chem. Sci.*, 2011, 2, 2078

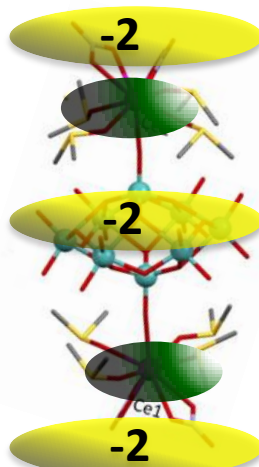
J. Tang, P. Zhang, *Lanthanide Single Molecule Magnets*, Springer, 2015

Single ion anisotropy and CF

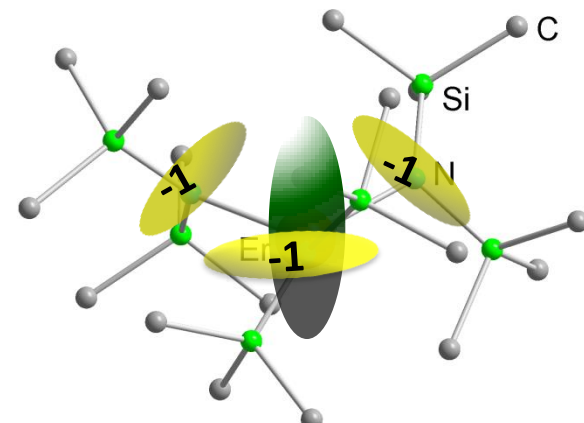
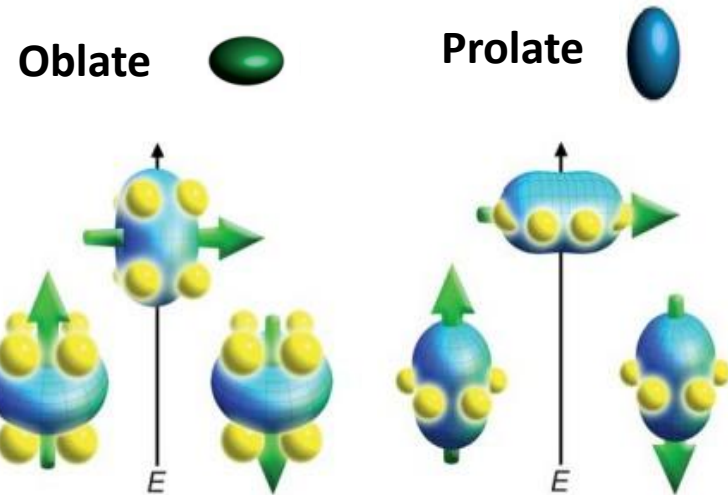
- “Oblate/Prolate model”



N. Ishikawa., et al. *J. Am. Chem. Soc.* 2003, 125, 8694



A. Ben Khélifa., et al. *Dalton Trans.*, 2015, 44, 16458

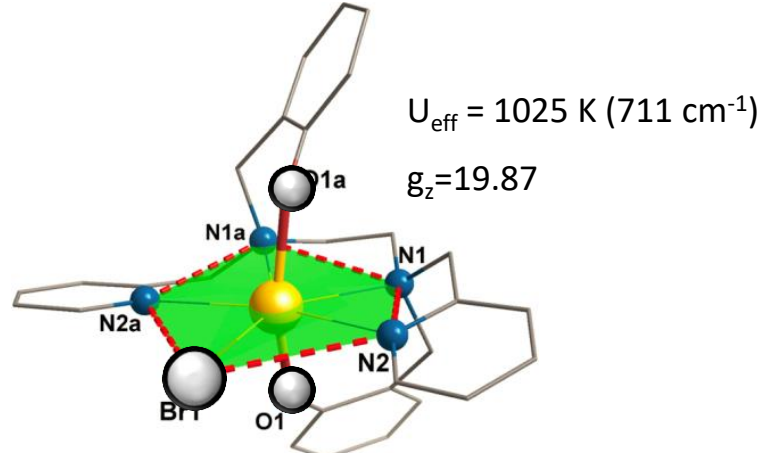
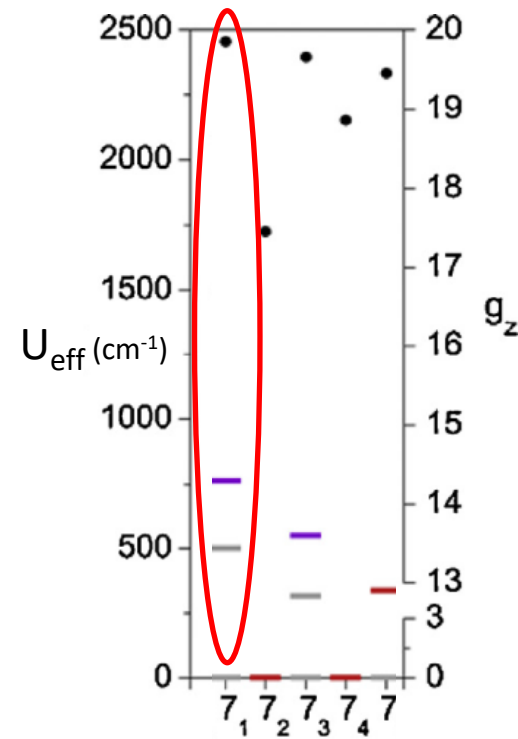
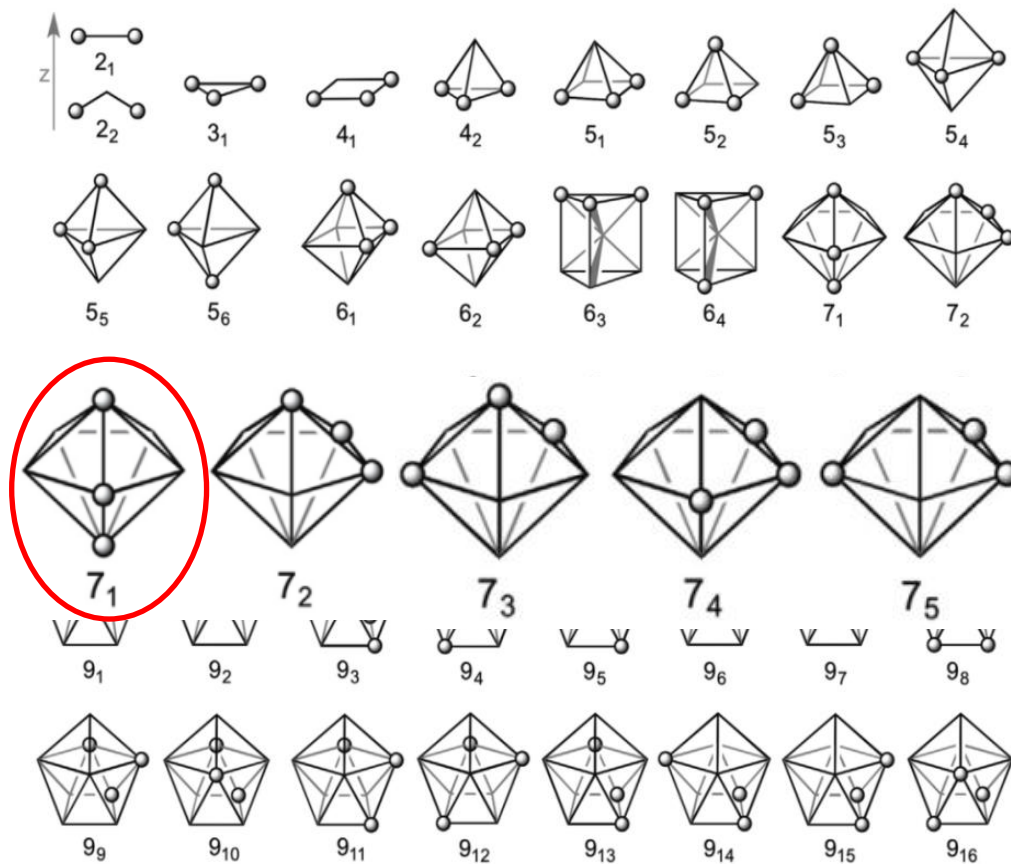


P. Zhang., et al. *J. Am. Chem. Soc.* 2014, 136, 4484

Single ion anisotropy and CF

- Localized charges electrostatic model

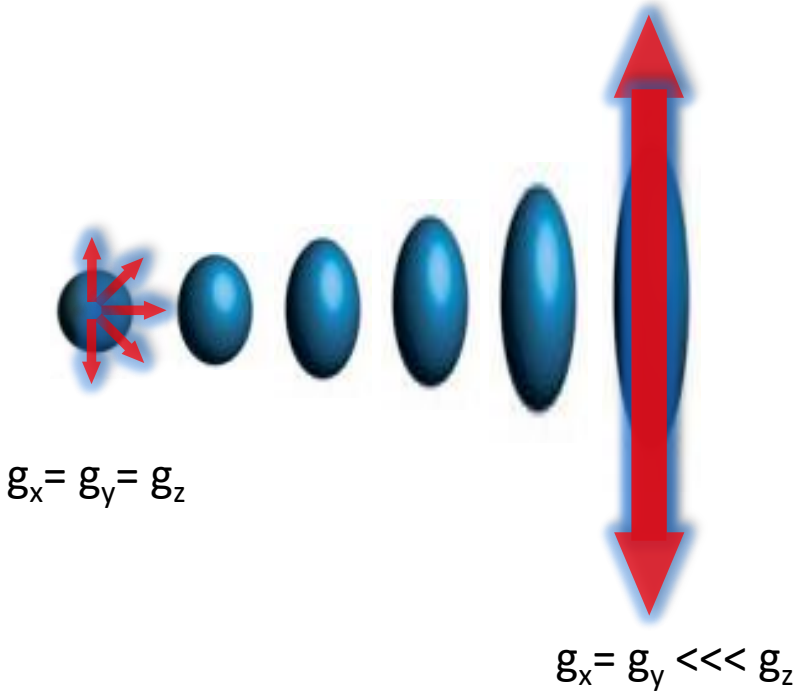
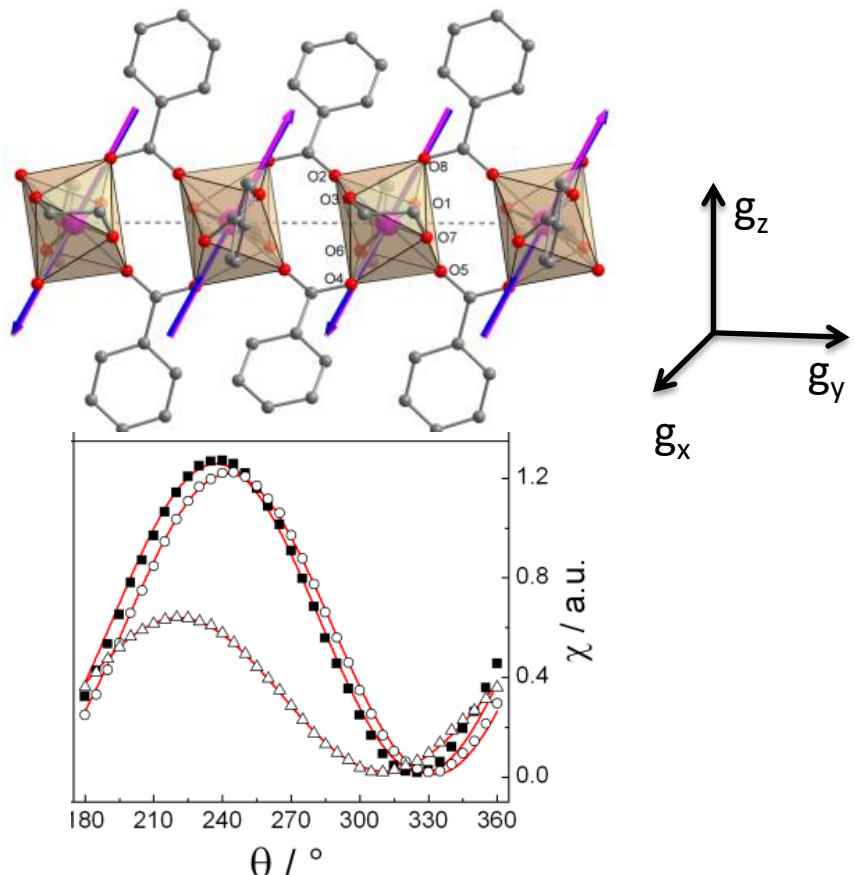
Neutral Dy^{III} complexes



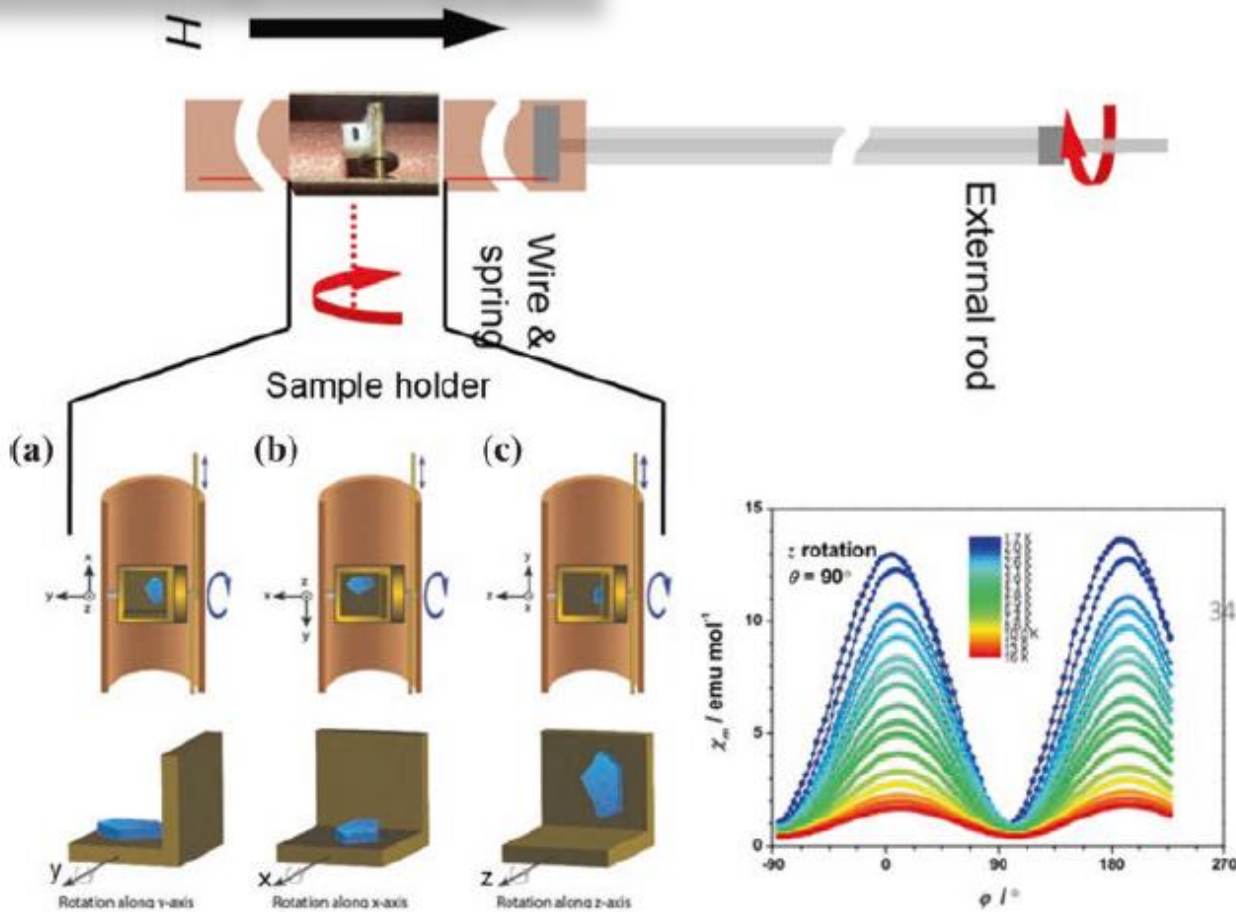
Quantification of Lanthanide(III) anisotropy in mononuclear molecules

Quantification of the anisotropy

- EPR
- Polarized neutron diffraction (PND)
- Single crystal magnetic measurements
 - Cantilever magnetometry
 - Angle-resolved magnetometry



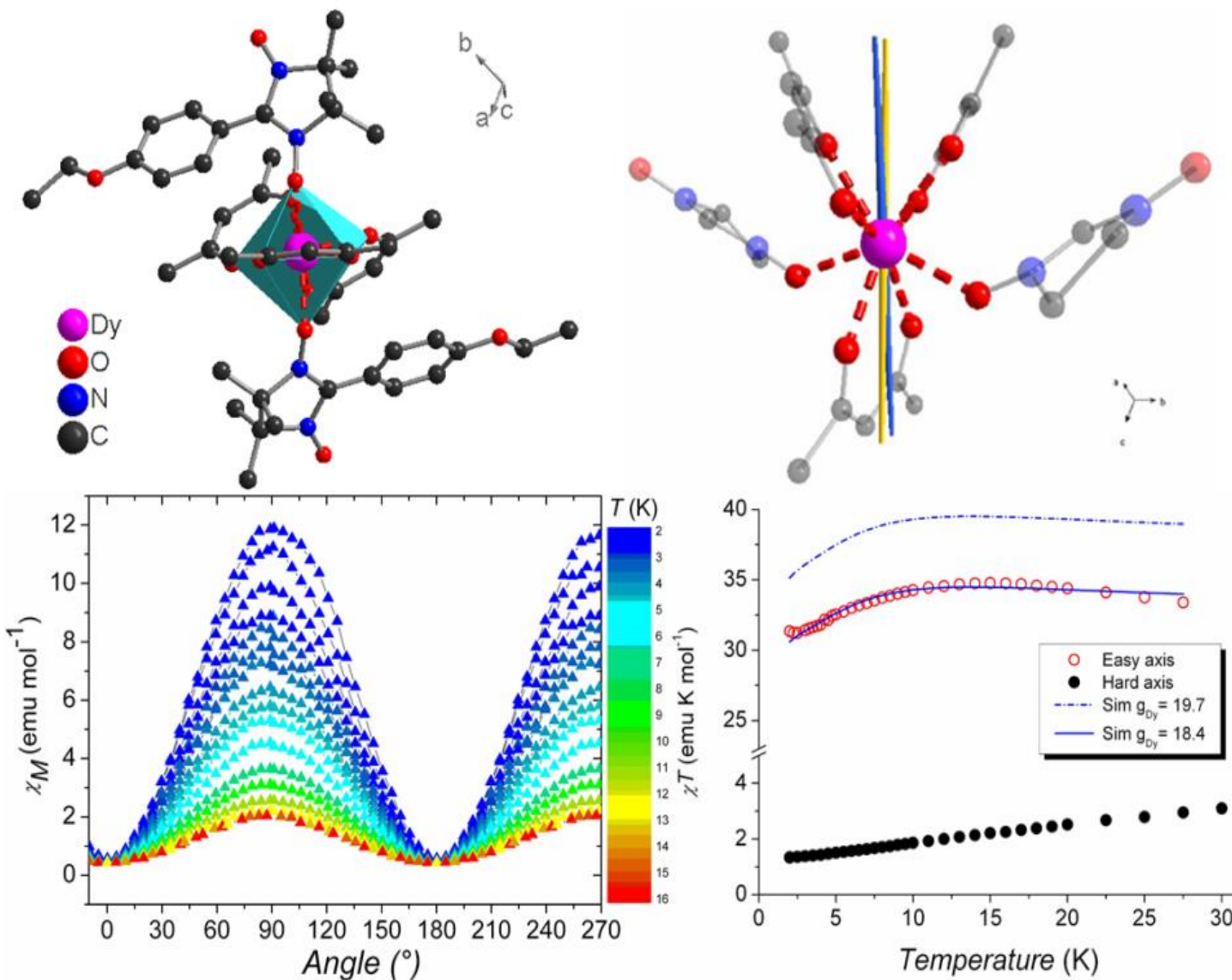
Angle-resolved magnetometry



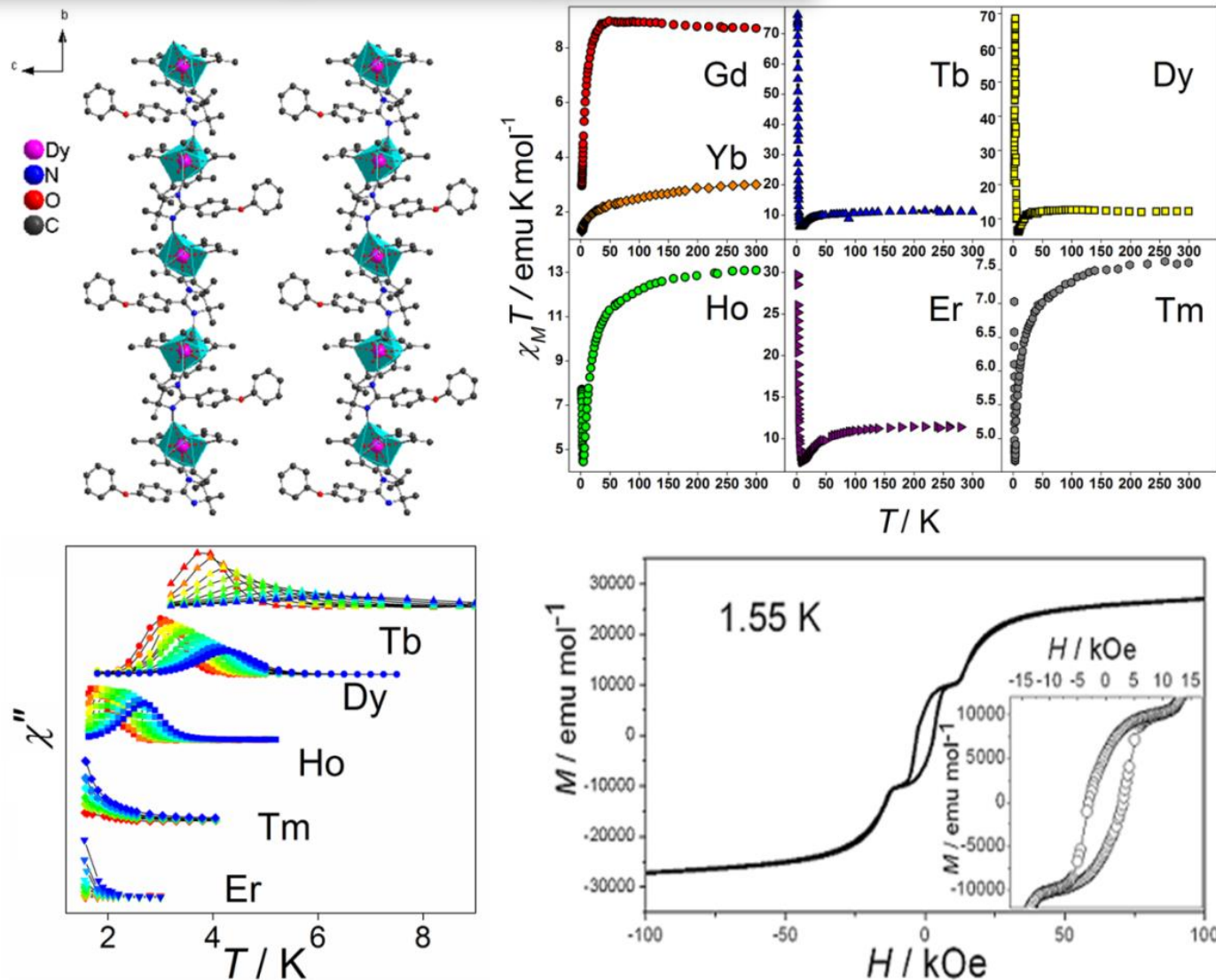
$$\chi^{\text{rot}\gamma}(\theta) = \chi_{\alpha\alpha}\cos^2(\theta) + \chi_{\beta\beta}\cos^2(\theta) + 2\chi_{\alpha\beta}\cos^2(\theta)$$

$$\chi = \begin{pmatrix} \chi_{\alpha\alpha} & \chi_{\alpha\beta} & \chi_{\alpha\gamma} \\ \chi_{\beta\alpha} & \chi_{\beta\beta} & \chi_{\beta\gamma} \\ \chi_{\gamma\alpha} & \chi_{\gamma\beta} & \chi_{\gamma\gamma} \end{pmatrix} \rightarrow \begin{pmatrix} \chi_x & 0 & 0 \\ 0 & \chi_y & 0 \\ 0 & 0 & \chi_z \end{pmatrix}$$

Angle-resolved magnetometry on SMM



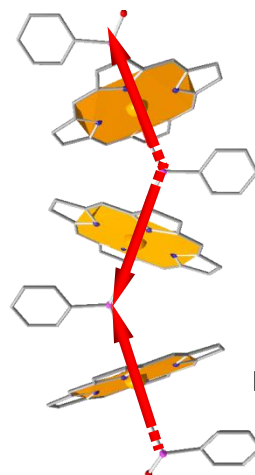
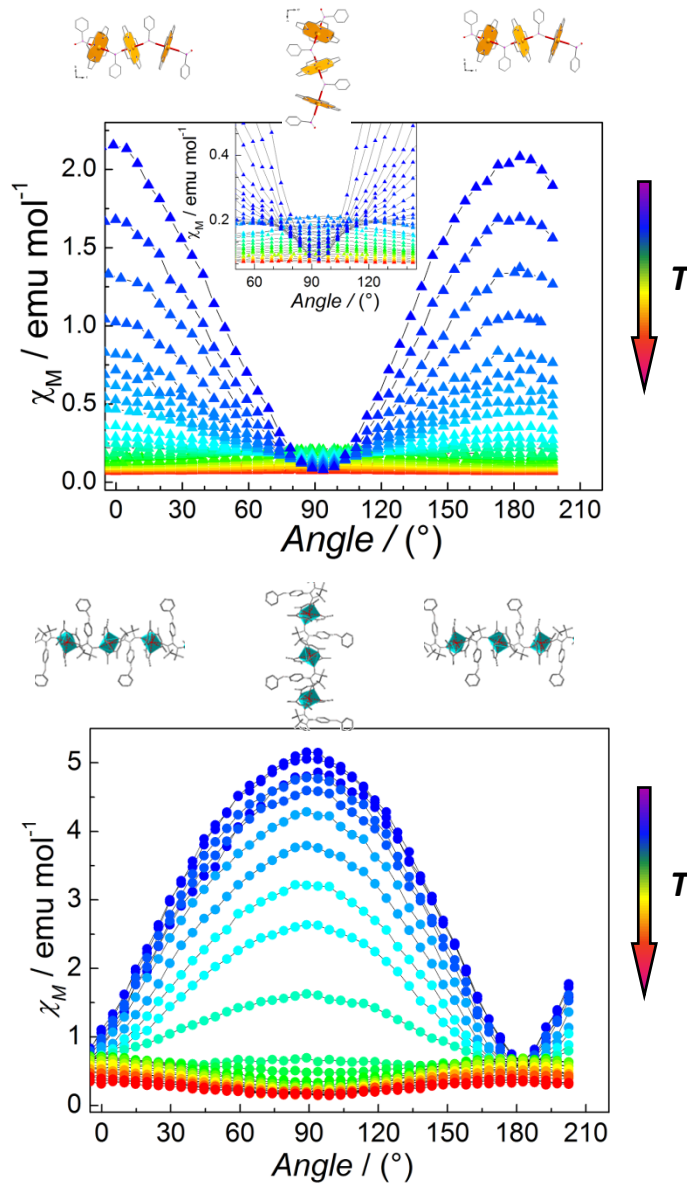
Angle-resolved magnetometry on SCM



- L. Bogani, et al., *Angew. Chem.* 2005, 44, 5817
 K. Bernot, et al., *J. Am. Chem. Soc.* 2006, 128, (24), 7947
 K. Bernot, et al., *Inorg. Chim. Acta*, 2007, 360, (13), 3807

Angle-resolved magnetometry on SCM

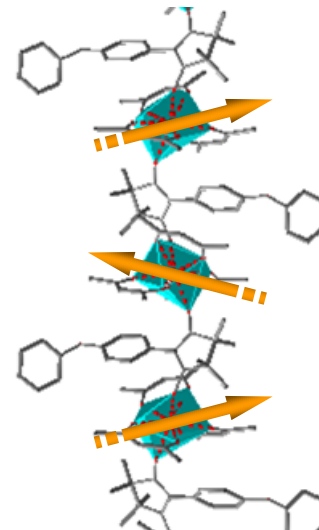
- Temperature dependance of the chain anisotropy



Mn^{III}-based SCM

→ Antiferromagnetic SCM
with weak canting

K. Bernot, et al., *J. Am. Chem. Soc.*, 2008, 130, 1619



Dy^{III}-based SCM

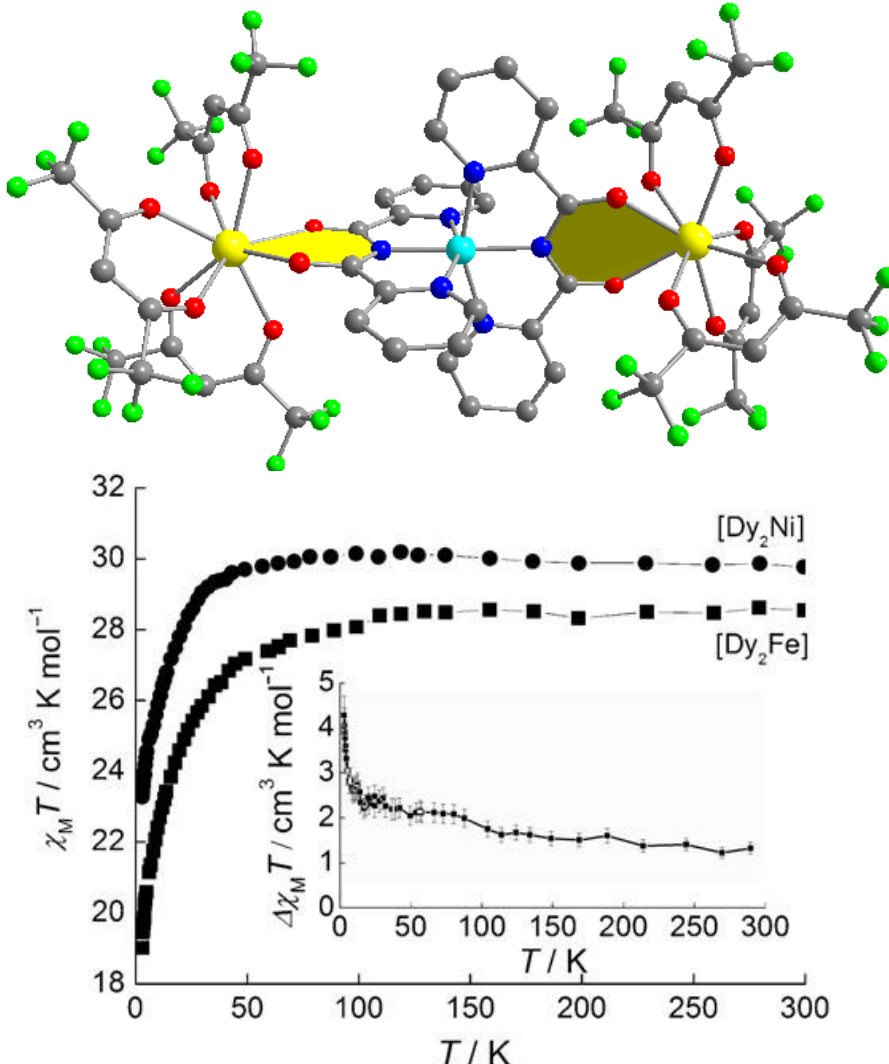
→ Antiferromagnetic SCM
with strong canting

K. Bernot, et al., *Phys. Rev. B*, 79, 134419 (2009).

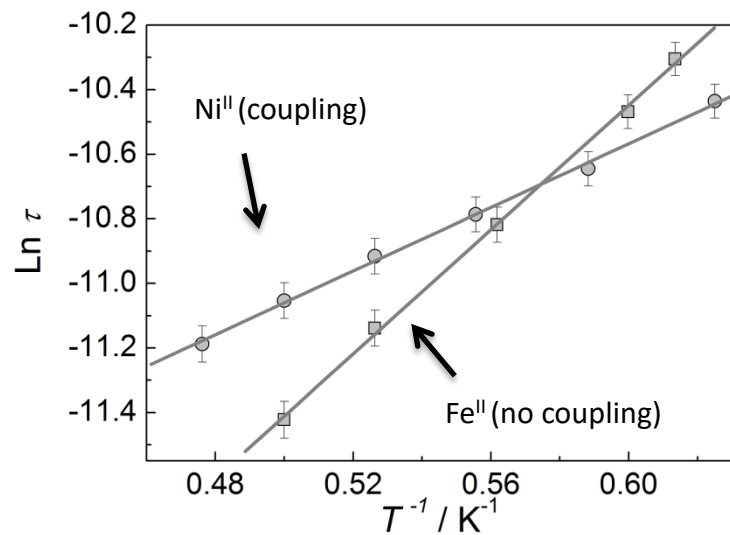
Lanthanide anisotropy in polynuclear molecules

Lanthanide anisotropy in polynuclear molecules

- **Dy^{III}-Fe^{II}-Dy^{III} and Dy^{III}-Ni^{II}-Dy^{III} SMMs**
 → Fe^{II} diamagnetic
 → Ni^{II} paramagnetic



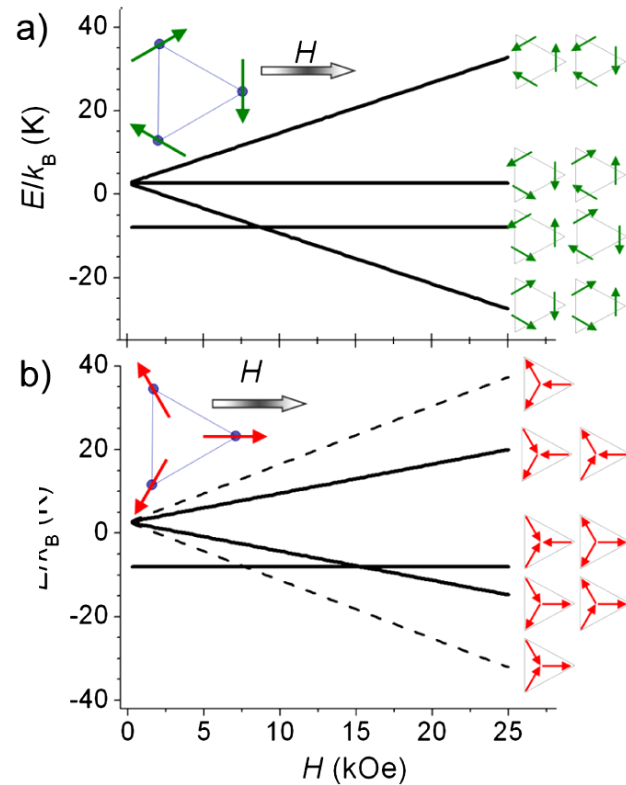
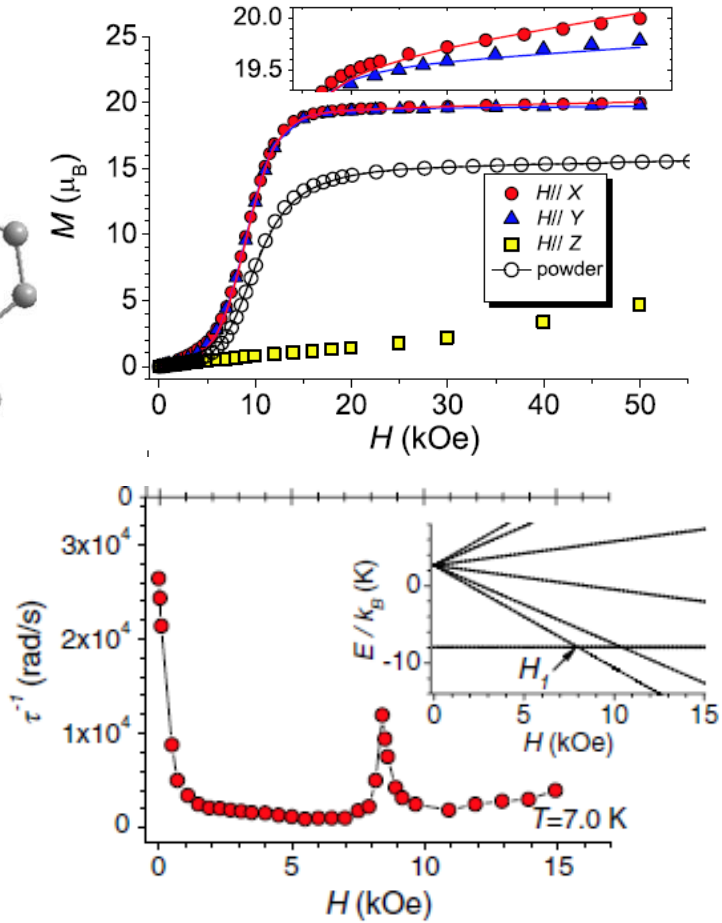
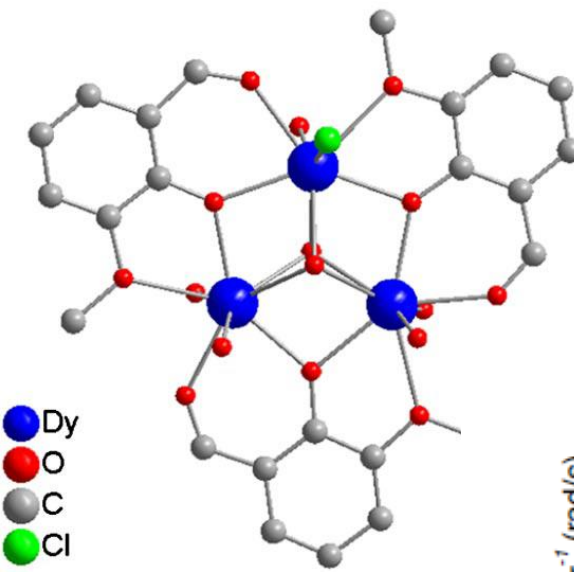
- **Ferromagnetic Dy-Dy coupling (dipolar)**
 via $\Delta\chi_M T$ method
- **Anisotropy axes are orthogonal**
 → coupling reduces SMM properties



→ Relative orientation of anisotropy axes is a key parameter

Lanthanide anisotropy in polynuclear molecules

- Dy^{III} triangle with non-magnetic ground state



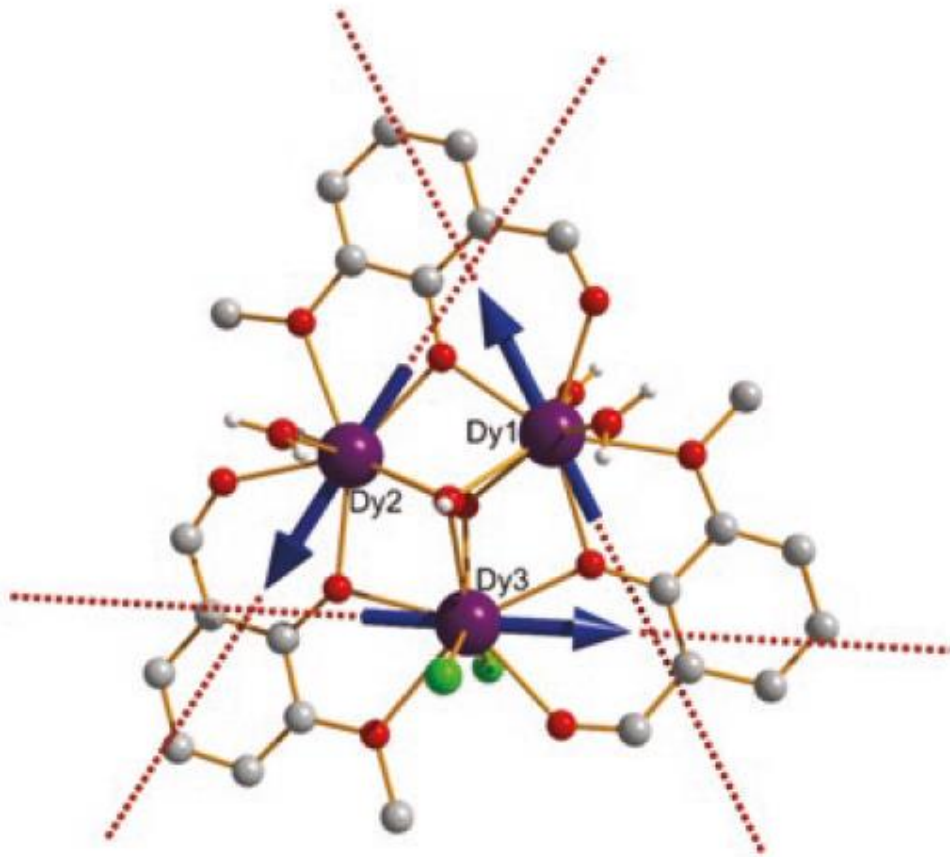
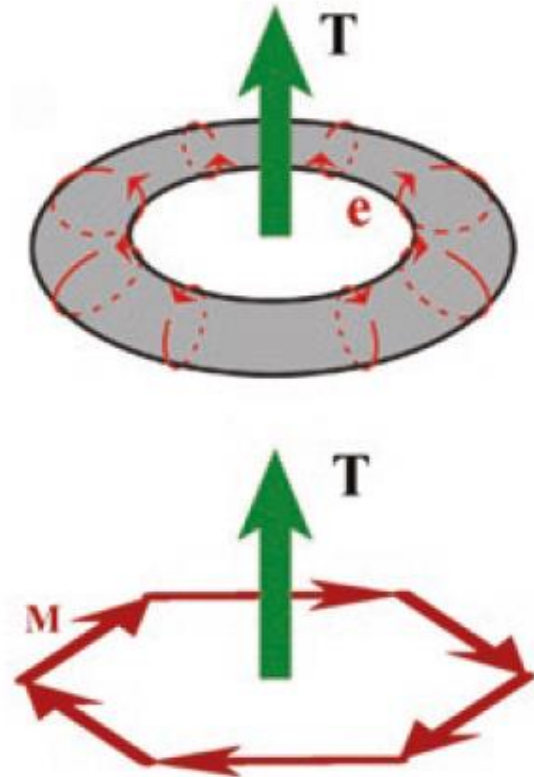
J. K. Tang, et al., *Angew. Chem.-Int. Edit.* **2006**, *45*, 1729

L. F. Chibotaru, et al. *Angew. Chem. Int. Ed.* **2008**, *47*, 4126

J. Luzon, et al., *Phys. Rev. Lett.* **2008**, *100*, 247205.

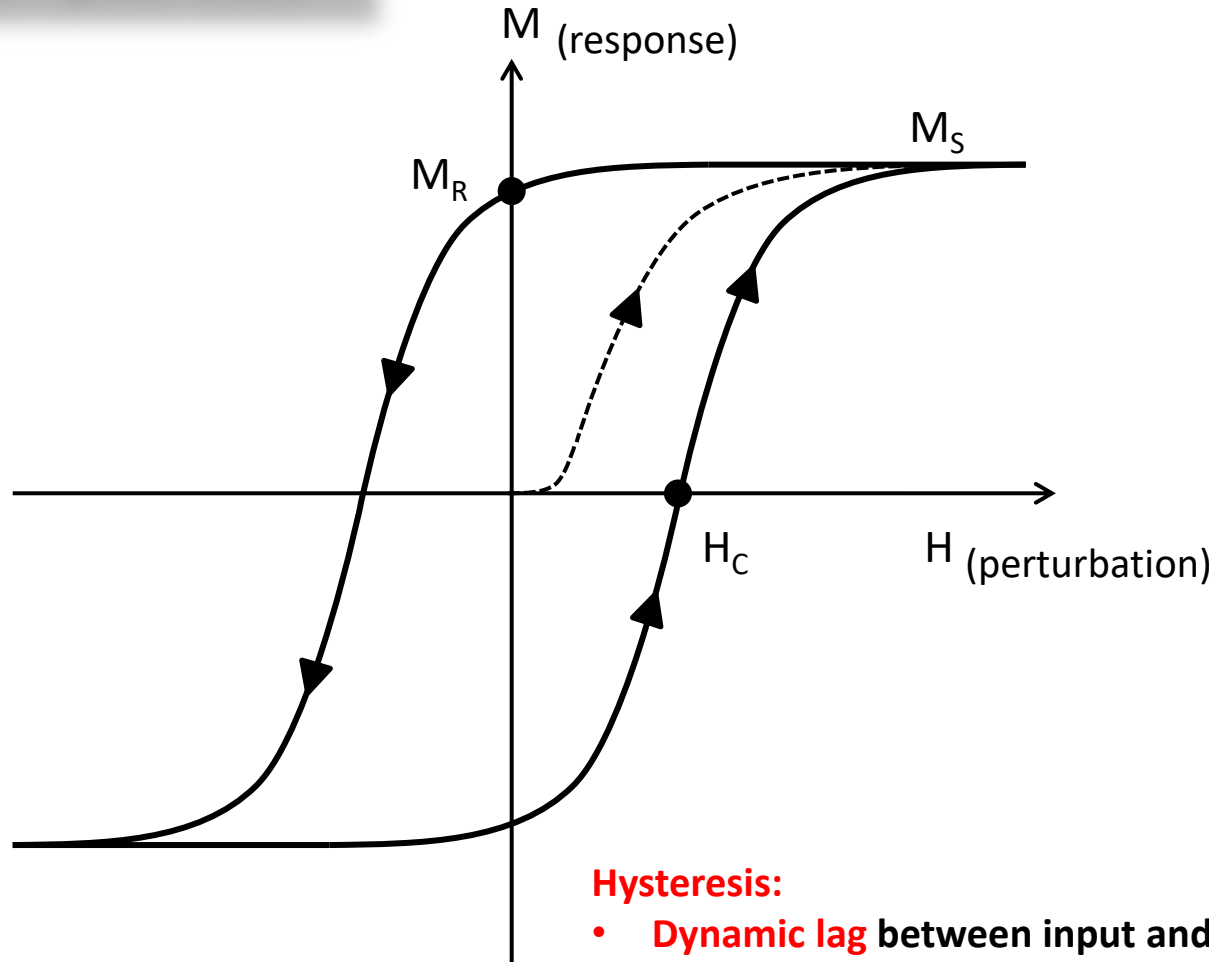
Lanthanide anisotropy in polynuclear molecules

- New class of molecules → **toroics SMM**



Molecular Magnetism : from 3d to 4f single-molecule magnets

Magnetic hystereses

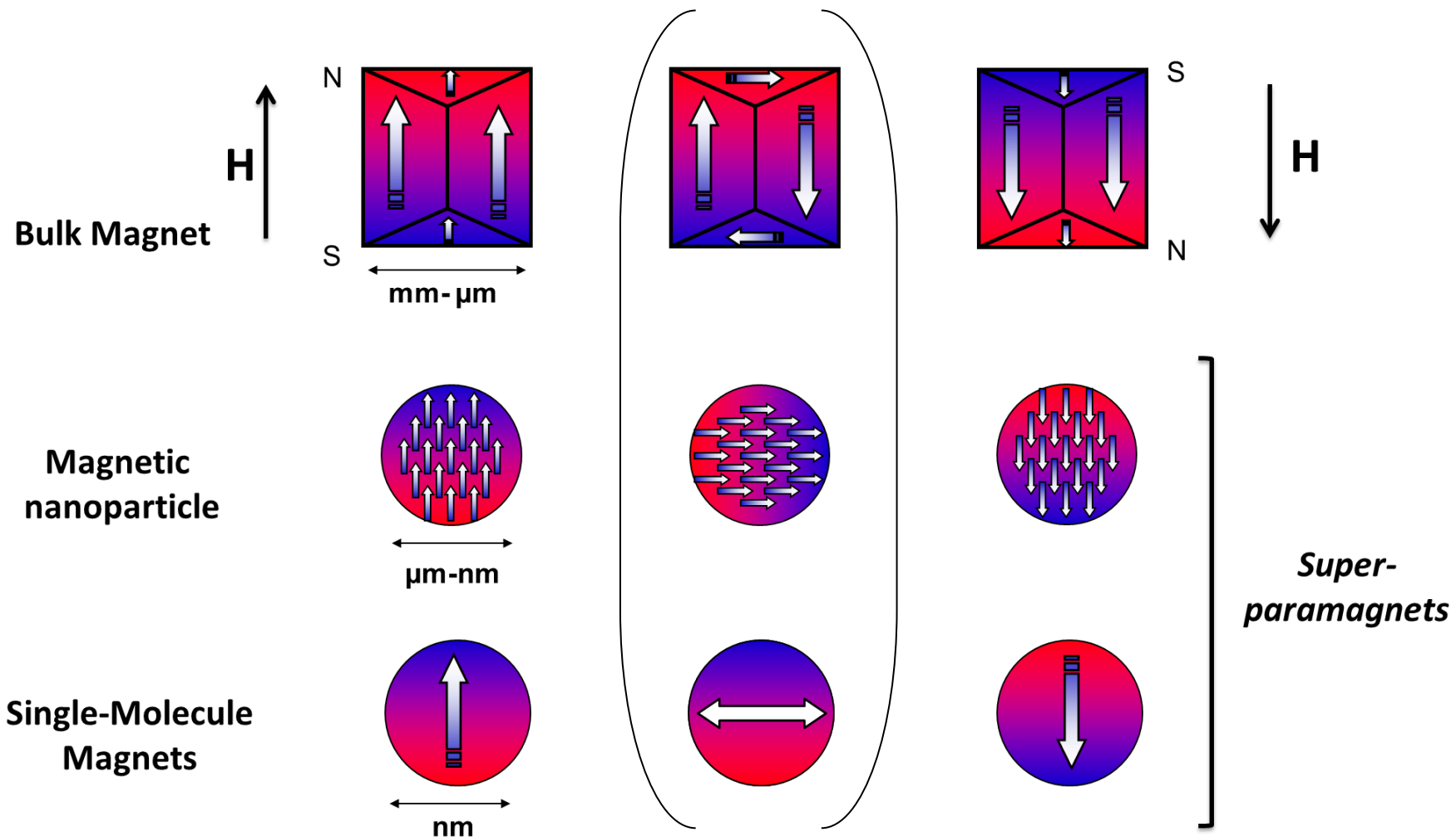


Hysteresis:

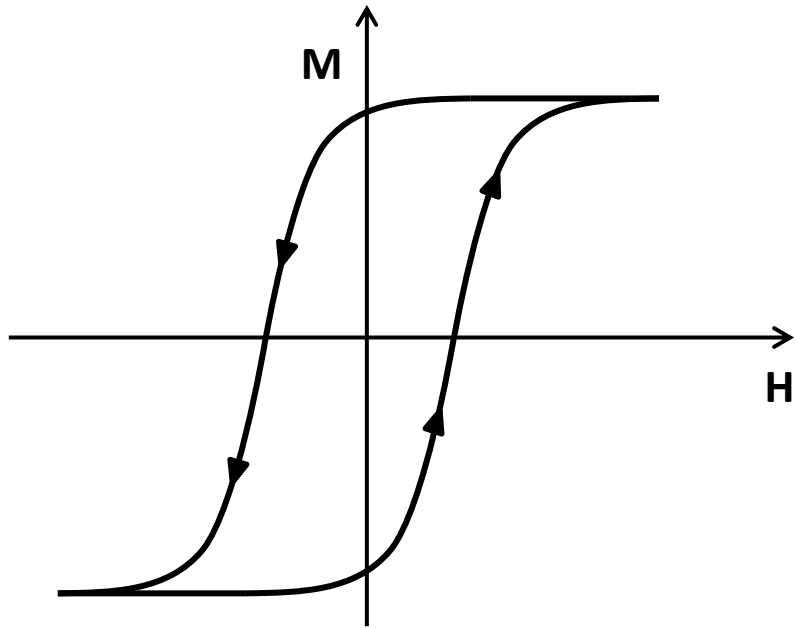
- **Dynamic lag** between input and output
- The dependance of the state of a system **on its history**
- Rate-dependant (disappear if perturbation is slow)
- Rate-independant

- M_S : Magnetization @ saturation
- M_R : Remanent magnetization $M@H=0$
- H_C : Coercitive field $H@M=0$

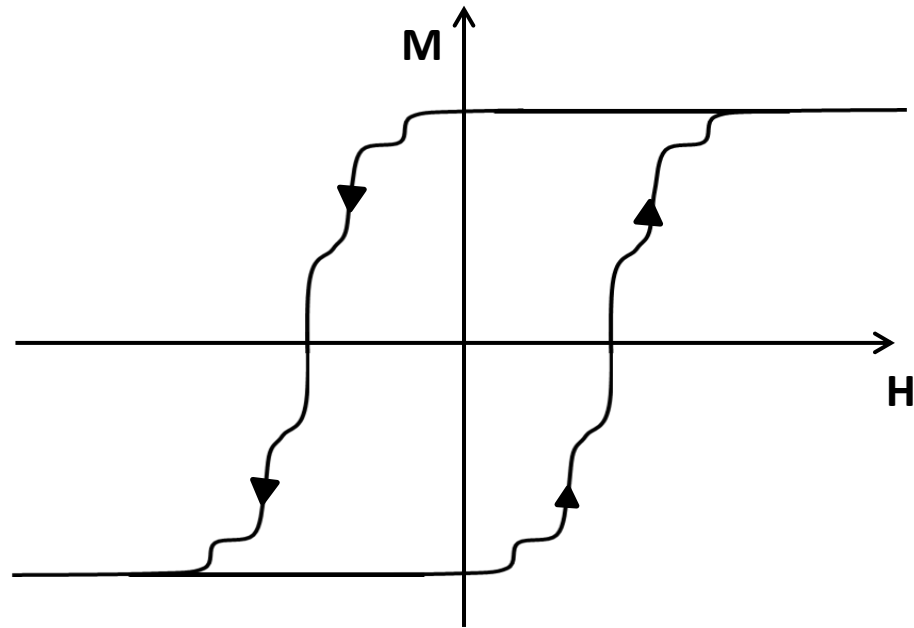
Magnetic hystereses



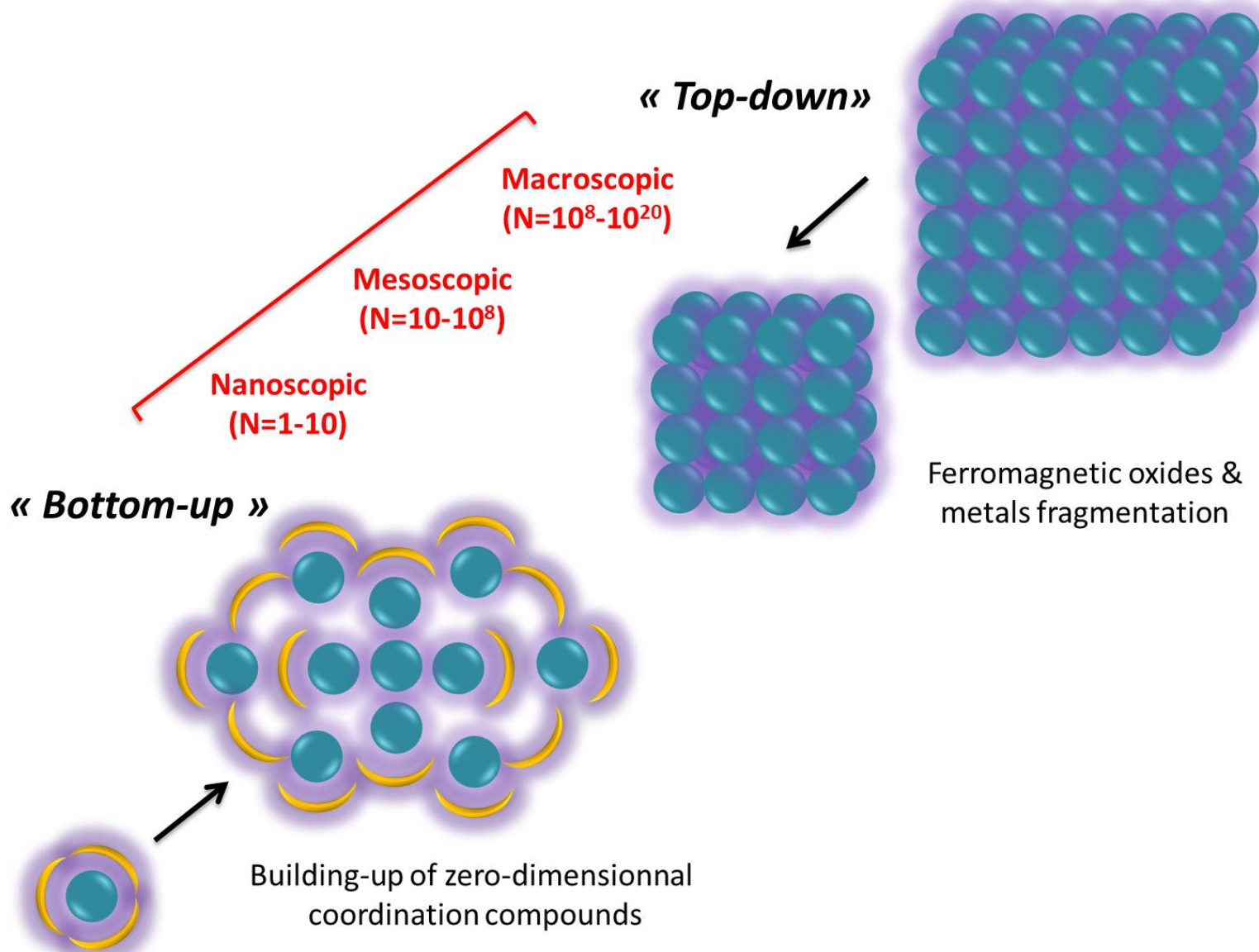
Nanoparticle



Single-Molecule Magnet

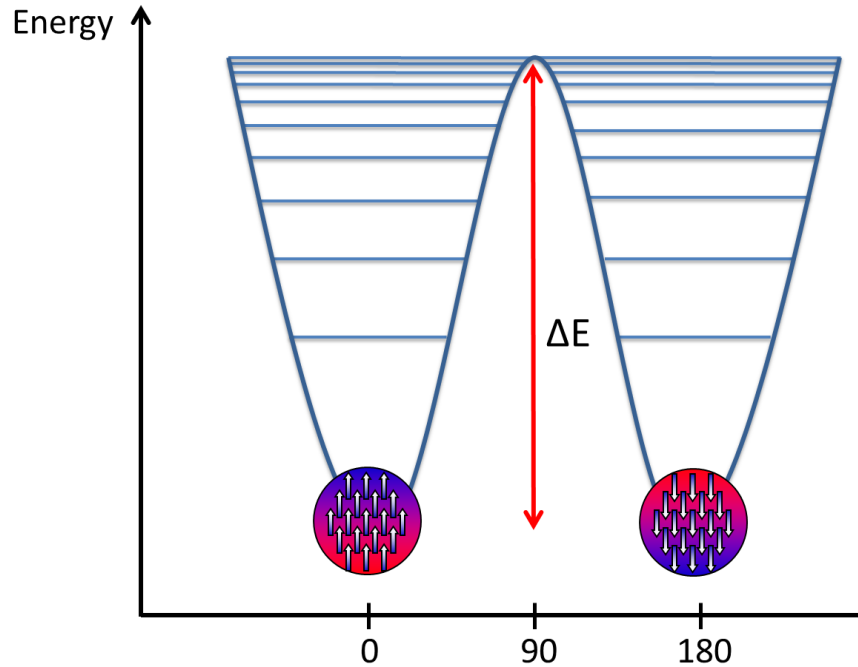


- Hard ($H_c > 5000$ Oe) or soft magnet-like hysteresis ($H_c < 125$ Oe)
- Hard-magnet-like hysteresis with **quantum effect** (molecular quantum tunneling of the magnetization)

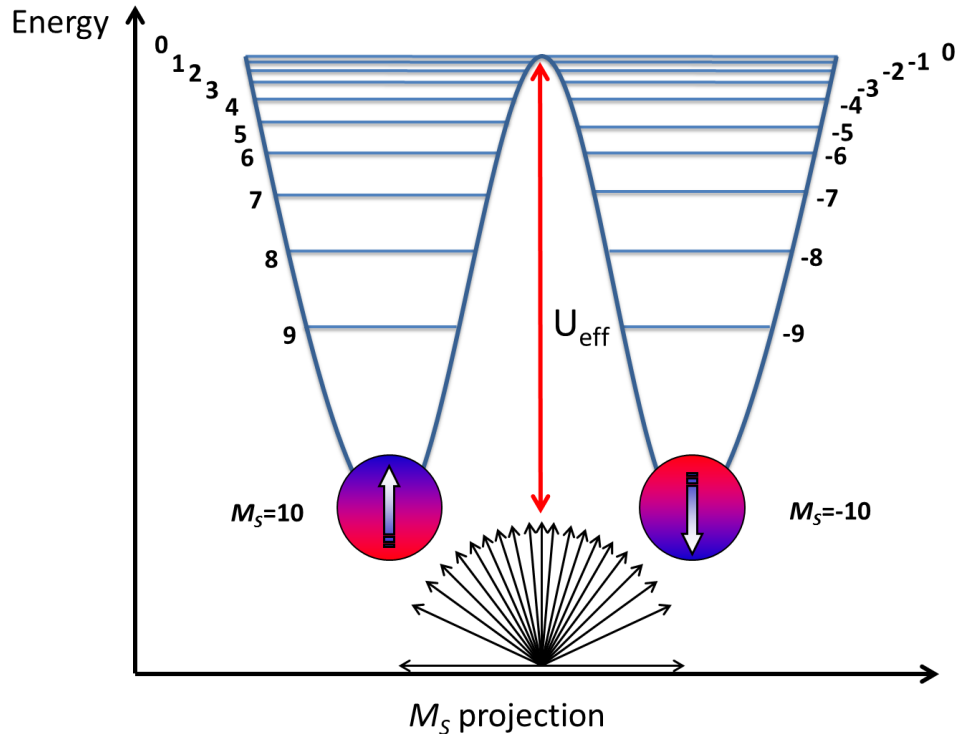


Spin reversal in Superparamagnets

Nanoparticle



Single-Molecule Magnet



Level's energies: $E = KV \sin^2 \phi - \mu_0 M V H \cos(\phi - \theta)$

K: anisotropy constant; V: volume; M: magnetization; H: magnetic field
 θ : particle magnetization angle; ϕ : magnetic field angle



M_s moment projections

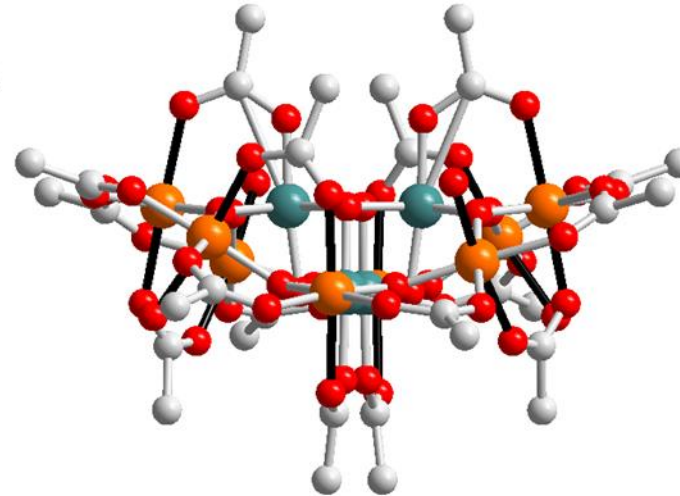
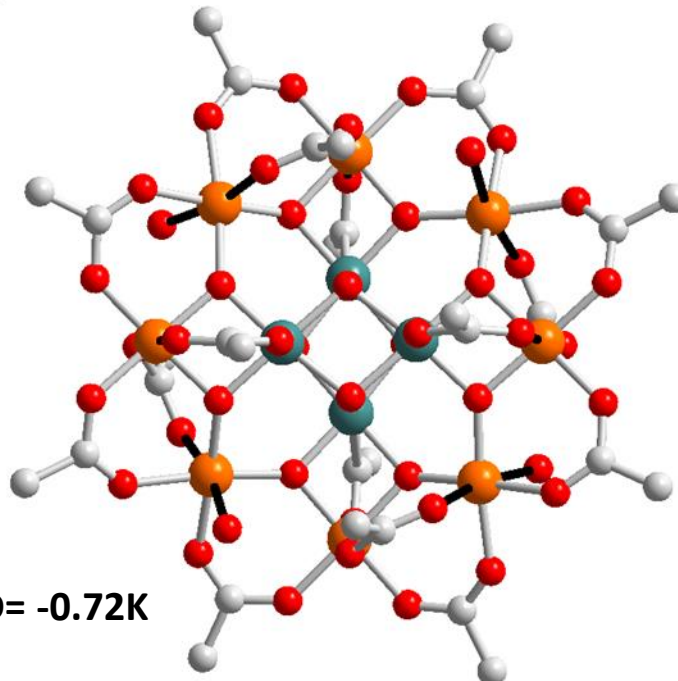
Relaxation above the barrier is $\tau = \tau_0 \exp(KV/k_B T)$

→ Stoner-Wohlfarth, Curling, nucléation/propagation/annihilation



$\tau = \tau_0 \exp(U_{\text{eff}}/k_B T)$
→(Orbach)

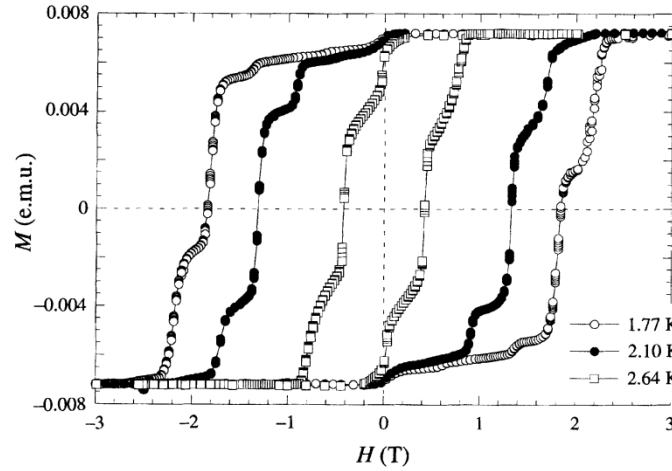
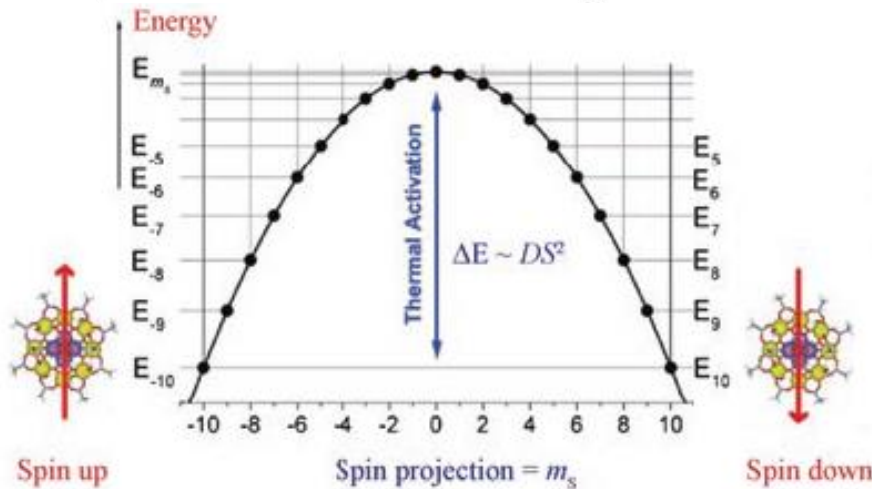
The iconic Mn_{12}



Spin $S = 10$

Anisotropy $D = -0.72\text{K}$

$U_{\text{eff}} = 72\text{K}$

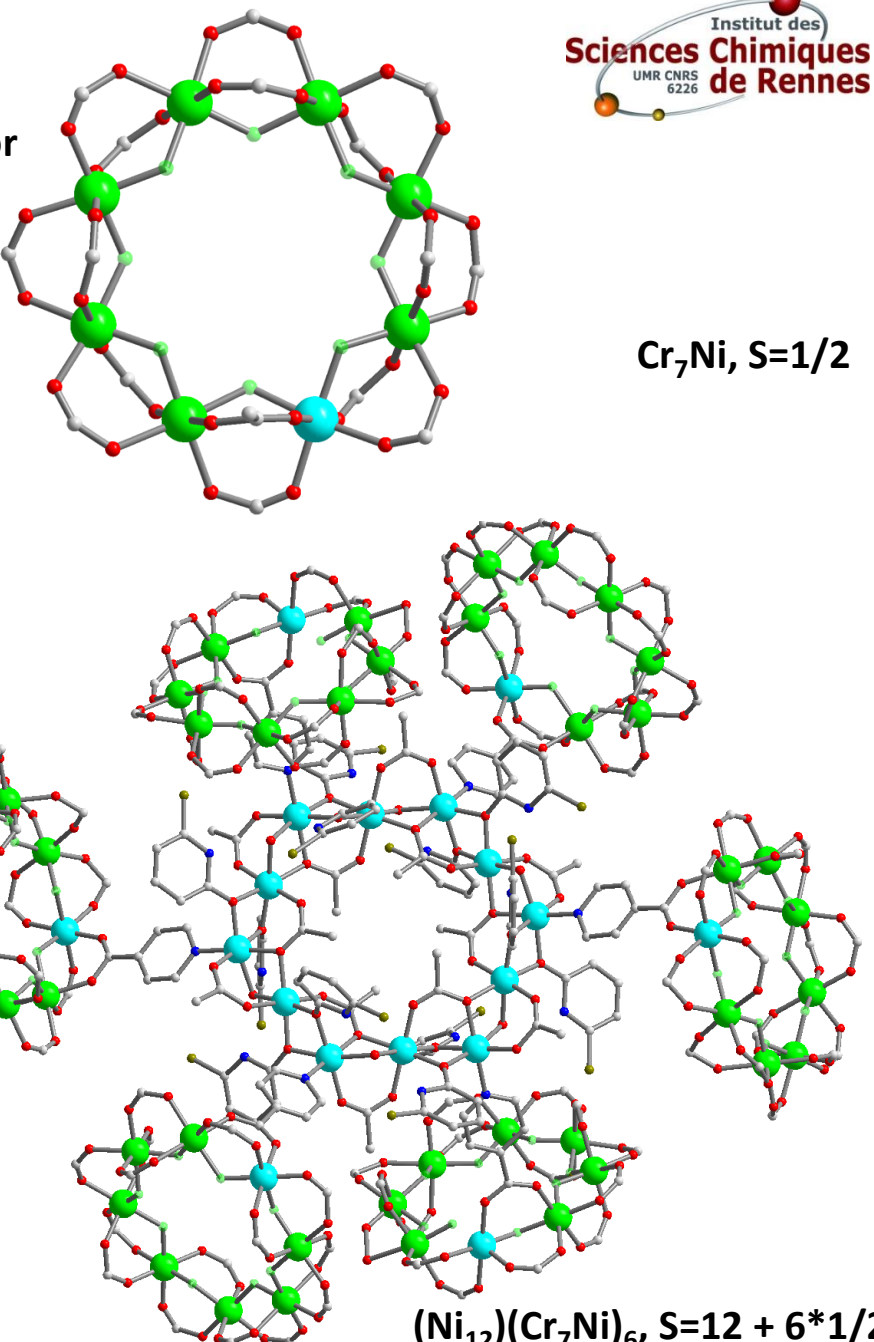
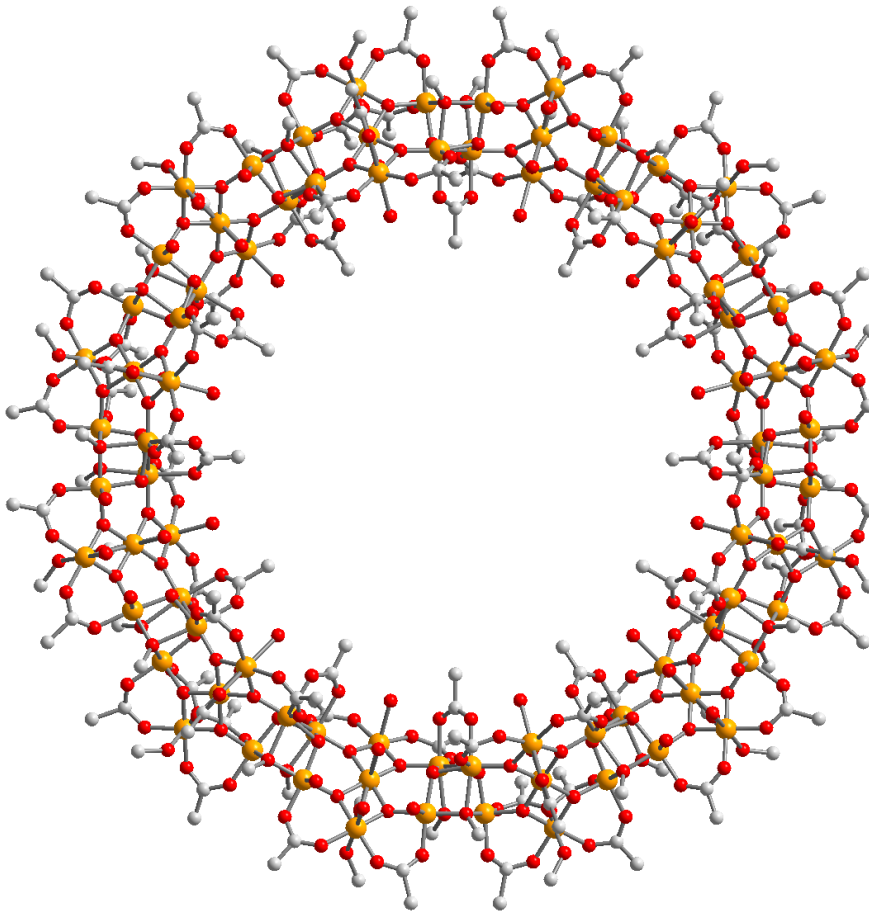


Thomas, L. et al., . *Nature* 1996, 383, 145-147.

J. Tang, P. Zhang, *Lanthanide Single Molecule Magnets*, Springer, 2015

Optimizing S.....

- Amazingly beautiful molecules but no efficiency for magnetic slow relaxation



Tasiopoulos, A. J. et al., *Angew. Chem.-Int. Edit.* 2004, 43, 2117

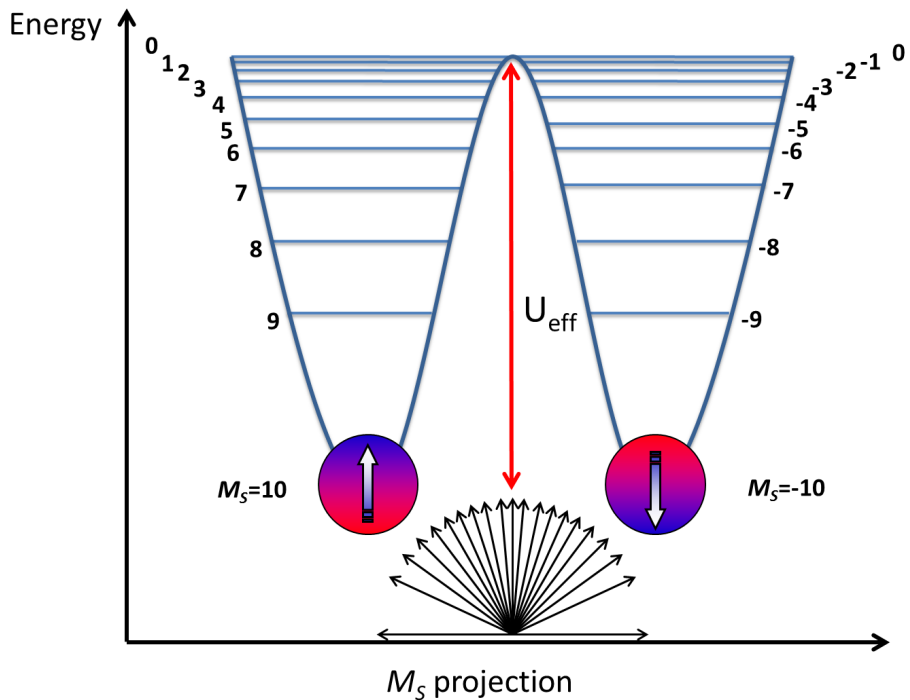
Timco, G. A.; et al.. *Nat Nano* 2009, 4, 173,

Andres, H. et al., *Chem. Eur. J.* 2002, 8, 4867.

Whitehead, G. F. S. et al., *Angew. Chem.-Int. Ed.* 2013, 52, 9932.

Spin reversal in Superparamagnets

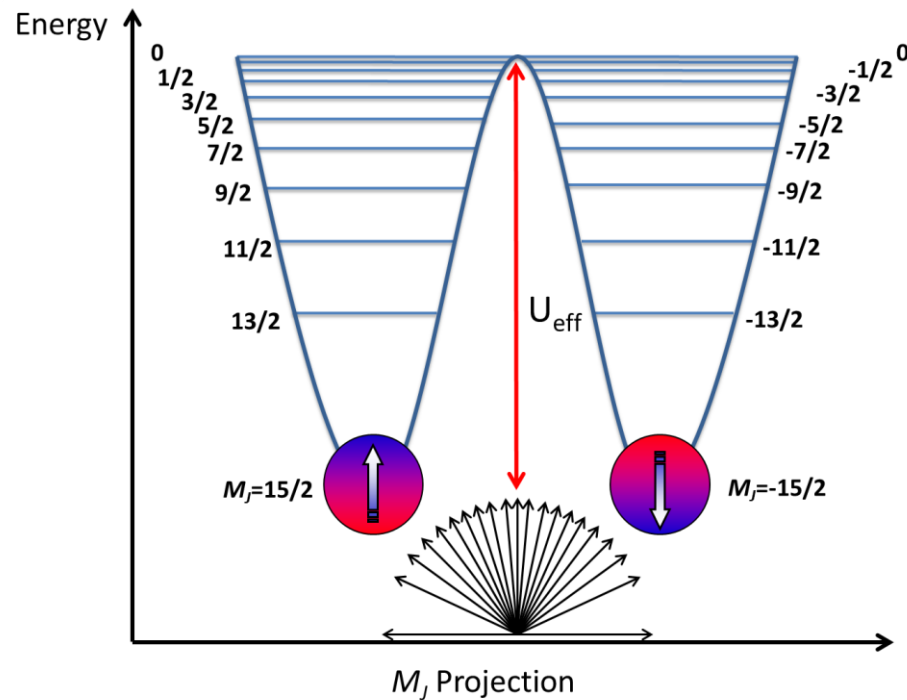
3d-SMM



$\text{Mn}_{12} \text{ S}=10$

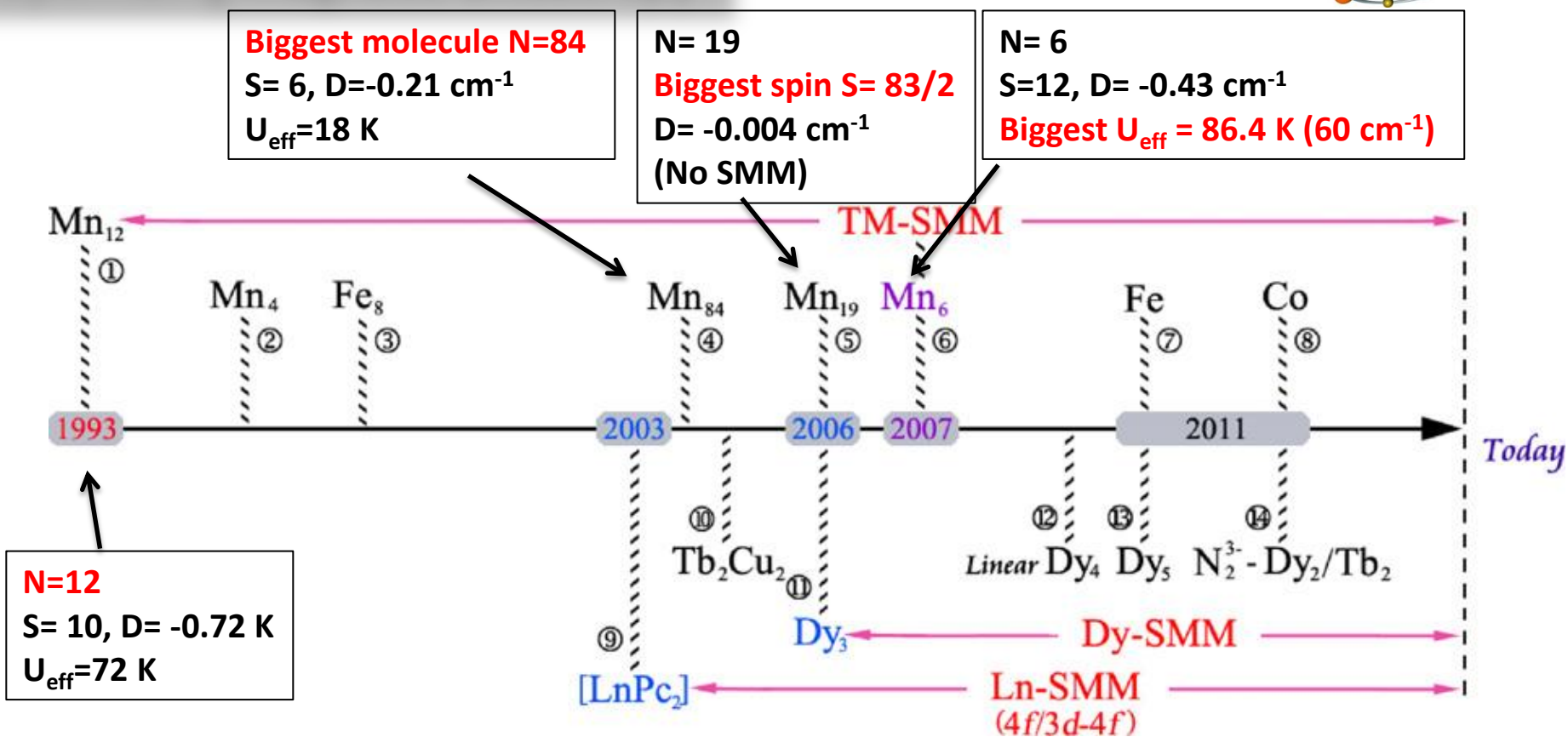
$$U_{\text{eff}} \rightarrow |D| S^2$$

4f-SMM



$\text{Dy } {}^6\text{H}_{15/2}$

Optimizing magnetic anisotropy



Polynuclear SMM:
still a lot to do with 3d ions, but 4f ions are more and more used to design SMM

Mn₆: Milios, C. J.; *J. Am. Chem. Soc.* 2007, 129, 2754

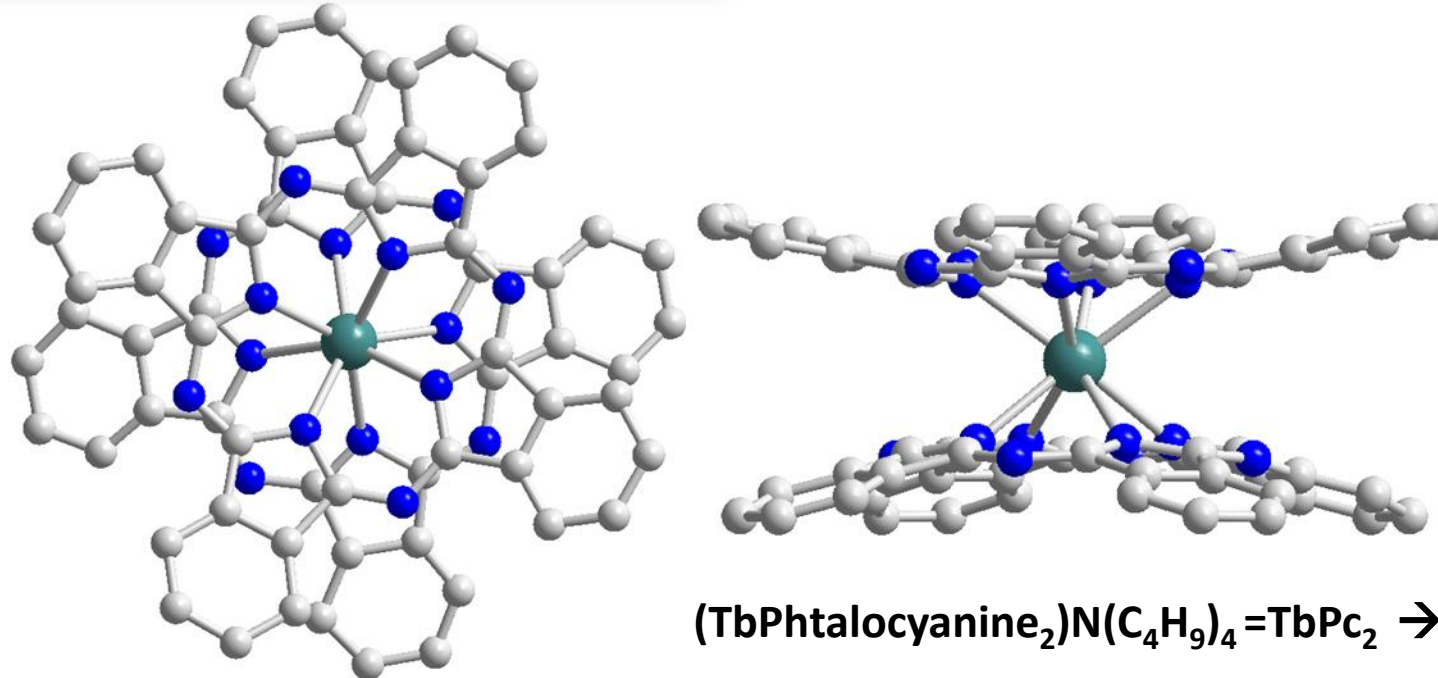
Mn₁₉: AkoO, A. M.; *Angew. Chem.-Int. Ed.* 2006, 45, 4926

Mn₈₄: Tasiopoulos, A. J.; *Angew. Chem.-Int. Edit.* 2004, 43, 2117

J. Tang, P. Zhang, *Lanthanide Single Molecule Magnets*, Springer, 2015

Zhang P. et al., *Coord. Chem. Rev.*, 2013, 257, 1728

The breakthrough of TbPc₂

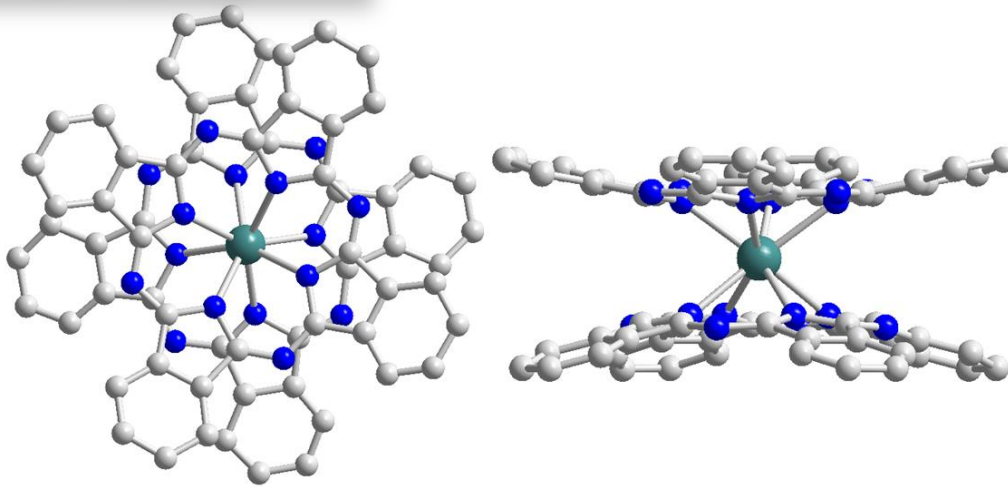


In 2003, a revolution in the design of SMM:

- No need for « giant spins » via polynuclear molecules
- Spins of 4f ions are enough and their anisotropy is huge

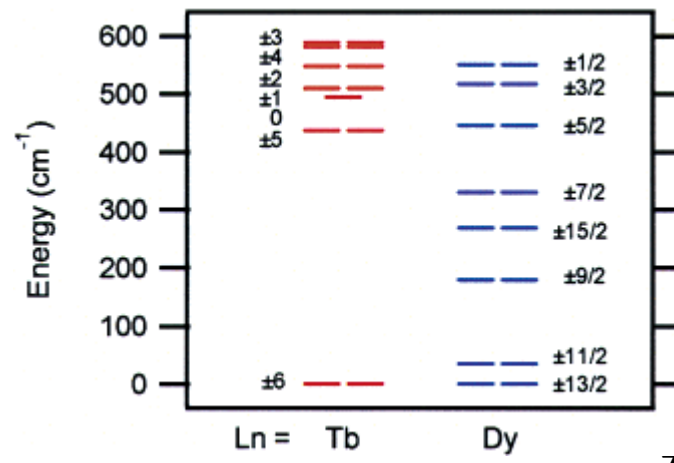
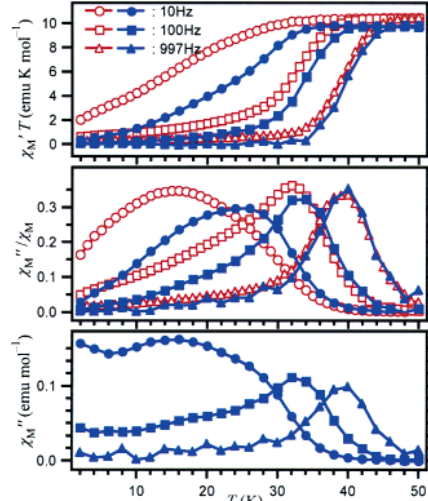
Spin optimization → → → Anisotropy optimization

The breakthrough of TbPc₂



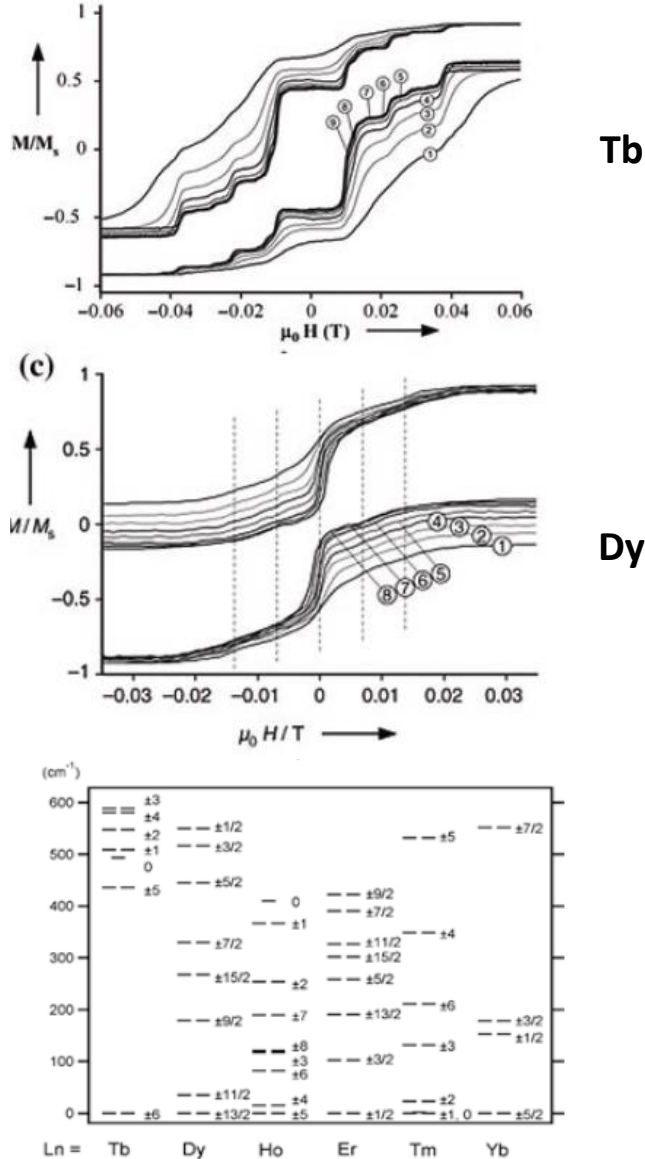
In 2003, a revolution in the design of SMM:

- SMM behavior is observable if N=1 provided its anisotropy is huge : Single Ion Magnet
→ better called « mononuclear SMM »
- Dilution in isomorphous matrix (Y^{III}) is possible and enhances magnetic relaxation
- Sublevels structure (spilling of M_J) can be determined by ¹H NMR



The breakthrough of TbPc₂

T= 0.04 K



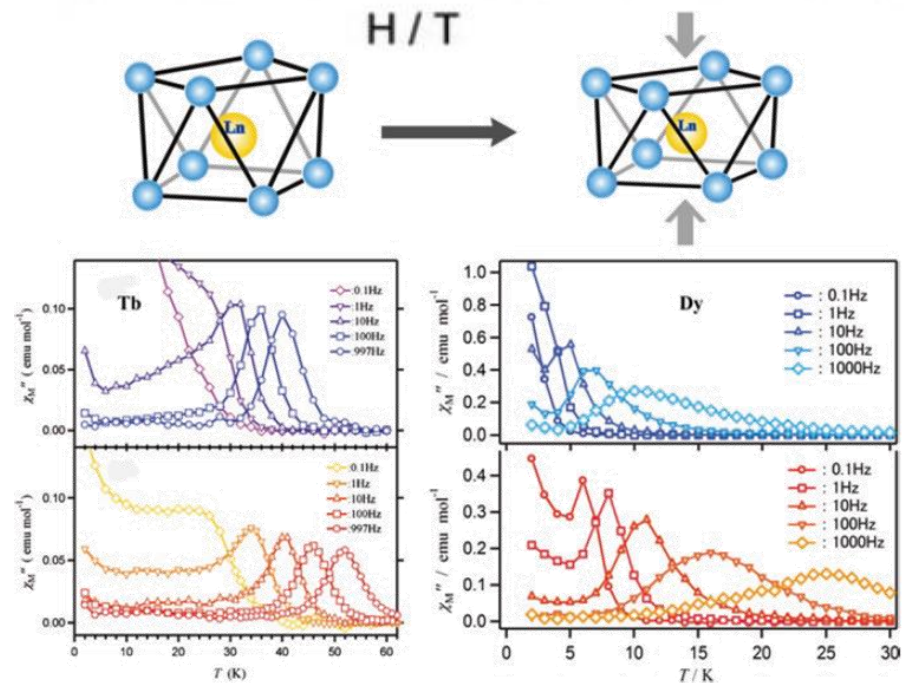
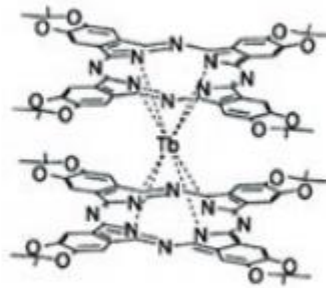
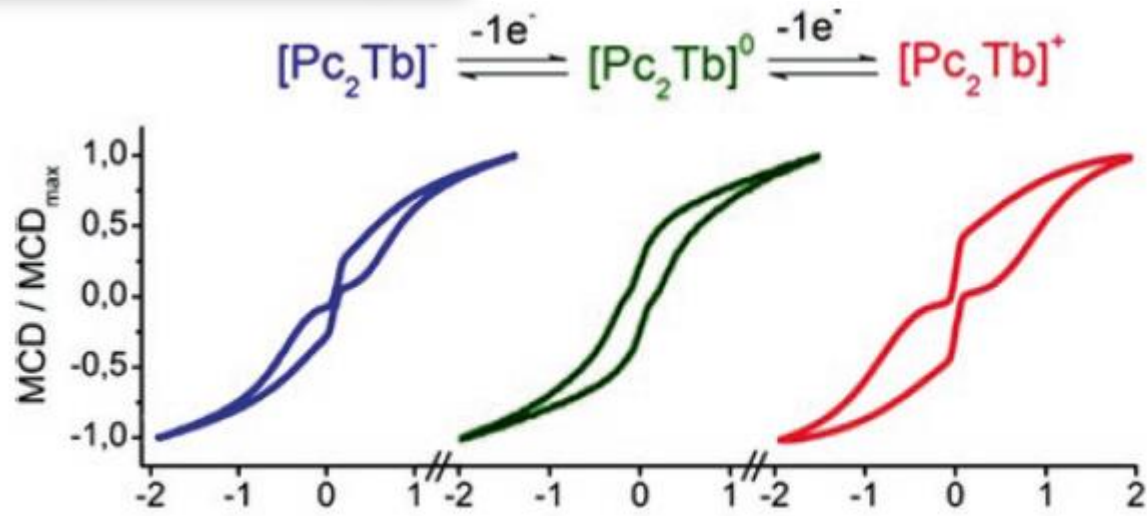
Wide possibilities of chemical engineering of LnPc₂

Molecule	$U_{\text{eff}}/\text{cm}^{-1}$	τ_0/s
[Tb(Pc-OPh) ₂]	504	2.16×10^{-11}
[Tb(Pc-Oph) ₂ ⁻ N(Me) ₄ ⁺	442	8.2×10^{-11}
[Tb(Pc-Oph) ₂ ⁻ N(Bu) ₄ ⁺	394	3.45×10^{-10}
[Tb(Pc)(Pc-Oph)]	652	1.1×10^{-11}
[Tb(Pc)(Pc-Oph) ⁻ N(Me) ₄ ⁺	450	3.0×10^{-10}
[Tb(Pc)(Pc-Oph) ⁻ N(Bu) ₄ ⁺	487	7.8×10^{-11}
[Tb(Pc)(Pc-Bu)]	642	2.21×10^{-11}
[Tb(Pc)(Pc-Bu) ⁻ N(Bu) ₄ ⁺	400	4.78×10^{-10}
[Tb(Pc-ODOP) ₂] (order)	480	
[Tb(Pc-ODOP) ₂] (disorder)	422	
[Tb(Pc-a) ₂ ⁻ N(Bu) ₄ ⁺	445	6.35×10^{-11}
[Tb(Pc-b) ₂ ⁻ N(Bu) ₄ ⁺	428	1.34×10^{-10}
[Tb(Pc-c) ₂ ⁻ N(Bu) ₄ ⁺	463	2.22×10^{-11}
[Tb(Pc-OBu) ₂] ₂	230	1.1×10^{-10}
[Dy(Pc-OBu) ₂] ₂	44	1.3×10^{-5}
[Dy(Pc-CN) ₂]	40	

Bagai, R.; Christou, G., "The Drosophila of Single-Molecule Magnetism: Mn₁₂". Chem. Soc. Rev. 2009, 38, 1011.

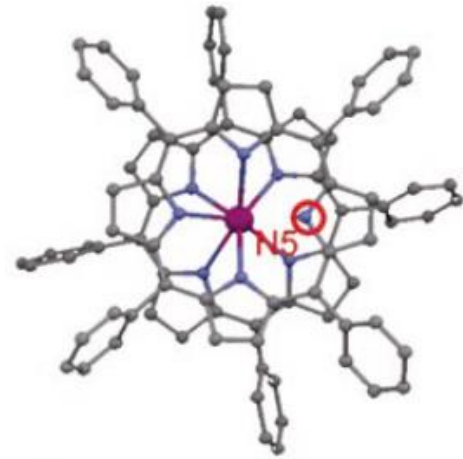
TbPc₂ is the 4f-SMM drosophila

Playing with TbPc₂

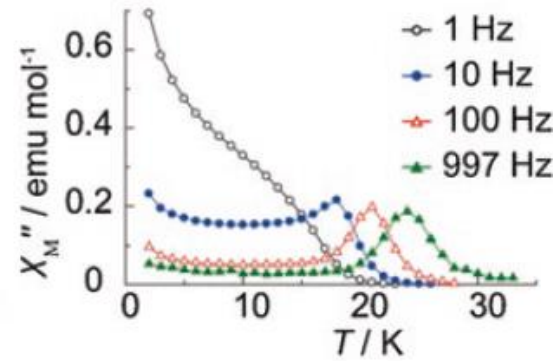
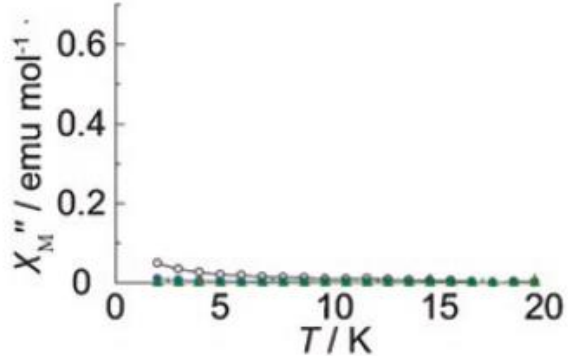
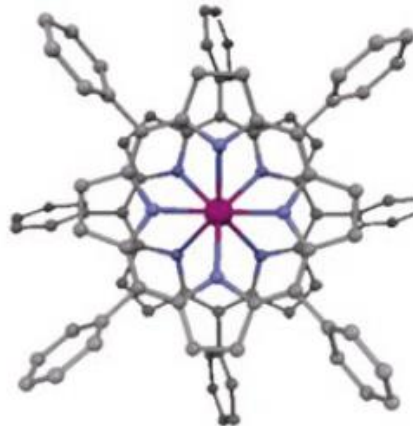


Phtolocyanine analogues (tetraphenylporphyrin) to test the electrostatics around Tb^{III} [TbH(TPP)₂]:

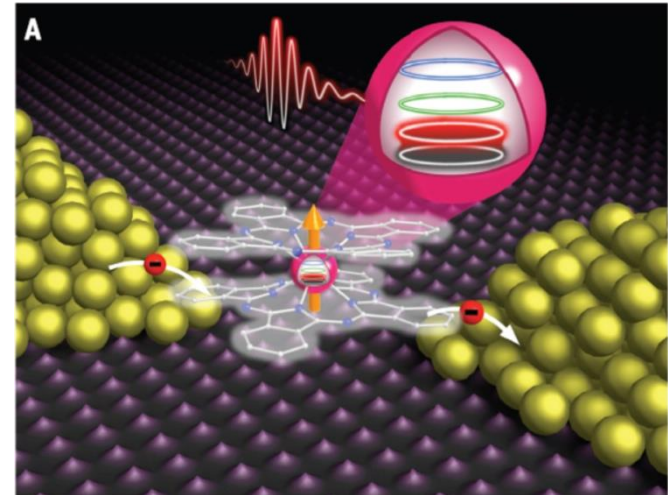
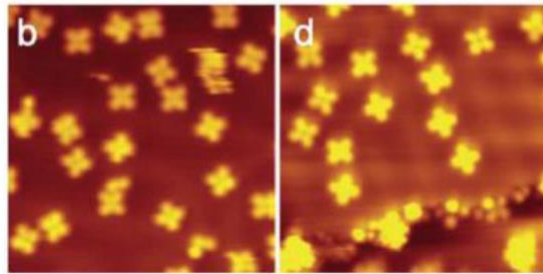
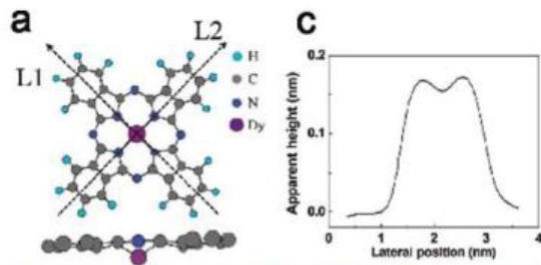
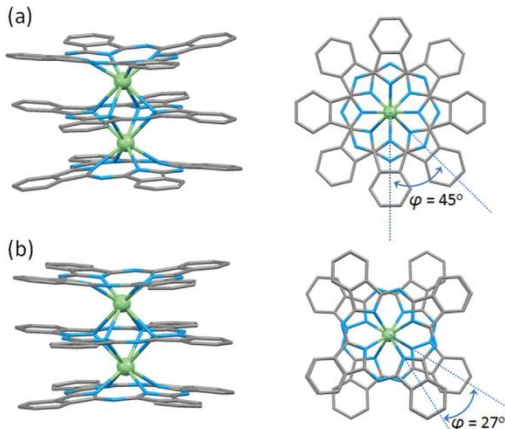
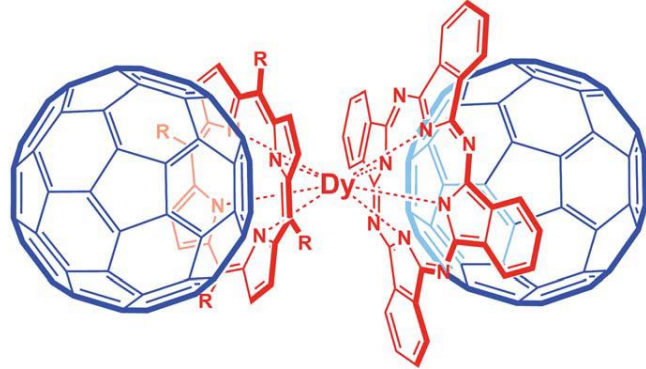
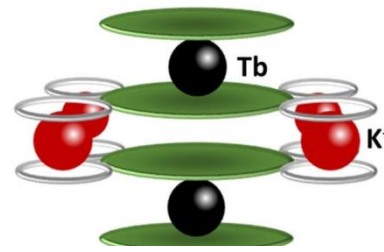
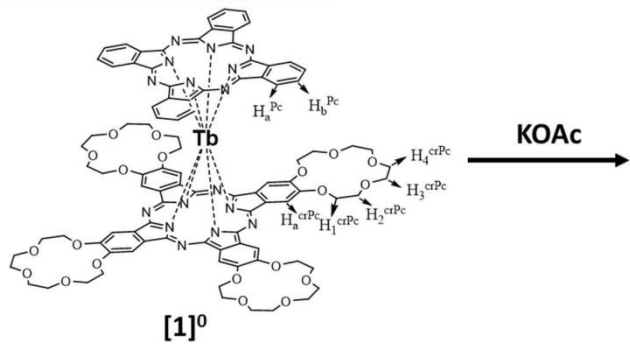
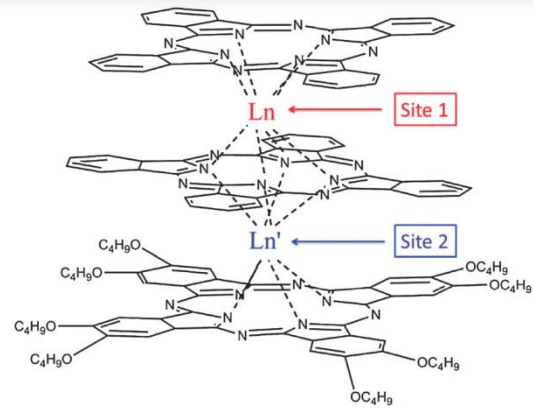
Protonated [TbH(TPP)₂]:



de-protonated [Tb(TPP)₂]⁻: U_{eff}= 407 K



The breakthrough of TbPc₂



Wang, H. et al., *Coord. Chem. Rev.* 2016, 306

Wang, H. et al., *Chem. Sci.* 2014, 5, 3214, 195.

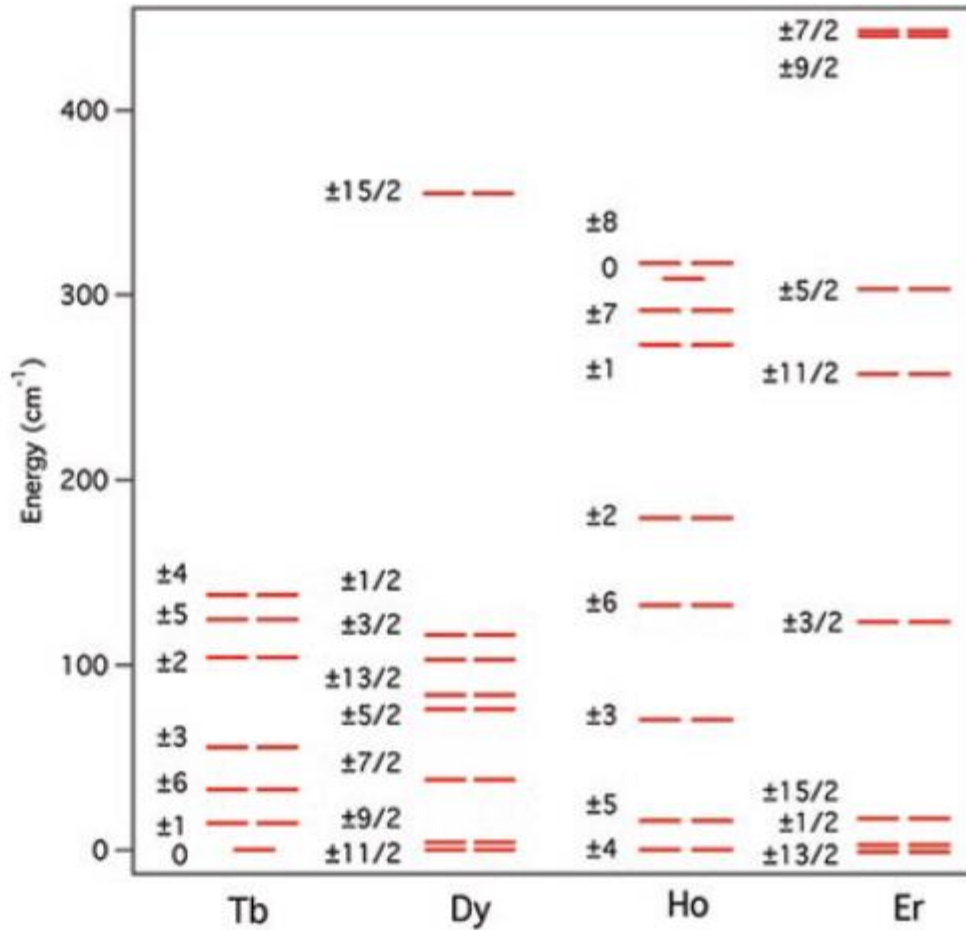
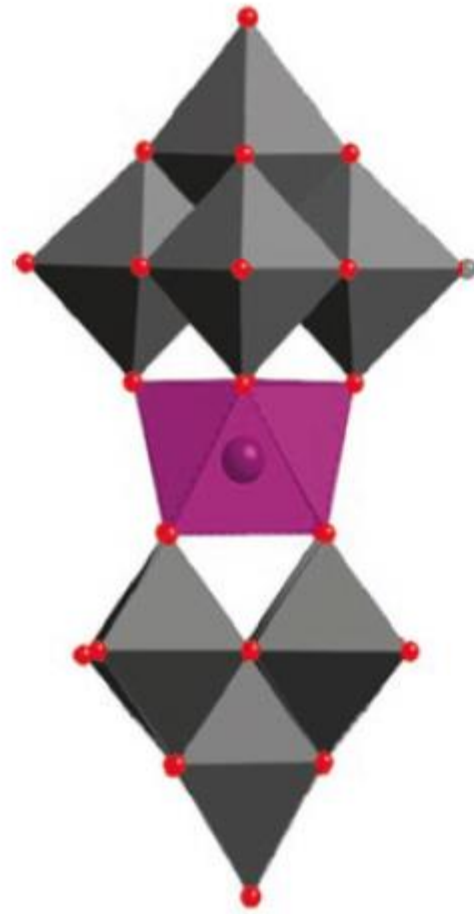
Katoh, K. et al., *Chem. Eur. J.* 2017, 23, 15377

Horii, Y., et al. *Chem. Eur. J.* 2018

Thiele , S., et al. *Science* 2014, 344, 1135

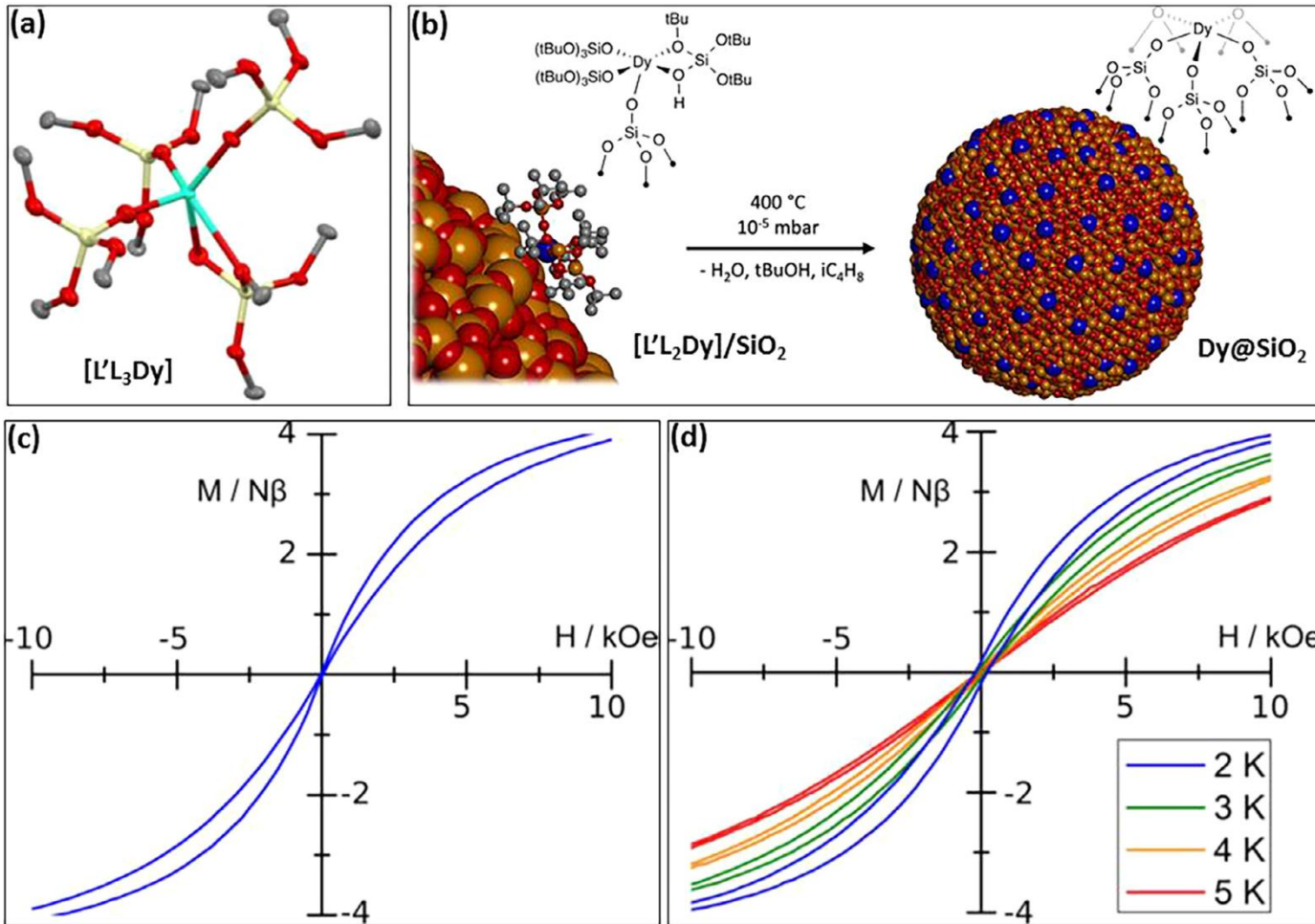
K. Katoh, et al., *Dalton Trans.* 2010, 39 4708

- Ln polyoxometalates → the second 4f-SIM family



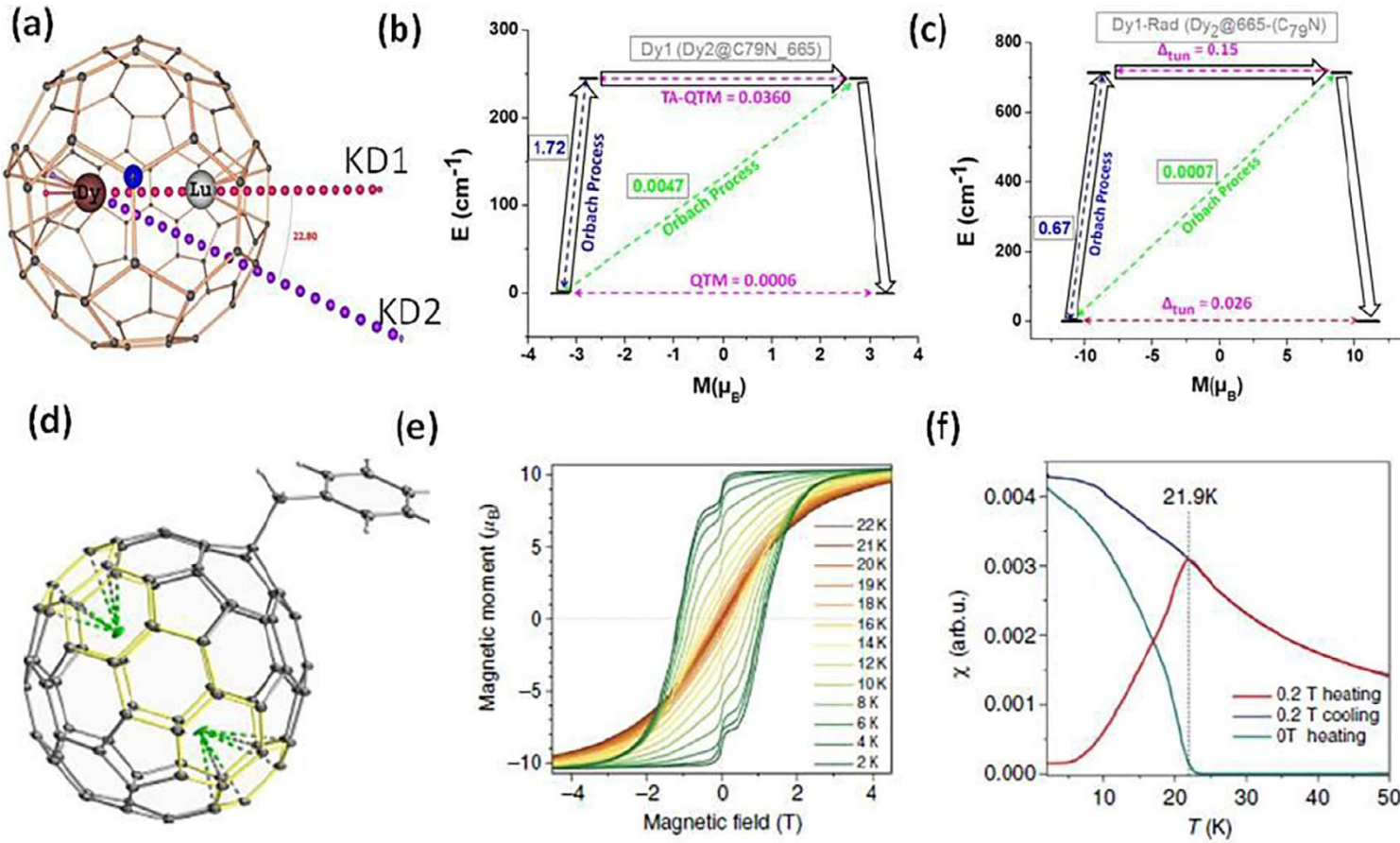
Low coordinate Ln^{III}

- via grafting on SiO₂ nanoparticles



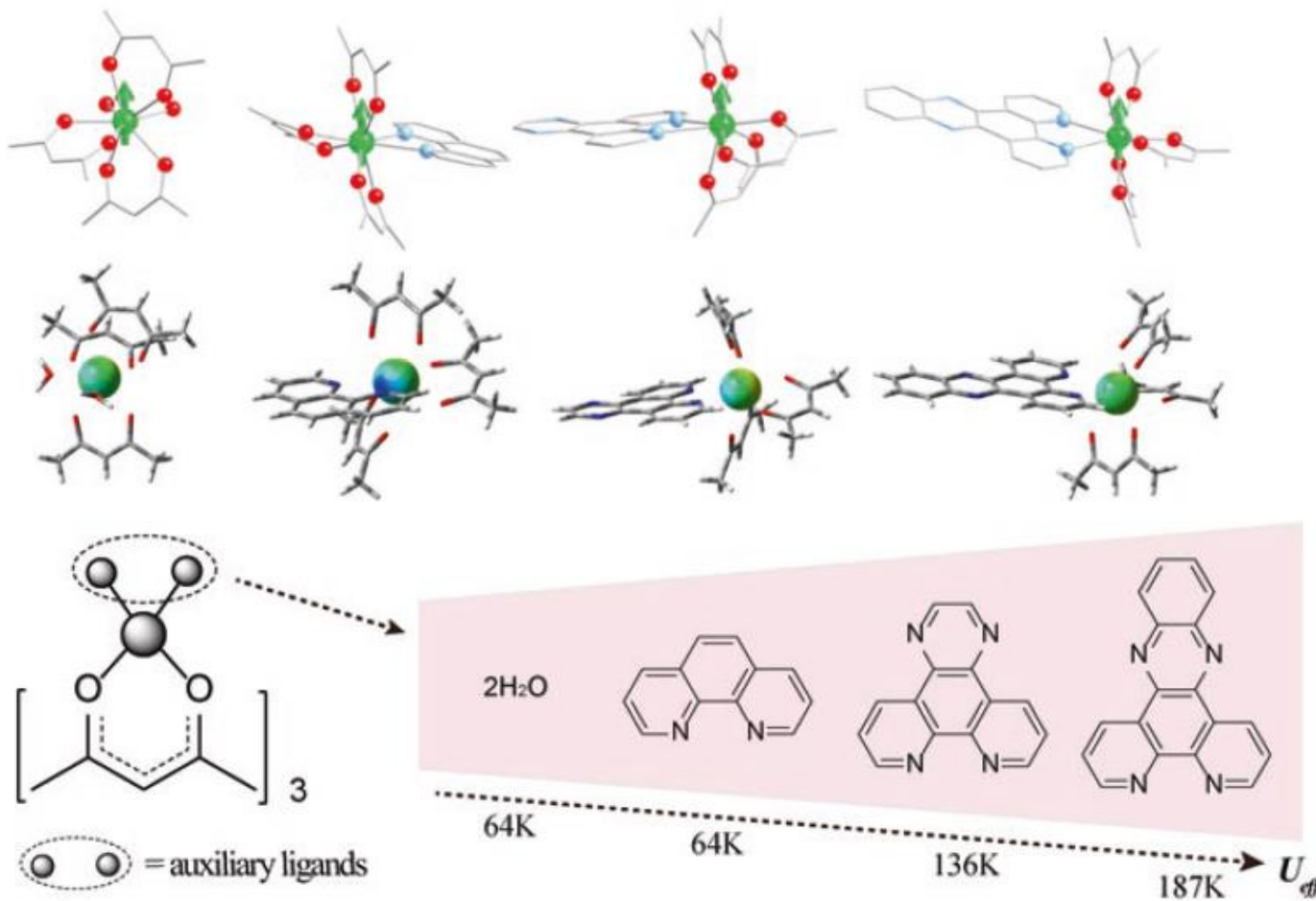
Low coordinate Ln^{III}

- via encapsulation in fullerenes derivatives

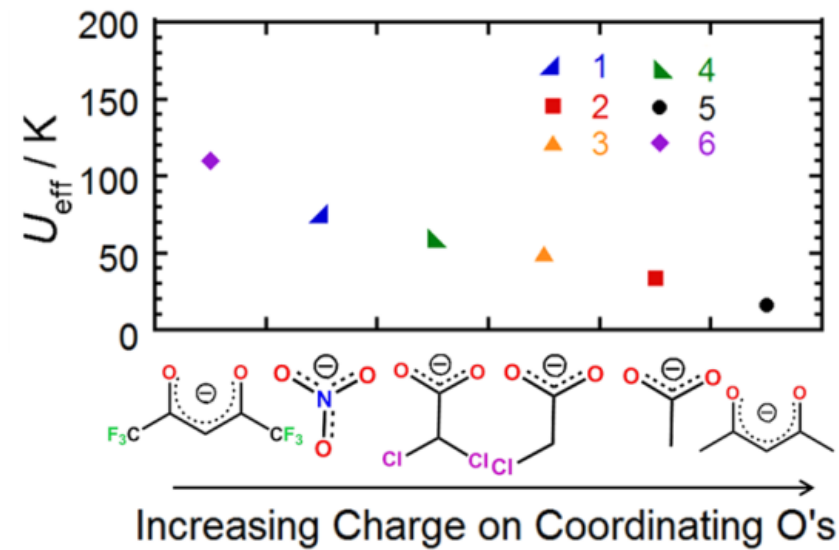
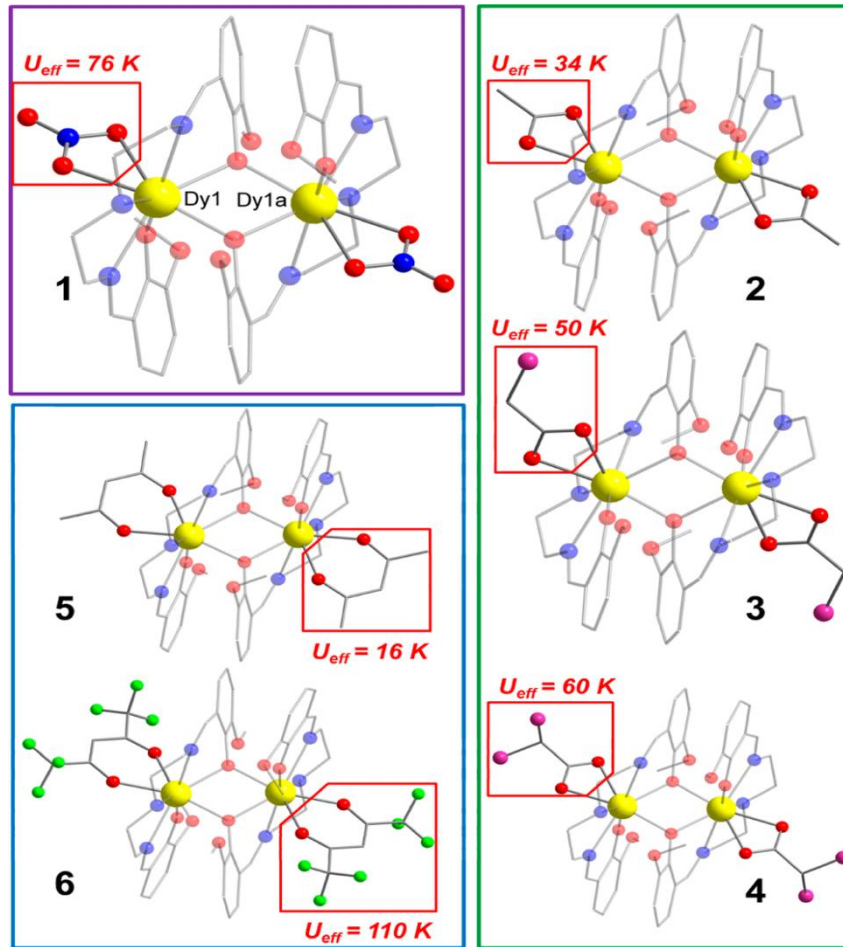


Electrostatics optimization in 4f-SMM

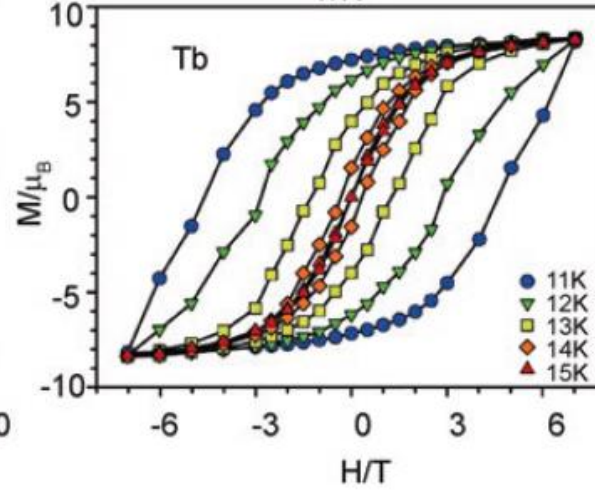
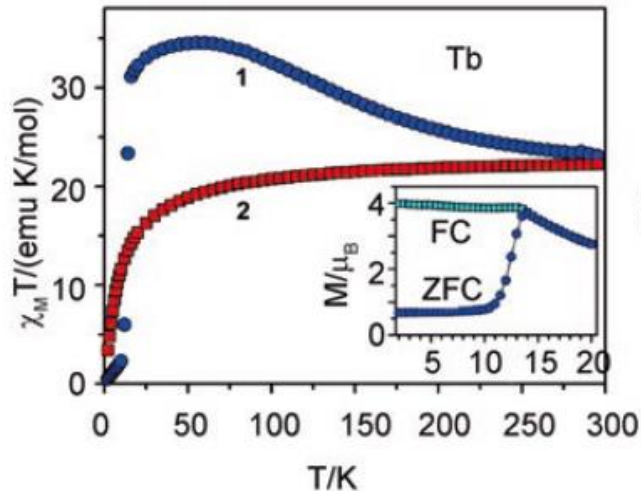
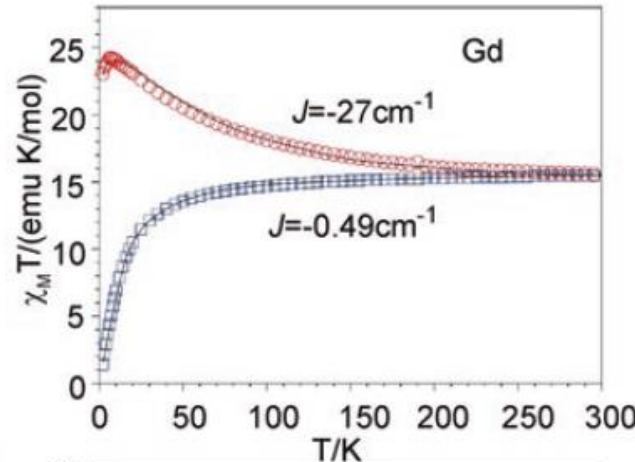
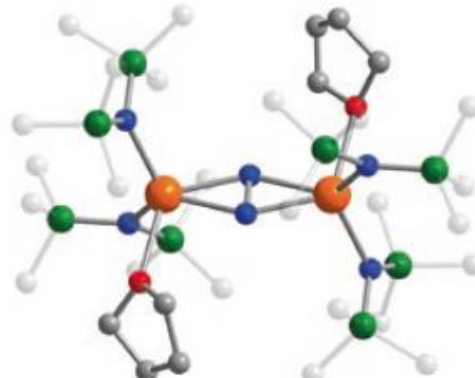
- Going for polynuclear 4f-SMM enhance the possibility of **electrostatic modulation of the Ln^{III} surrounding (ancillary or bridging ligand tuning)**



Electrostatics optimization in 4f-SMM

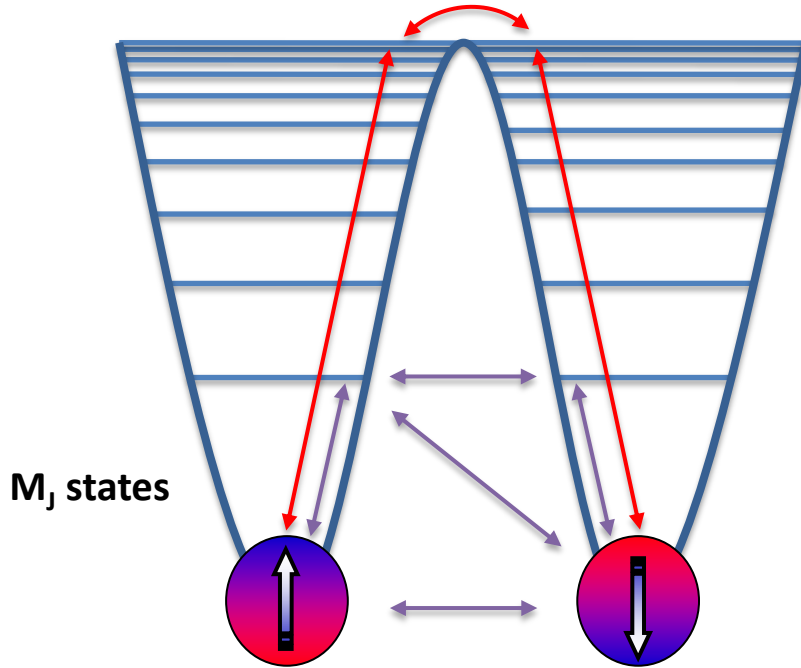
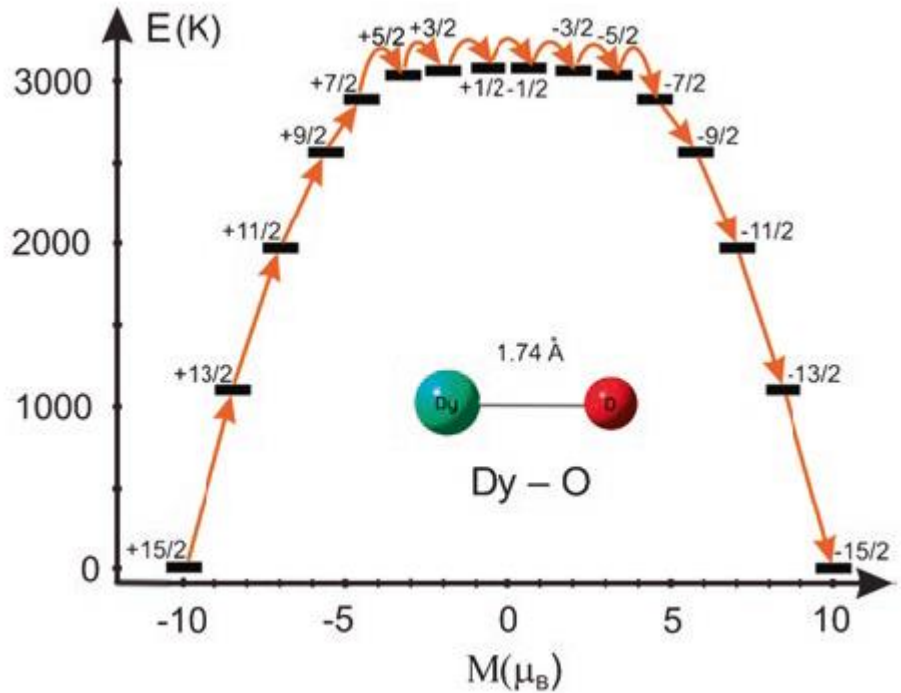


Ln^{III} coupling



- Need for **radical ligands otherwise** 4f-4f interactions are weak (dipolar + very small exchange)
- Need for **small ligands** → N₂³⁻

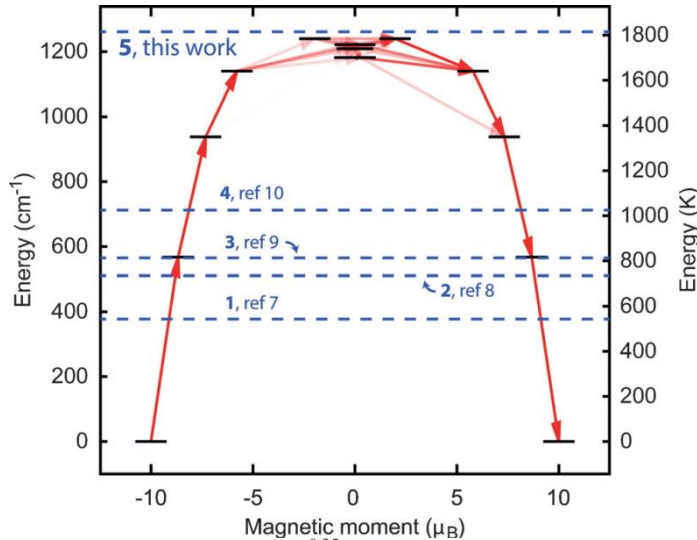
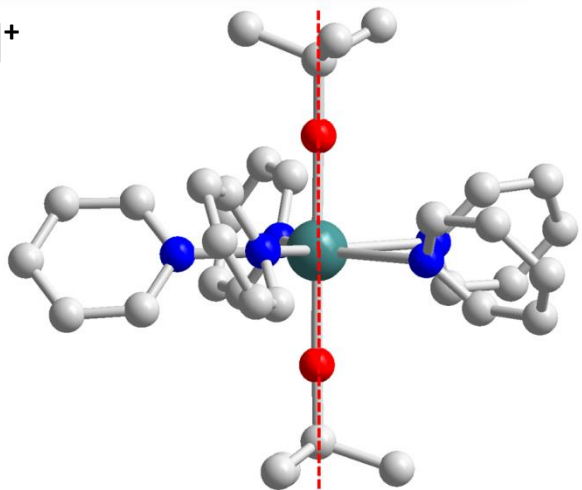
Theoretical approach of U_{eff}



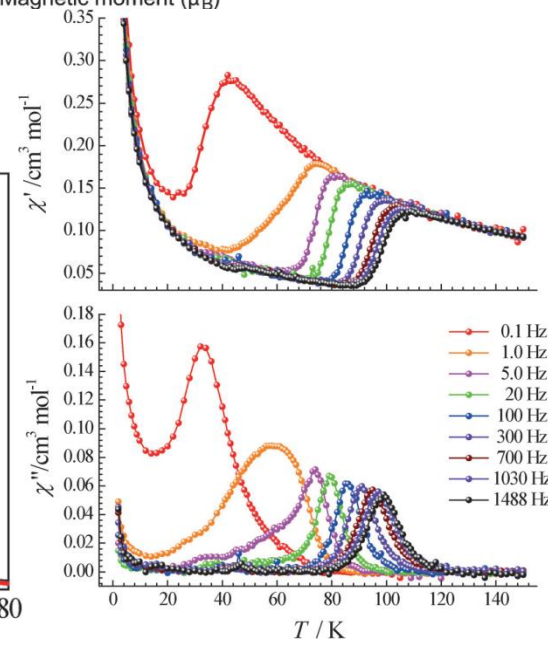
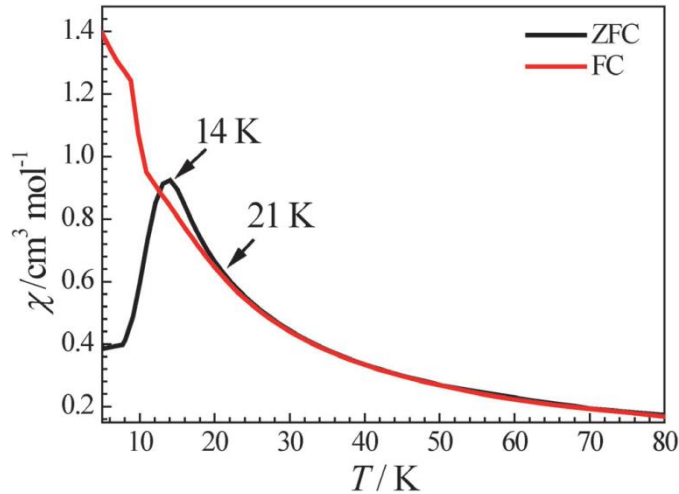
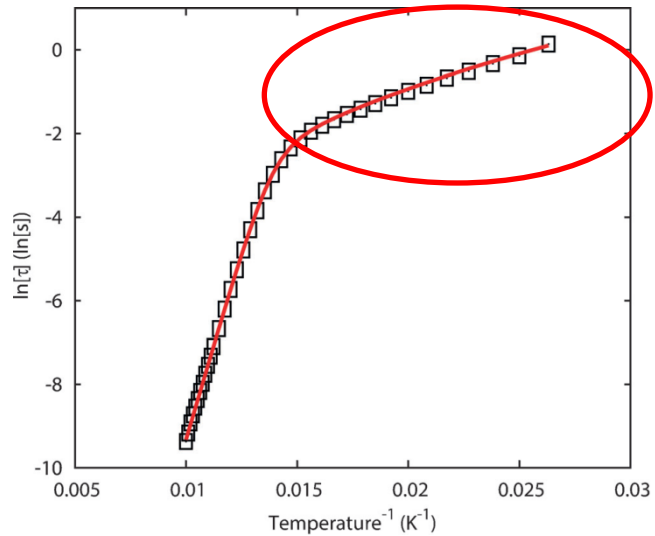
- For a Dy-O distance of 1.74 Å, theoretical value of U_{eff} can be as high as $U_{\text{eff}} \approx 3000$ K
- If under-barrier relaxation mechanisms are suppressed, very high T_B can be targeted

Closer to the perfect Dy symmetry

$[\text{Dy}(\text{O}^{\text{t}}\text{Bu})_2(\text{Py})_5]^+$
 O-Dy-O = 178.9°
 $U_{\text{eff}} = 1815 \text{ K}$
 $T_B = 14 \text{ K}$



- Optimization of the $M_J = 15/2$ stabilization by increasing the O-Dy-O angle (closer to 180°)
- Underbarrier relaxation at low T still possible



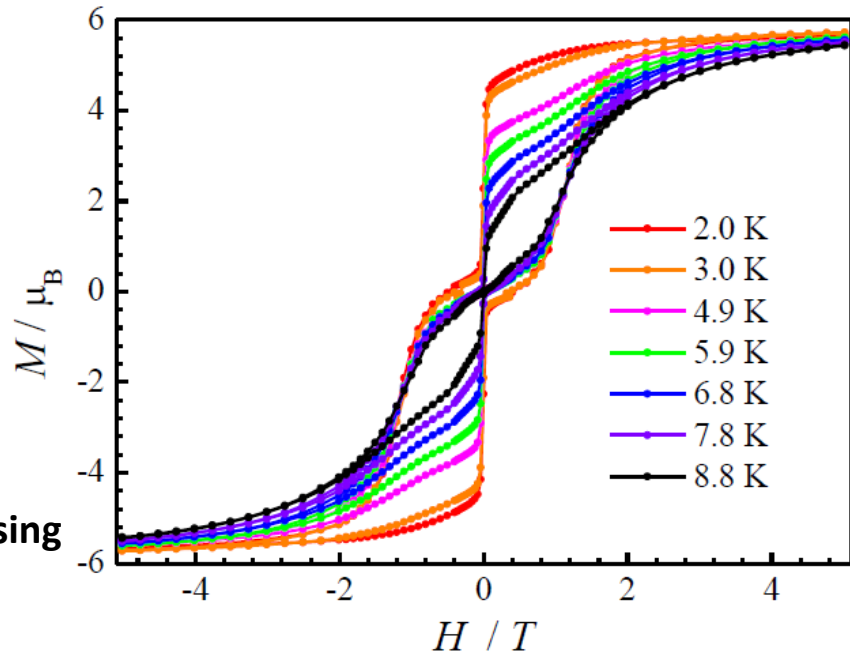
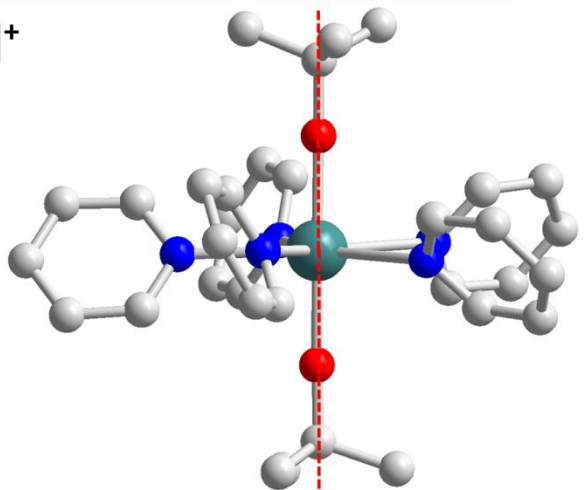
Closer to the perfect Dy symmetry



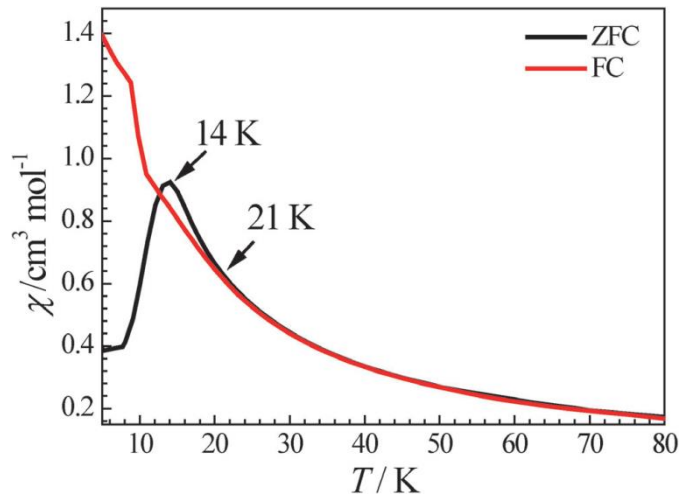
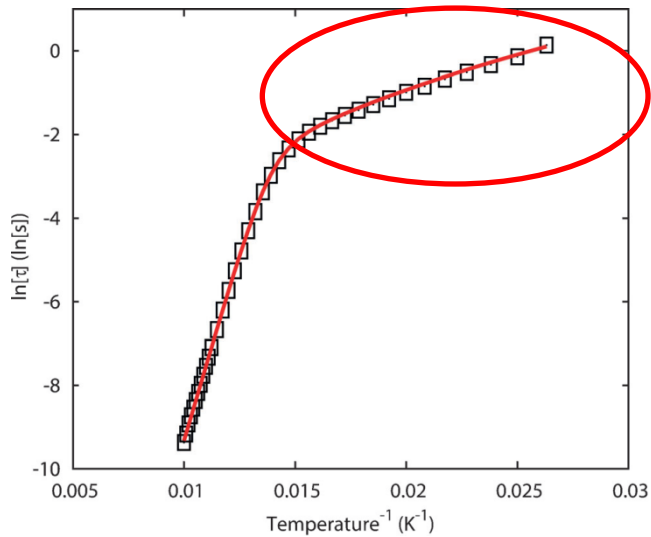
O-Dy-O = 178.9°

$U_{\text{eff}} = 1815 \text{ K}$

$T_B = 14 \text{ K}$



- Optimization of the $M_J = 15/2$ stabilization by increasing the O-Dy-O angle (closer to 180°)
- Underbarrier relaxation at low T still possible

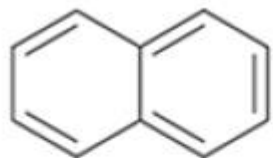


Going above N₂(l) temperature region

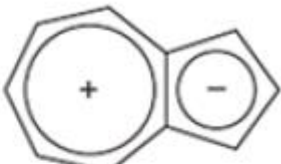
Neutral aromatic species



Benzene
6C, 6π

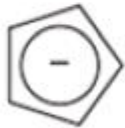


Naphthalene
10C, 10π



Azulene
10C, 10π

Charged aromatic species



Cyclopentadienyl
5C, 6π



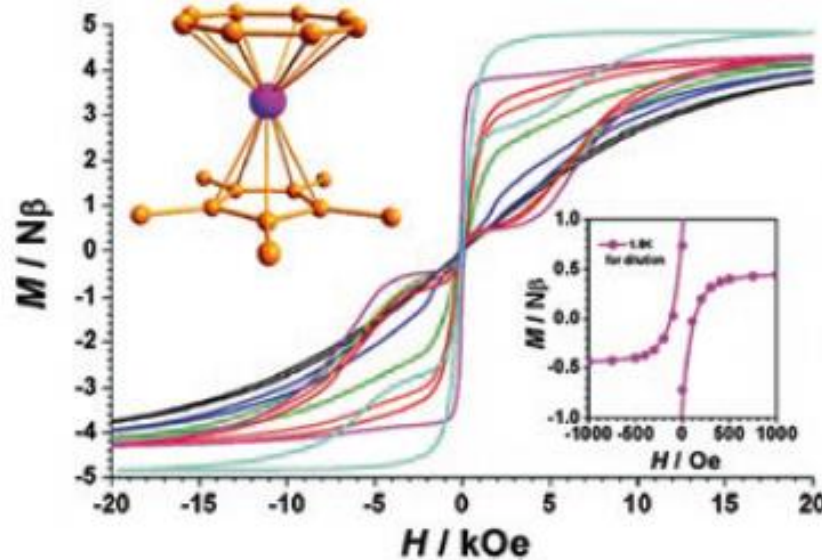
Tropylium
7C, 6π



Cyclooctatetraene
dianion
8C, 10π



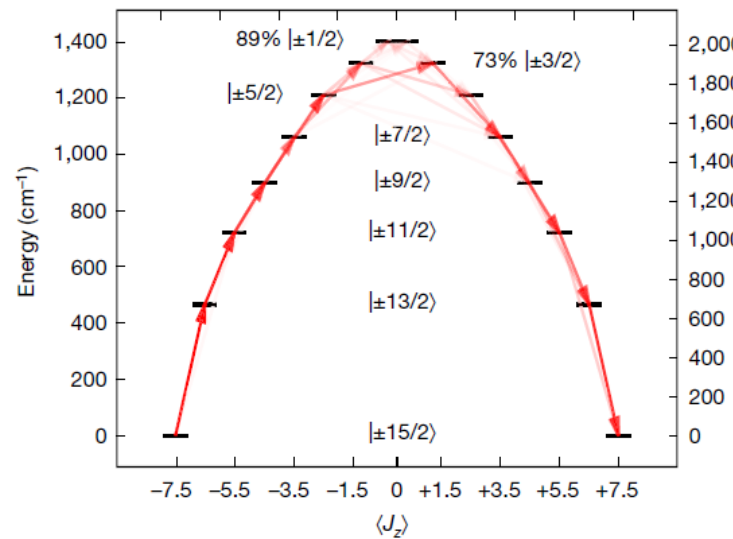
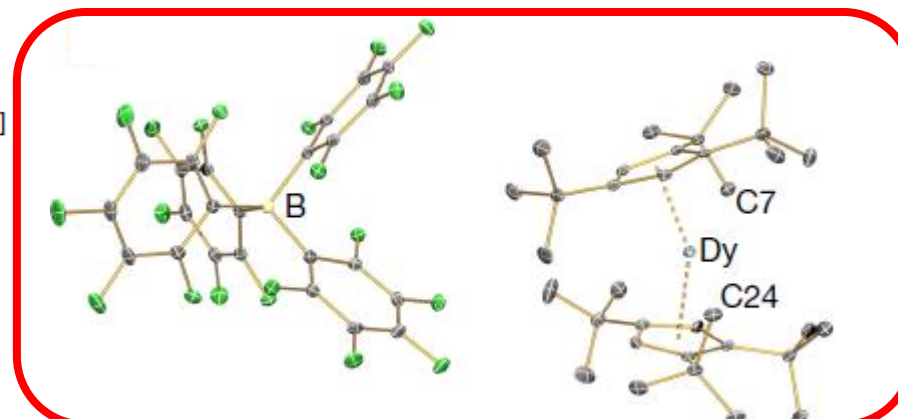
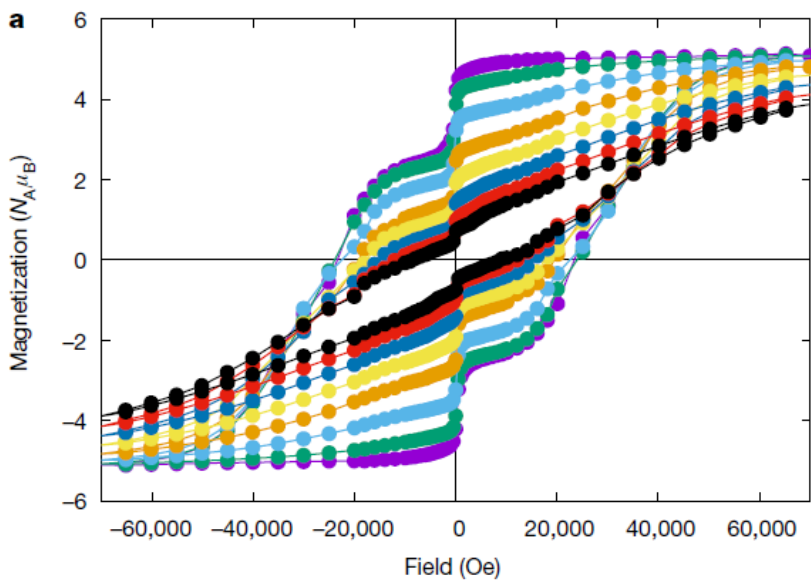
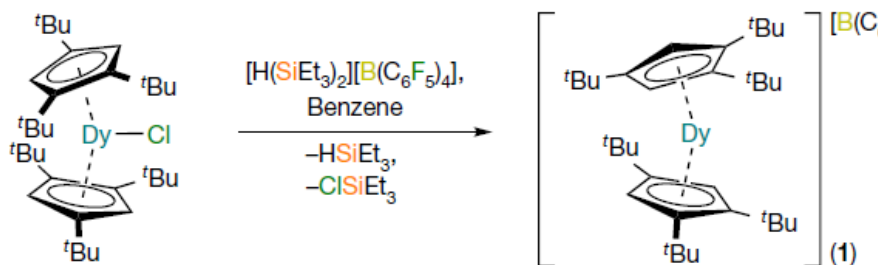
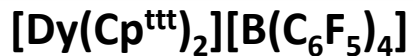
Benzene
tetraanion
6C, 10π



LnCOT family: a curiosity but maybe more.....

Pentamethylcyclopentadienide (C_5Me_5 , Cp*)
Cyclooctatetraenide ($\text{C}_8\text{H}_8^{2-}$, COT).

Going above N₂(I) temperature region



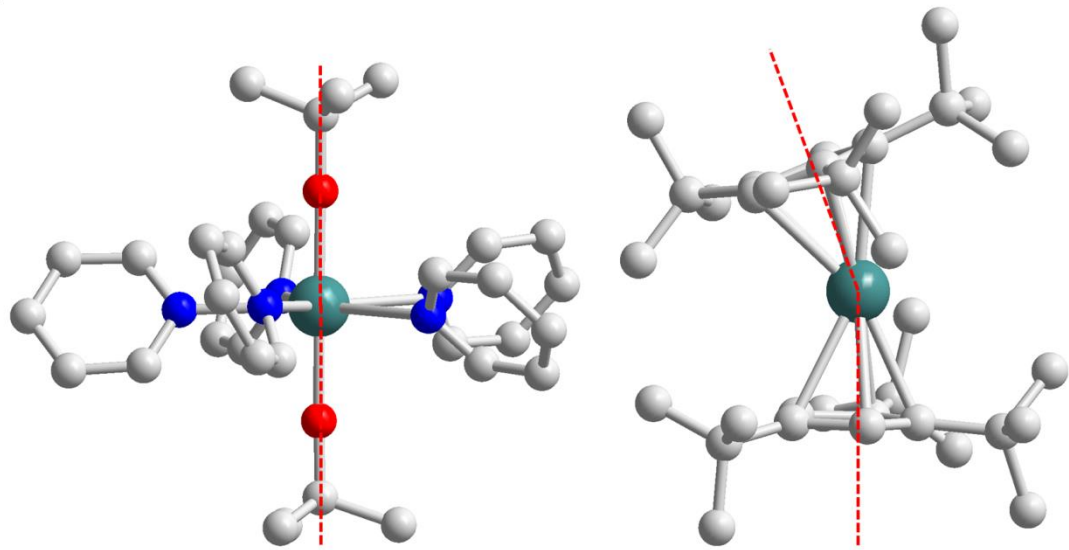
Blocking temperature as high as $T_B=60\text{K}$

$U_{\text{eff}} = 1760\text{ K}$

Cp-Dy-Cp = 152.8°

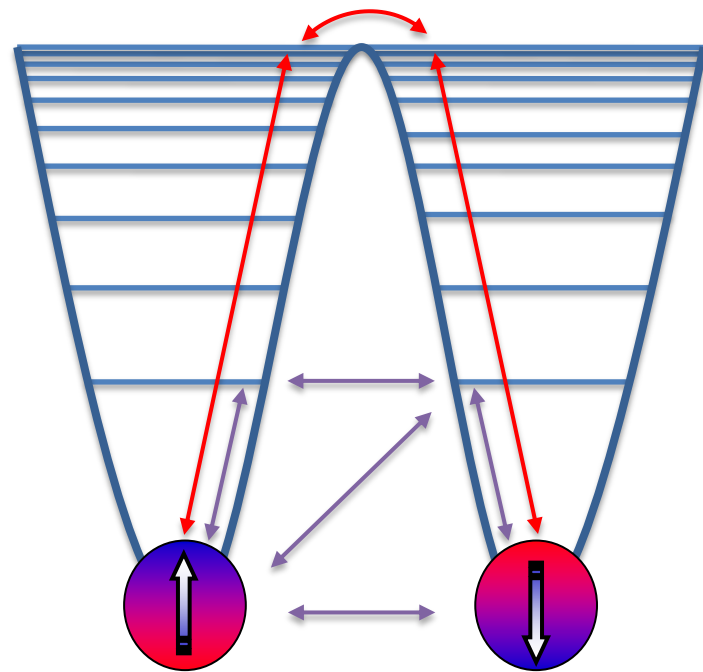
Movie

Going above N₂(I) temperature region



$[\text{Dy}(\text{O}^{\text{t}}\text{Bu})_2(\text{Py})_5]^+$,
angle O-Dy-O = 178.9°,
 $\text{U}_{\text{eff}} = 1815 \text{ K}$,
 $T_B = 14 \text{ K}$

$[\text{Dy}(\text{Cp}^{\text{ttt}})_2]^+$
angle Cp-Dy-Cp = 152.8°,
 $\text{U}_{\text{eff}} = 1760 \text{ K}$,
 $T_B = 60 \text{ K}$



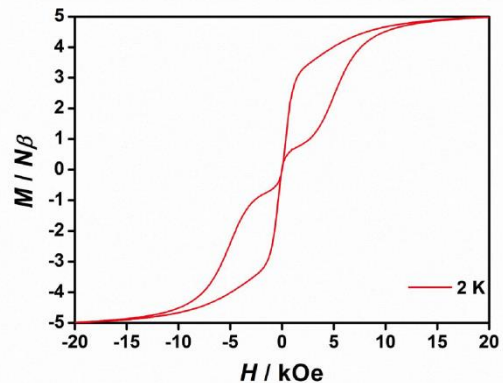
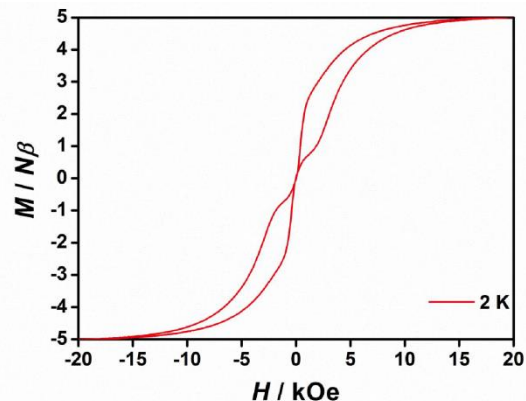
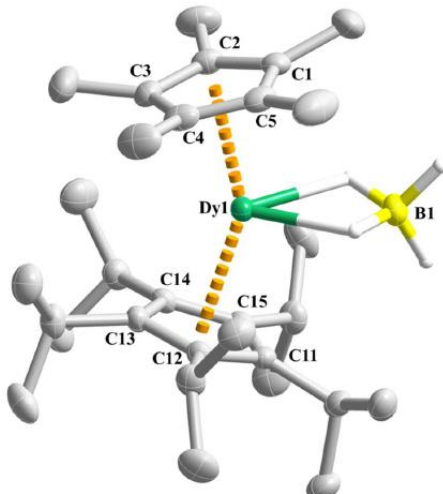
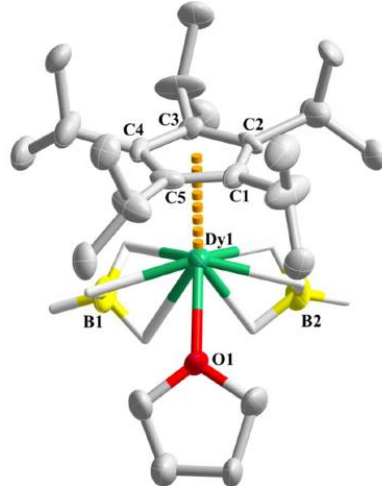
- **Optimization of spin-phonon coupling by increasing the « rigidity » of the molecule skeleton (vibration modes)**

Going above N₂(I) temperature region

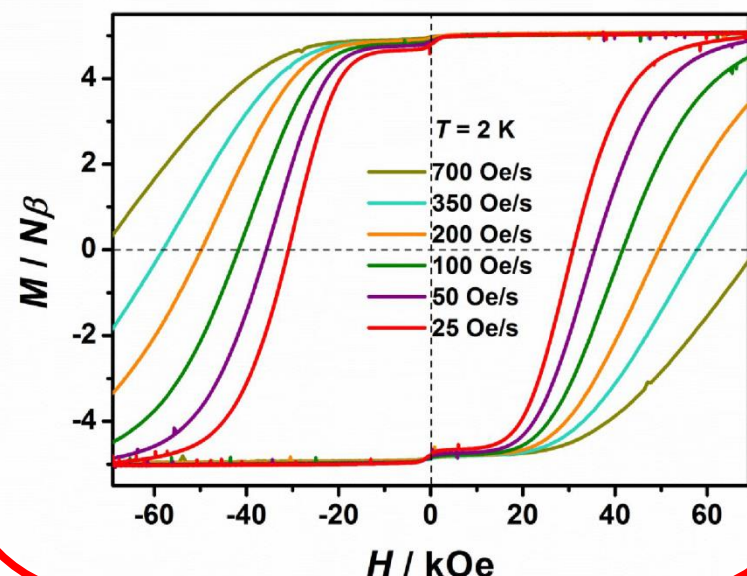
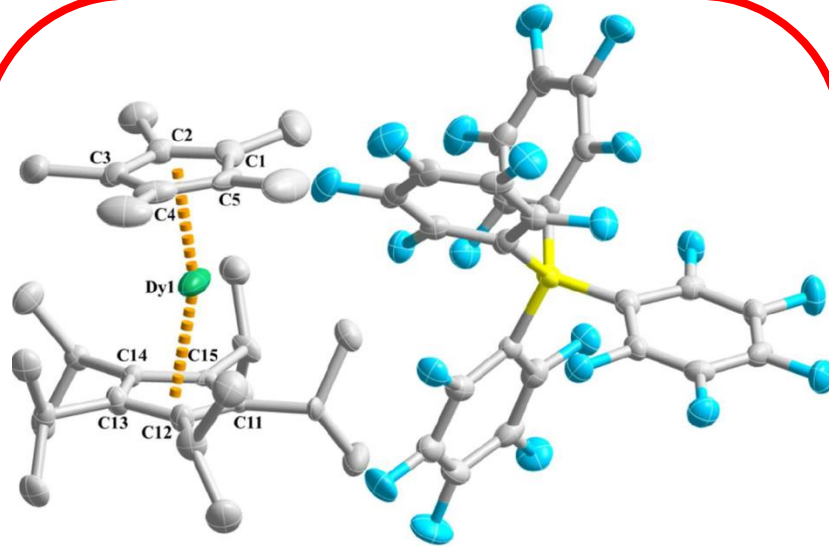
$[(\text{Cp}^{\text{iPr}_5})\text{Dy}(\text{Cp}^*)]^+$

$U_{\text{eff}} = 2217 \text{ K}$,

$T_B = 80 \text{ K}$ record blocking temperature for a SMM

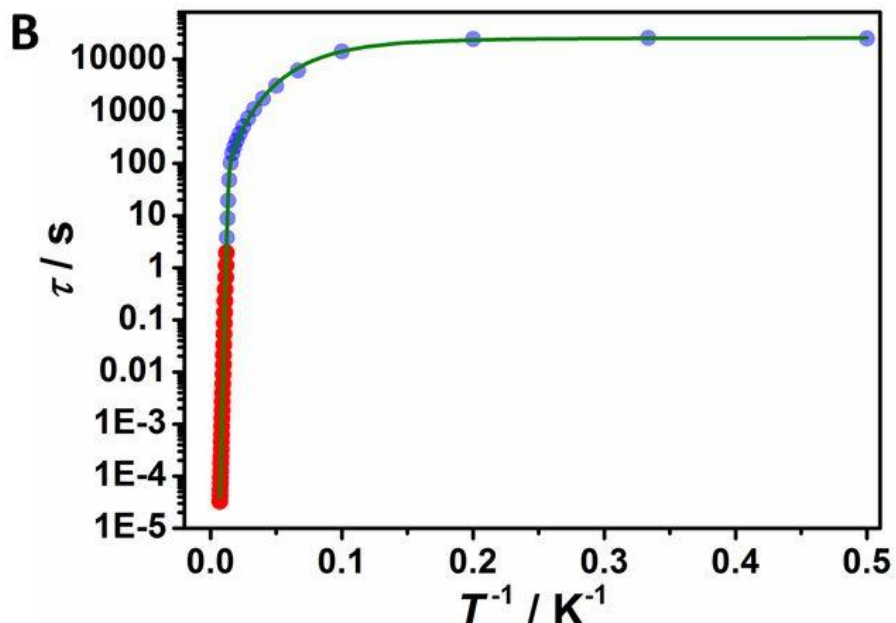
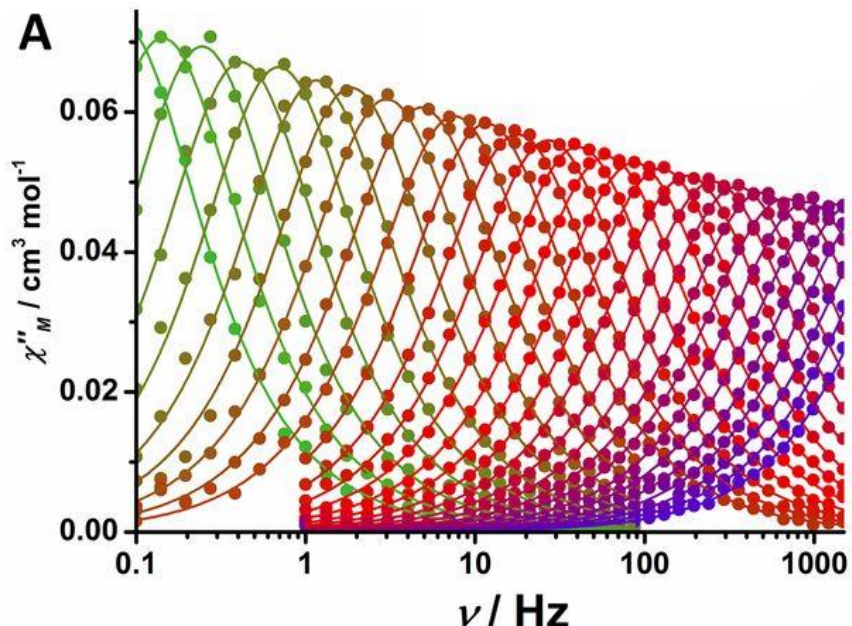


Hard magnet-like behavior



Going above N₂(l) temperature region

Underbarrier relaxation pathways are still present at low T but for relaxation times that are extremely slow



movie

Going above N_2 (I) temperature region



angle Cp-Dy-Cp = 165.5° , $U_{\text{eff}} = 2217\text{K}$,
 $T_B = 80\text{ K}$

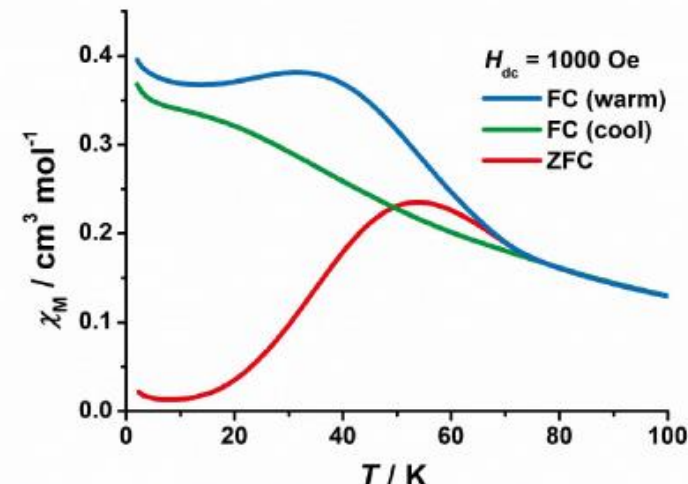
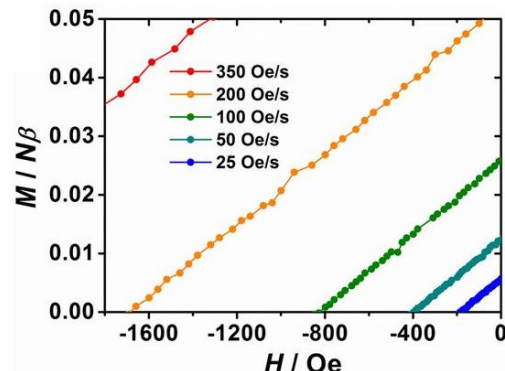
Hard magnet-like behavior

Table S9. Coercive fields for 3 at different sweep rate at 2 K, corresponding to Fig. S49.

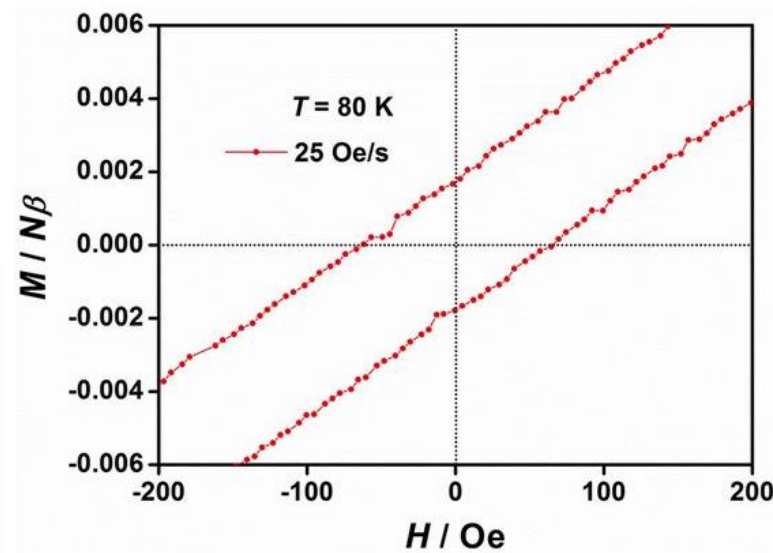
Sweep rate / Oe s ⁻¹	Coercive field / Oe
700	> 70000
350	58146
200	49741
100	41722
50	35632
25	30893

Table S10. Coercive fields at different sweep rate at 77 K, corresponding to Fig. S50.

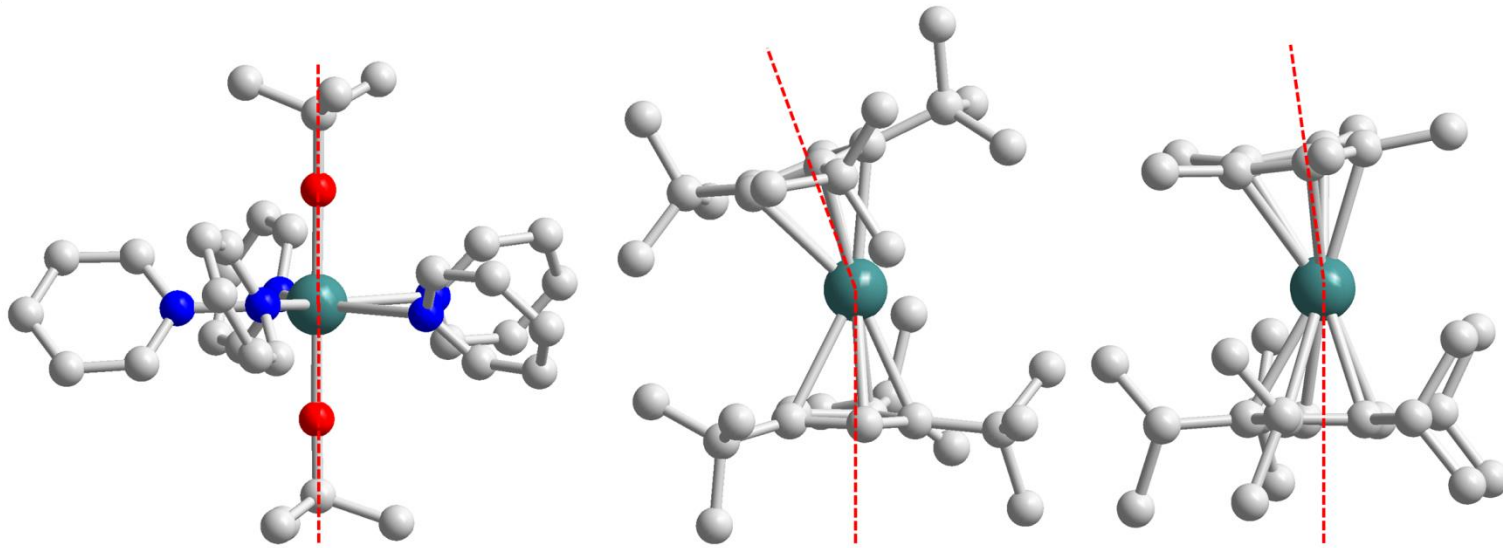
Sweep rate / Oe s ⁻¹	Coercive field / Oe
700	5802
350	2946
200	1688
100	825
50	398
25	191



1. Field-cooled (FC, blue line) and zero-field-cooled (ZFC, red line) variable-temperature ac susceptibility for 3_{nv} under 1000 Oe DC filed in warm mode (2 K/min) from 2 to 100



Going above N₂ temperature region



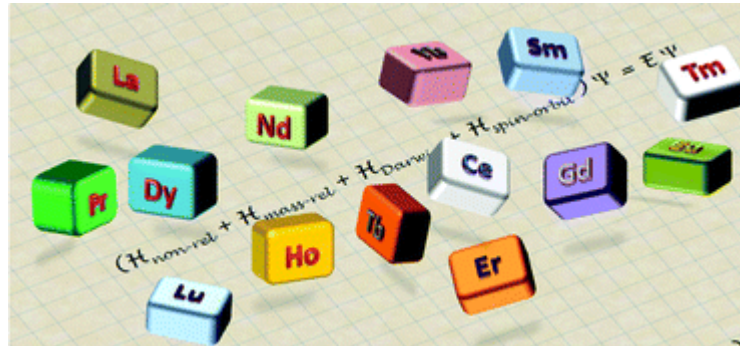
[Dy(O^tBu)₂(Py)₅]⁺,
angle O-Dy-O= 178.9°,
 $U_{\text{eff}} = 1815 \text{ K}$
 $T_B = 14 \text{ K}$

[Dy(Cp^{ttt})₂]⁺
angle Cp-Dy-Cp= 152.8°,
 $U_{\text{eff}} = 1760 \text{ K}$
 $T_B = 60 \text{ K}$

[(Cp^{iPr₅})Dy(Cp^{*})]⁺
angle Cp-Dy-Cp= 165.5°,
 $U_{\text{eff}} = 2217 \text{ K}$,
 $T_B = 80 \text{ K}$

- Optimization of spin-phonon coupling by increasing the « rigidity » of the molecule skeleton (vibration modes)
- Optimization of the $M_J = 15/2$ stabilization (electrostatics around Dy^{III}) by increasing the X-Dy-X angle (closer to 180°)

Key Points



- Rare-Earth (RE) elements are **not rare**
- RE have **similar chemical properties**
- Their high cost is due to the separation cost of indiv. RE oxide and to the high demand
- LS (spin-orbit)> CF (crystal field), J is a good quantum number
- M_s states on 3d, M_j states on 4f, (energy barrier is DS^2 and U_{eff} resp.)
- M_j states can be investigated by **luminescence spectroscopy**
- Magnetic anisotropy can be investigated by **angular-resolved magnetometry**
- Spin and magnetic anisotropy are the two ingredients for SMM behavior
- Giant spins (polynuclear molecules) do not always provide SMM behavior
- Strong anisotropy of single-ion can be enough to provide SMM behavior
- TbPc_2 was the first family of 4f-SMM
- Strong axiality of the electrostatics around Dy^{III} is needed
- Vibration modes (molecule rigidity) could be responsible for under-barrier relaxation
- Organometallic 4f molecules verify these last two requisites and affords high-performance **4f-SMM**
- The quest for stable (air, moisture,...), depositable (surfaces) and addressable SMMs continues...

Somes references on 4f-SMM

- Bar, A. K. et al., *Coord. Chem. Rev.* **2018**, 367, 163
- Zhang P. et al., *Coord. Chem. Rev.*, **2013**, 257, 1728
- Woodruff, D. N., et al. *Chem. Rev.* **2013**, 113, 5110
- F. Pointillart, et al. *Coord. Chem. Rev.*, **2017**, 346, 150
- **Lanthanides and Actinides in Molecular Magnetism**; Ed. R.A. Layfield, M. Murugesu, Wiley-VCH, **2015**
- Kahn, O. **Molecular Magnetism**; Wiley-VCH: Weinheim, **1993**
- Du Trémolet De Lacheisserie, E. **Magnétisme**, Presses Universitaires de Grenoble, **1999**
- Benelli, C.; Gatteschi, D. **Introduction to Molecular Magnetism: From Transition Metals to Lanthanides**, **2015**
- Verdaguer, M.; Launay, J.-P. - **Electrons in Molecules; from Basic Principles to Molecular Electronics**; OUP, **2013**
- Ribas, J. **Coordination Chemistry**; Wiley-vch: Weinheim, **2008**
- Carlin, R. J. **Magnetochemistry**; Springer: Berlin, **1986**
- Clérac, R.; Winpenny, R. E. P. **Single-Molecule Magnets and Related Phenomena**. In 50 Years of Structure and Bonding – the Anniversary Volume, Springer, **2016**; 35
- J. Tang, P. Zhang, **Lanthanide Single Molecule Magnets**, Springer, **2015**